Mittuniversitetet
MID SWEDEN UNIVERSITY

Thesis for the degree of Doctor of Technology, Sundsvall 2015

DISTRIBUTIONS OF FIBER CHARACTERISTICS AS A TOOL TO EVALUATE MECHANICAL PULPS

Sofia Reyier Österling

Supervisors:
Professor Per Engstrand
Professor Hans Höglund
MSc Olof Ferritsius
MSc Rita Ferritsius
MSc Hans Ersson
Professor Per Gradin

FSCN – Fibre Science and Communication Network
Faculty of Science, Technology and Media
Mid Sweden University, SE-851 70 Sundsvall, Sweden

ISSN 1652-893X
Mid Sweden University Doctoral Thesis 211
ISBN 978-91-86694-66-1

FSCN
PART OF MID SWEDEN UNIVERSITY

Akademisk avhandling som med tillstånd av Mittuniversitetet i Sundsvall framläggs till offentlig granskning för avläggande av teknologie doktorsexamen i kemiteknik, onsdag den 25 februari 2015, klockan 09.15 i sal L111 på Mittuniversitetet i Sundsvall, Sverige. Seminariet kommer att hållas på engelska.

DISTRIBUTIONS OF FIBER CHARACTERISTICS AS A TOOL TO EVALUATE MECHANICAL PULPS

Sofia Reyier Österling

The image on the cover illustrates length weighted BIN-distributions and micrographs from a scanning electron microscope of fibers from the P16/R30 fraction, magnified 600 times, of two pulp streams of the same news grade pulp, a TMP made from Norwegian spruce (Picea abies) refined in double disc refiners.

The QR code accesses material and images which are related to this study. All scientific material is also available at Mid Sweden University, Sundsvall, Sweden.

FSCN – Fibre Science and Communication Network
Faculty of Science, Technology and Media
Mid Sweden University, SE-851 70 Sundsvall, Sweden

Telephone: +46 (0)771-975 000

Printed by Service and Maintenance Office, Mid Sweden University, Sundsvall, Sweden, 2015

DISTRIBUTIONS OF FIBER CHARACTERISTICS AS A TOOL TO EVALUATE MECHANICAL PULPS

Sofia Reyier Österling

FSCN – Fibre Science and Communication Network, Faculty of Science, Technology and Media, Mid Sweden University, SE-851 70 Sundsvall, Sweden
ISSN 1652-893X, Mid Sweden University Doctoral Thesis 211; ISBN 978-91-86694-66-1

ABSTRACT

Mechanical pulps are used in paper products such as magazine or news grade printing papers or paperboard. Mechanical pulping gives a high yield; nearly everything in the tree except the bark is used in the paper. This means that mechanical pulping consumes much less wood than chemical pulping, especially to produce a unit area of printing surface. A drawback of mechanical pulp production is the high amounts of electrical energy needed to separate and refine the fibers to a given fiber quality. Mechanical pulps are often produced from slow-growing spruce trees of forests in the northern hemisphere resulting in long, slender fibers that are well suited for mechanical pulp products. These fibers have large varieties in geometry, mainly wall thickness and width, depending on seasonal variations and growth conditions. Earlywood fibers typically have thin walls and latewood fibers thick.

The background to this study was that a more detailed fiber characterization involving evaluations of distributions of fiber characteristics, may give improved possibilities to optimize the mechanical pulping process and thereby reduce the total electric energy needed to reach a given quality of the pulp and final product. This would result in improved competitiveness as well as less environmental impact.

This study evaluated the relation between fiber characteristics in three types of mechanical pulps made from Norway spruce (*Picea abies*), thermomechanical pulp (TMP), stone groundwood pulp (SGW) and chemithermomechanical pulp (CTMP). In addition, the influence of fibers from these pulp types on sheet characteristics, mainly tensile index, was studied. A comparatively rapid method was presented on how to evaluate the propensity of each fiber to form sheets of high tensile index, by the use of raw data from a commercially available fiber analyzer (FiberLab™). The developed method gives novel opportunities of evaluating the effect on the fibers of each stage in the mechanical pulping process and has a potential to be applied also on-line to steer the refining and pulping process by the characteristics of the final pulp and the quality of the final paper.

The long fiber fraction is important for the properties of the whole pulp. It was found that fiber wall thickness and external fibrillation were the fiber characteristics that contributed the most to tensile index of the long fiber fractions in five mechanical pulps (three TMPs, one SGW, one CTMP). The tensile index of handsheets of the long fiber fractions could be predicted by linear regressions using a combination of fiber wall thickness and degree of external fibrillation. The predicted tensile index was denoted *BIN*, short for *B*onding ability *IN*fluence. This resulted in the same linear correlation between *BIN* and tensile index for 52 samples of the five mechanical pulps studied, each fractionated into five streams (plus feed) in full size hydrocyclones. The Bauer McNett P16/R30 (passed 16 mesh wire, retained on a 30 mesh wire) and P30/R50 fractions of each stream were used for the evaluation. The fibers of the SGW had thicker walls and a higher degree of external fibrillation than the TMPs and CTMP, which resulted in a correlation between *BIN* and tensile index on a different level for the P30/R50 fraction of SGW than the other pulp samples. A *BIN* model based on averages weighted by each fiber´s wall volume instead of arithmetic averages, took the fiber wall thickness of the SGW into account, and gave one uniform correlation between *BIN* and tensile index for all pulp samples (12 samples for constructing the model, 46 for validating it). If the *BIN* model is used for predicting averages of the tensile index of a sheet, a model based on wall volume weighted data is recommended. To be able to produce *BIN* distributions where the influence of the length or wall volume of each fiber is taken into account, the *BIN* model is currently based on arithmetic averages of fiber wall thickness and fibrillation.

Fiber width used as a single factor reduced the accuracy of the *BIN* model. Wall volume weighted averages of fiber width also resulted in a completely changed ranking of the five hydrocyclone streams compared to arithmetic, for two of the five pulps. This was not seen when fiber width was combined with fiber wall thickness into the factor "collapse resistance index". In order to avoid too high influence of fiber wall thickness and until the influence of fiber width on *BIN* and the measurement of fiber width is further evaluated, it is recommended to use length weighted or arithmetic distributions of *BIN* and other fiber characteristics.

A comparably fast method to evaluate the distribution of fiber wall thickness and degree of external fibrillation with high resolution showed that the fiber wall thickness of the latewood fibers was reduced by increasing the refining energy in a double disc refiner operated at four levels of specific energy input in a commercial TMP production line. This was expected but could not be seen by the use of average values, it was concluded that fiber characteristics in many cases should be evaluated as distributions and not only as averages.

BIN distributions of various types of mechanical pulps from Norway spruce showed results that were expected based on knowledge of the particular pulps and processes. Measurements of mixtures of a news- and a SC (super calendered) grade TMP, showed a gradual increase in high-*BIN* fibers with higher amounts of SC grade TMP. The *BIN* distributions also revealed differences between the pulps that were not seen from average fiber values, for example that the shape of the *BIN* distributions was similar for two pulps that originated from conical disc refiners, a news grade TMP and the board grade CTMP, although the distributions were on different *BIN* levels. The SC grade TMP and the SC grade SGW had similar levels of tensile index, but the SGW contained some fibers of very low *BIN* values which may influence the characteristics of the final paper, for example strength, surface and structure. This shows that the *BIN* model has the potential of being applied on either the whole or parts of a papermaking process based on mechanical or chemimechanical pulping; the evaluation of distributions of fiber characteristics can contribute to increased knowledge about the process and opportunities to optimize it.

Keywords: Fiber, fibre, fiber characteristics, fiber dimension, fiber properties, mechanical pulp, FiberLab, raw data, distribution, fiber wall thickness, *BIN*, bonding ability influence, bonding indicator, bonding ability, fiber width, fibrillation, collapse resistance, laboratory sheet, fiber analyzer, optical analyzer, TMP, CTMP, SGW, sheet model, prediction, fiber characterization, hydrocyclone, fractionation, kernel density estimation, *KDE*, diffusion mixing, acoustic emission, F0.90, Norway spruce, *Picea abies*

SAMMANDRAG

Mekanisk pappersmassa används för att tillverka bland annat kataloger, dagstidningar och kartong. Mekanisk massa framställs med högt materialutbyte, och nästan allt i veden utom barken används till pappret. Det gör att den mekaniska massaprocessen är mer materialeffektiv än den kemiska, särskilt sett till mängd material som krävs för att tillverka en given tryckyta. En nackdel med den mekaniska massatillverknings-processen är den stora mängden elektrisk energi som krävs för att frilägga fibrerna från veden och bearbeta dem till en fördefinierad fiberkvalitet. Mekanisk massa tillverkas ofta av långsamväxande barrträd som växer på det norra halvklotet. Fibrer från dessa träd är långa och slanka och passar bra till produkter som tillverkas av mekanisk massa. Dessa fibrer har dock väldigt olika geometri, främst väggtjocklek och vidd (diameter), på grund av årstidsvariationer och skillnader i växtbetingelser. Vårvedsfibrer har typiskt tunna fiberväggar, och sommarvedsfibrer tjocka.

Bakgrunden till den här studien var att en mer detaljerad karakterisering av fibrerna, bland annat fördelningen av fiberegenskaper, skulle kunna förbättra möjligheterna att optimera den mekaniska massaprocessen, och därmed minska den totala mängden elektrisk energi som krävs för att nå en viss kvalitet på massan och den färdiga produkten. Det skulle resultera i både ökad konkurrenskraft och minskad miljöpåverkan.

I den här studien utvärderades relationen mellan fiberegenskaper i tre typer av mekanisk massa gjord på norsk gran (*Picea abies*), termomekanisk massa (TMP), slipmassa (SGW) och kemitermomekanisk massa (CTMP). Även fibrernas påverkan på labark, främst dragindex, för de olika massatyperna undersöktes. Studien resulterade i en jämförelsevis snabb metod för att karakterisera varje fibers förmåga att bidra till ark med högt dragindex. Metoden baseras på användning och hantering av rådata från en kommersiellt tillgänglig fiberanalysator (FiberLab™) och möjliggör utvärdering av hur fibrerna påverkas i varje del av den mekaniska massa-processen. Metoden har också möjlighet att appliceras som ett online-verktyg för att styra raffinerings- och massatillverkningsprocessen baserat på den slutliga massans egenskaper och den färdiga produktens kvalitet.

Långfiberfraktionen är viktig för den mekaniska massans kvalitet, och långfiberfraktioner från fem mekaniska massor från norsk gran (*Picea abies*) utvärderades: tre TMP, en SGW och en CTMP. Studien visade att fiberväggtjocklek och yttre fibrillering var de två fiberegenskaper som påverkade dragindex hos laboratorieark av långfiberfraktionen mest. Det var möjligt att prediktera dragindex för laboratorieark gjorda av långfiberfraktionen med linjärregression genom att kombinera fiberväggstjocklek och yttre fibrillering. Det predikterade värdet kallades *BIN*, en förkortning för "*B*onding ability *IN*fluence".

Predikteringen gav samma linjära korrelation mellan *BIN* och dragindex för 52 prover från de fem studerade mekaniska massorna, där varje massa hade fraktionerats till fem olika strömmar (plus injekt) i fullstora hydrocykloner. Bauer McNett fraktionerna P16/R30 (passerar en 16 mesh vira, retenderas på en 30 mesh vira) och P30/R50 användes till utvärderingen. Fibrerna från SGW hade tjockare väggar och högre uppmätt fibrilleringsgrad än de tre TMP och CTMP. Detta resulterade i att *BIN* och dragindex korrelerade på en annan nivå för P30/R50 fraktionen för SGW jämfört med alla de andra massafraktionerna. När *BIN* modellen baserades på medelvärden som var viktade med avseende på varje fibers väggvolym istället för på aritmetiska medelvärden, så reflekterades SGW-fibrernas tjockare väggar i medelvärdet och korrelationen var densamma mellan *BIN* och dragindex för samtliga massaprover (12 prover för att konstruera modellen och 46 för att validera den). Om *BIN* modellen används för att prediktera ett arks medelvärde av dragindex, så rekommenderas att basera modellen på väggvolymviktade data. För att göra viktade *BIN*-distributioner där inflytandet av varje fibers längd eller väggvolym tas i beaktande, så baseras *BIN*-modellen i nuläget på aritmetiska medelvärden av väggtjocklek och fibrillering.

När fibervidd togs med som en enskild faktor, minskade *BIN*-modellens noggrannhet. Väggvolym-viktade medelvärden av fibervidd kastade dessutom om ordningen mellan de fem hydrocyklon-strömmarna till den motsatta ordningen jämfört med aritmetisk fibervidd, för två av de fem massorna. När fibervidd kombinerades med väggtjocklek till faktorn ”collapse resistance index” ändrades ingen rangordning mellan aritmetiska och väggvolym-viktade medelvärden. För att undvika alltför stark inverkan av fiberväggtjocklek i fördelningar, och tills inverkan av fibervidd på *BIN* och hur fibervidd mäts är fullständigt utrett, rekommenderas att använda längdviktade eller aritmetiska fördelningar av *BIN* och andra fiberegenskaper.

En relativt snabb metod att utvärdera fördelningarna av väggtjocklek och fibrillering med hög upplösning visade att de tjockväggiga fibrernas väggtjocklek minskade när raffineringsenergin ökades i en dubbeldisk-raffinör i en kommersiell produktionslinje för TMP, som styrdes till fyra nivåer av specifik energiförbrukning. Detta var förväntat men kunde inte visas genom utvärdering av enbart medelvärden, och en slutsats av studien var att fiberegenskaper i många fall bör utvärderas som fördelningar och inte bara medelvärden.

BIN-fördelningar av olika typer av mekaniska massor från norsk gran visade förväntade resultat baserat på kännedom om massornas egenskaper och de processer som använts för att tillverka massorna. Det bekräftades också av mätningar på blandningar av två TMP för tidnings- respektive SC (super calendered) kvalitet. I blandningarna ökade mängden fibrer med högt *BIN*-värde när andelen SC-massa ökade. *BIN*-fördelningarna belyste också skillnader mellan

massorna som inte kunde observeras med medelvärden, till exempel att de två massor som tillverkats i raffinörer med konisk disk (CD-raffinörer) hade liknande form på *BIN*-fördelningarna, men på olika *BIN*-nivåer. Två massor som båda användes till SC-papper, en TMP och en SGW, hade liknande nivåer i dragindex men *BIN*-distributioner visade att SGW-massan innehöll en andel fibrer med väldigt lågt *BIN*-värde, något som kan påverka slutprodukten, till exempel arkets styrka, yta och struktur. Det här visar att *BIN*-modellen har potential att appliceras på hela eller delar av en papperstillverkningsprocess baserad på en mekanisk och kemimekanisk massatillverkningsprocess, där utvärdering av fördelningar av fiberegenskaper kan bidra till en ökad kunskap om processen och möjligheter att förbättra och optimera den.

TABLE OF CONTENTS

LIST OF PAPERS

The thesis is mainly based on the following papers, herein referred to by their Roman numerals. The papers were published in, or submitted to, peer-reviewed journals. The thesis also contains material which was not published elsewhere.

Paper I **Measuring the bonding ability distribution of fibers in mechanical pulps**
Reyier, S., Ferritsius, O., Shagaev, O.
TAPPI Journal, 2008, 7(12): 26-32

Paper II **The influence of mechanical pulp fiber dimensions on long fiber tensile index and density**
Reyier, S., Ferritsius, O., Ferritsius, R.
Nordic Pulp and Paper Research Journal, 2012, 27(5): 844-859

Paper III **Weighted averages and distributions of fibre characteristics of mechanical pulps – Part I: Various methods of weighting data from an optical analyser can give averages that rank pulps differently**
Reyier Österling, S., Ferritsius, O., Ferritsius, R., Stångmyr J.
Submitted to *Appita Journal*

Paper IV **Development of TMP fibers in LC- and HC-refining**
Ferritsius, R., Reyier Österling, S., Ferritsius, O.
Nordic Pulp and Paper Research Journal, 2012, 27(5): 860-871

Paper V **Weighted averages and distributions of fibre characteristics of mechanical pulps – Part II: Distributions of measured and predicted fibre characteristics by using raw data from an optical fibre analyser**
Reyier Österling, S., Ferritsius, O., Ferritsius, R., Johansson, C.A., Stångmyr, J.
Submitted to *Appita Journal*

AUTHOR'S CONTRIBUTION TO THE PAPERS

The author's contributions to the papers in the thesis are as follows:

Paper I	Planning for and participating in two pilot trials (hydrocyclone fractionation). Experimental work including preparation of pulp samples for analysis of cross-sectional SEM images and laboratory sheet characteristics by technicians at Stora Enso Research Centre, Falun, Sweden. Acoustic emission analyses were performed with assistance from Staffan Nyström, Mid Sweden University, and were compared to results of fracture toughness testing at PFI, Norway. Results from the acoustic emission analyses were evaluated and interpreted together with Professor Per Gradin and Professor Per Isaksson, Mid Sweden University, and Anders Hansson, at that time at Stora Enso Research Centre Falun. Interpreting results and writing the article together with Olof Ferritsius and Oleg Shagaev (formerly at Kadant Noss).
Paper II	Planning for and participating in three pilot trials (hydrocyclone fractionations). Experimental work including preparation of pulp samples for analysis of cross-sectional SEM images and laboratory sheet characteristics by technicians at Stora Enso Research Centre, Falun, Sweden. MorFi lab analyses were performed at CTP with assistance from Dr. Michael Lecourt, FCBA, Grenoble, France. Interpreting results, developing methods for *BIN* and writing the article together with Olof and Rita Ferritsius.
Paper III	Experimental work. Evaluating results and writing the manuscript together with Olof and Rita Ferritsius. Methods of weighting averages of fiber characteristics from the FiberLab analyzer were developed together with Christer A. Johansson and Jakob Stångmyr.
Paper IV	Limited parts of the experimental work, interpretation of results together with Rita and Olof Ferritsius. Writing the article together with Rita and Olof Ferritsius.
Paper V	Experimental work. Evaluating results and writing the manuscript together with Olof Ferritsius and Rita Ferritsius. Methods of producing distributions with high resolution of data of fiber characteristics from the FiberLab analyzer were developed together with Christer A. Johansson and Jakob Stångmyr.

RELATED MATERIAL

Results related to this work have been published and/or presented at international conferences as follows:

Ways to measure the bonding ability distribution of fibers in mechanical pulps
Reyier, S., Ferritsius, O., Shagaev, O. (2007)
Proceedings (article and oral presentation by co-author), *International Mechanical Pulping Conference*, Minneapolis, USA, May 6 – 9, CD-ROM, 15pp

Some aspects of fiber bonding ability in mechanical pulps
Reyier, S., Ferritsius, O., Shagaev, O. (2007)
Proceedings (extended abstract, presentation images and oral presentation), *PIRA International Refining & Mechanical Pulping Conference,* Arlanda, Sweden, December 12 – 13, CD-ROM, 19pp

BIN: A method of measuring the bonding ability distribution in mechanical pulps
Reyier, S., Ferritsius, O. (2008)
Proceedings (extended abstract, presentation images and oral presentation), *Fundamental Pulp Research Seminar,* Espoo, Finland, May 21 – 22, 11pp

BIN – A method to measure the distribution of fiber bonding ability
Reyier, S., Ferritsius, O., Ferritsius, R. (2009)
Proceedings (article and poster presentation), *International Mechanical Pulping Conference,* Sundsvall, Sweden, May 31 – June 4, pp. 292-297

The influence of process design on the distribution of fundamental fibre parameters
Ferritsius, O., Ferritsius, R., Reyier, S. (2009)
Proceedings (article and oral presentation), *International Mechanical Pulping Conference*, Sundsvall, Sweden, May 31 – June 4, pp. 160-168

The development of fiber characteristic distributions in mechanical pulp refining
Reyier, S., Ferritsius, O., Ferritsius, R. (2011)
Proceedings (article and oral presentation by co-author), *International Mechanical Pulping Conference,* Xi'an, China, June 27 – 29, pp. 40-43

Optimizing the process energy efficiency requires fast and accurate analysis of pulp quality – Do we have such?
Reyier Österling, S., Ferritsius, R., Ferritsius, O. (2013)
Proceedings (extended abstract, presentation images and oral presentation), *Fundamental Pulp Research Seminar,* Åre, Sweden, January 29 – 31, electronic archive at FSCN, Mid Sweden University, 39pp

PREFACE

This study was a co-operation between Stora Enso and the Mechanical Pulp Industrial Research College of Mid Sweden University, FSCN (Fibre Science and Communication Network), Sundsvall, Sweden. Financial support was given by the Swedish Knowledge foundation (KK-stiftelsen).

The project started as a master thesis study in October 2005 at the Royal Institute of Technology, Stockholm, Sweden, supervised by Professor Mikael Lindström, Hans Ersson, development manager at Stora Enso Kvarnsveden mill, Borlänge, Sweden, and Olof Ferritsius, mechanical fiber research manager at Stora Enso Research Centre Falun, Sweden. In 2006 the project continued as an industrial licentiate project and after 2008 as a part-time industrial doctorate project performed parallel to work in the development department of Stora Enso Kvarnsveden mill / Stora Enso Printing and Reading R&D. The project was paused during 2012 and 2013 and resumed again in April 2014.

Supervisors in the doctorate project have been Professor Per Engstrand and Professor Hans Höglund, Mid Sweden University, FSCN, MSc Hans Ersson, former R&D manager at Stora Enso Kvarnsveden mill, MSc Olof Ferritsius, Mid Sweden University, FSCN (formerly at Pöyry AB and Stora Enso Research Centre Falun), MSc Rita Ferritsius, Stora Enso Kvarnsveden mill and Mid Sweden University, FSCN (formerly at Pöyry AB and Stora Enso Research Centre Falun) and Professor Per Gradin, Mid Sweden University, FSCN. In the last part of the study, supervisory tasks were mainly undertaken by PhD Mats Rundlöf, Capisco.

Hydrocyclone fractionations took part at Kadant Noss, Norrköping, Sweden. Laboratory evaluations and trials were mainly performed at Stora Enso Research Centre, Falun, and Stora Enso Kvarnsveden Mill. Supplementary and comparing testing was performed at Mid Sweden University, Sundsvall (acoustic emission), Innventia, formerly STFI-Packforsk, Stockholm, Sweden (Simons' Staining), Paper and Fiber Research Institute, PFI, Trondheim, Norway (fracture testing of long fiber Formette sheets in connection to acoustic emission testing) and Centre Technique du Papier, CTP, Grenoble, France (MorFi Lab and CyberBond evaluations).

Maybe you will only read a few pages of this thesis, and that is okay.

Just promise that the next time you hold a magazine, paperboard product or newspaper in your hands you'll take some time to admire the fibers in it.

They are worth it.

1. INTRODUCTION

Mechanical pulps are used in paper products such as magazine or news grade printing papers or paperboard. These pulps are often produced from slow-growing spruce trees of forests in the northern hemisphere resulting in long, slender fibers that are well suited for mechanical pulp products (Wood and Karnis 1991). The northern countries Sweden, Finland, and Norway are important producers of wood based products. Access to wood raw material, water and relatively cheap electrical energy have resulted in a long pulp and paper industry tradition and Sweden is a large net exporter of pulp and paper. The export value of forestry products in 2013 was SEK 120 billion ($120 \cdot 10^9$), about 12.6 billion Euro. In 2013, Sweden produced 10.8 million ($10.8 \cdot 10^6$) tons paper and 11.7 million tons pulp, of which three percent was made from mechanical and chemimechanical pulp, corresponding to 9.7% of the total world production of mechanical pulp in 2012/2013. (Source: Skogsindustrierna.org).

Mechanical pulping gives a high yield; nearly everything in the tree except the bark is used in the paper. This means that mechanical pulping consumes much less wood than chemical pulping, especially to produce a unit area of printing surface. The pulp used for producing printing paper is mainly manufactured by thermomechanical pulping, TMP, in which the separation of the fibers from the wood matrix is achieved by mechanical forces at high temperature and steam pressure. This requires large amounts of electrical energy and generally, higher specific energy consumption leads to higher sheet strength (Liimatainen *et al.* 1999, page 124). In order to keep cost and environmental impact as low as possible, all mills producing mechanical pulps are trying to optimize their processes with respect to the total electric energy consumption in producing one ton of pulp of a specified quality. The general principle of steering a refiner with respect to pulp- and fiber characteristics is outlined below, Figure 1.1.

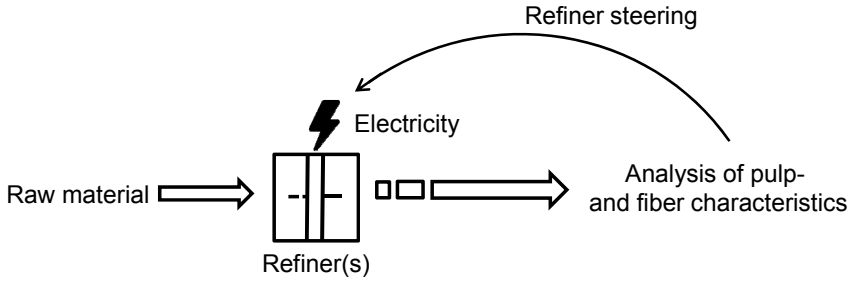

Figure 1.1. In order to separate the fibers from the wood matrix and treat the walls and surfaces of these fibers, electric energy is required. The refining process is continuously steered to produce a pulp which fulfills the requirements of fiber characteristics set by the final product, at the lowest possible specific energy consumption.

The average specific energy consumption for paper production in Sweden is close to 1750 kWh per ton paper (Source: Skogsindustrierna) for all fiber based paper qualities, chemical as well as mechanical pulps. Mechanical and chemimechanical pulps are commonly produced with an electric energy input of 1000 to 3000 kWh per ton pulp, depending on the product type and requirements of the final product. Naturally, the electric energy is one of the biggest costs for TMP mills. Energy is recycled from the TMP processes and the excess heat is often used for *e.g.* district heating. Steam from the TMP process is also utilized for drying the sheet on the paper machines in integrated pulp- and paper mills, but to decrease the total energy consumption in manufacturing TMP is a mill top priority. The mechanisms of mechanical pulp refining are complex and by no means fully understood, which makes optimization of the process with respect to electrical energy consumption to a given quality even more challenging.

Mechanical pulping results in long fibers having intact fiber walls, small particles coming off the fiber wall, fines, and also in larger fragments and broken parts of fibers. All parts of the mechanical pulp are important for the final product, but it has been shown that the long fibers of a pulp set the level of the total pulp strength (Lindholm 1980, Corson 1980, Lindholm 1983, Mohlin 1989, Rundlöf 2002, page 14).

The product group "printing paper" refers to papers printed in continuous printing presses used for newspapers, glossy journals, magazines or similar products. To withstand the forces of the printing press without breaking, the sheet strength is vital. Other requirements for printing paper are brightness/whiteness and surface properties well adjusted for the printing technique of the specific product, to ensure good reproduction of printed text and images as well as opacity to allow double-sided printing. Printing paper of low grammage may be as thin as three fibers in thickness, and every fiber's influence on the fiber network may therefore be high.

In order to know that the right level of fiber treatment has been reached in manufacturing TMP, evaluations of pulp and fibers are made both on-line and in the laboratory. Mechanical pulp fiber dimensions, for example fiber wall thickness, show wide distributions due to both raw material inhomogeneity and the mechanical pulping process. Despite the large differences in fiber geometry found in pulp produced from northern hemisphere wood and the effect the pulp fibers have on the final product, evaluations of fiber characteristics in an intermediate or final pulp are mainly focused on averages, such as the average fiber width. Moreover, the important fiber characteristics wall thickness and external fibrillation are seldom used in continuous fiber evaluation, probably due to challenges in the measurement techniques.

The background of this study was that average values of fiber dimensions may not fully characterize a mechanical pulp with respect to the fibers' ability to form sheets of high strength, and that a method to evaluate distributions of fiber dimensions would contribute to a more profound knowledge about each stage in a mechanical pulping process. To be able to evaluate how various fiber types develop in a process stage, rapid methods are needed to evaluate distributions of fiber characteristics. Below are some examples of a wide range of process related questions all of which need such methods to be answered, both for fine tuning and re-designing existing processes and for optimizing the functionality of new pulping lines:

Example 1. Which fibers were affected by the increased specific energy input in a given refining stage? Was the wall thickness of the thick-walled fibers causing harm in the printing paper surface really reduced, or did the increased energy result in more treatment of the already thin-walled fibers? Was it then worth the cost of increasing the electrical energy consumption?

Example 2. The average fibrillation index seems to have increased after the reject refiner and the average fiber wall thickness decreased, just as intended. Which fiber types were affected? All fibers equally or thin-walled more than thick-walled or *vice versa*? Would it be more energy efficient and beneficial to final product quality to separate the thick-walled and the thin-walled fibers and use them for different products, than to try to refine them together?

Example 3**.** How efficient was each screening stage in separating thick-walled fibers from thin-walled and fibers of high fibrillation from fibers of low fibrillation? Was the screening efficiency influenced by operation adjustments?

Example 4. What ratio between bulky and collapsed fibers resulted in the best final product quality? How was this ratio affected by changes in refining operations?

Attempts at answering these questions and many more could bring us closer to understanding more of the fundamentals of each stage in the refining process, and increase the chances of reducing the total energy consumption in producing mechanical pulps.

1.1 Objectives of the study

The overall aim of this study was to contribute to more efficient mechanical pulping, *i.e.* to be able to produce a final product of a given quality at the lowest possible total specific energy consumption. This may be achieved by a more detailed assessment of "pulp quality" which then could enable control of the process to produce a specified pulp quality. More accurate assessment of the pulp quality also provides increased knowledge of the different process stages in a mechanical pulping line which is valuable in designing or re-designing the line and enables optimization of the process with respect to both quality and use of electric energy.

The purpose of this study was to extract information about mechanical pulp quality from optical measurements and image analysis of individual fibers in a pulp suspension and to find out if this provides more useful information than traditional testing methods and analyses resulting in mean values.

The objectives were:

1. To identify which geometrical fiber dimensions that influence the tensile index of laboratory sheets made from various long fiber fractions of mechanical and chemithermomechanical pulps made from Norway spruce (*Picea abies*).
2. To evaluate to what extent the information from individually measured fibers, combined into a model, can be used to predict pulp properties.
3. To develop a rapid method that easily and with high resolution shows distributions of measured and modelled fiber characteristics. This approach could eventually provide measures of pulp quality useful for controlling the process.

1.2. Summary of papers

Figure 1.2 below contains a summary of the main content of the five papers and the objectives which were addressed in each paper.

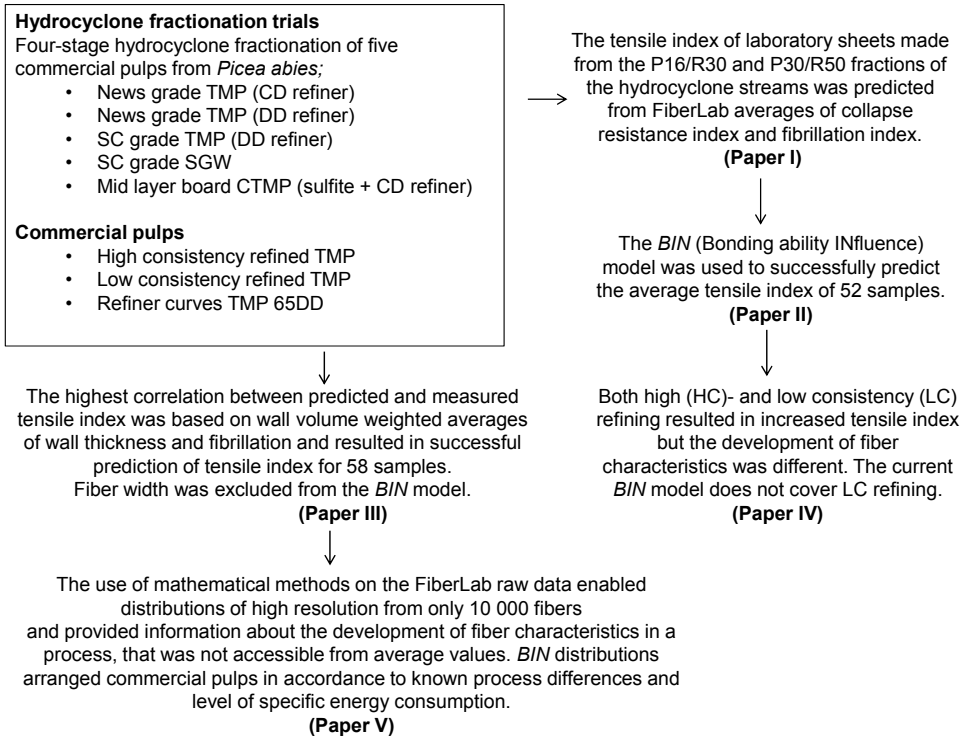

Figure 1.2. Overview of the contents of the five papers.

Paper I contains results from two of the five hydrocyclone fractionation trials. It shows that the tensile index of handsheets made from long fibers (Bauer McNett P16/R30 fractions) of two TMPs could be predicted from FiberLab data, *i.e.* averages of collapse resistance index and fibrillation index. Also the P30/R50 fractions of the two TMPs fit in the same model. The predicted tensile index in combination with the amount of pulp fraction per hydrocyclone stream was used to form "distributions" containing a few points. Acoustic emission was used to characterize these sheets by recording acoustic events during tensile testing. This seemed to reveal information about the fracture process of these sheets that could not be seen using traditional testing methods, in addition the fracture toughness could be predicted based on data from the acoustic emission. This paper refers to objective 1.

Paper II was based on results from all five hydrocyclone fractionations using three TMPs, one SGW and one CTMP. This paper showed that the tensile index of the Bauer McNett fractions P16/R30 and P30/R50 was positively influenced by

fibrillation index and negatively by arithmetic averages of fiber wall thickness index, fiber width index and collapse resistance index. The predicted tensile index was denoted *BIN* (*B*onding ability *IN*fluence). The *BIN* model was calculated from arithmetic averages based on collapse resistance index and fibrillation index data of individual fibers from twelve samples of the P16/R30 fractions of hydrocyclone fractionated TMP. Forty-six samples from the P16/R30 and P30/R50 fractions were used for validating the model. Neither collapse resistance index nor fibrillation index was sufficient to form a correlation on the same level for all pulps, but the two measures needed to be combined. Only the samples from the SGW P30/R50 fractions were slightly outside the *BIN* model. Results from the FiberLab analysis were compared to results from cross-sectional analysis of scanning electron microscope (SEM) images and results from the MorFi Lab fiber analyzer. There was a high correlation for fiber width between results from the MorFi and FiberLab analyzers, but the SEM method was not accurate enough to distinguish the small differences in fiber width between the pulp fractions evaluated. It is possible that too few fibers (600 – 1200) were used in the SEM method. For fiber wall thickness, the FiberLab and the SEM methods correlated but at different levels for different pulp types. In the FiberLab results there was a small but consistent difference in the fiber wall/width ratio between the P16/R30 and P30/R50 fractions. At a given fiber width index the fiber wall thickness was higher for the P30/R50 fraction than the P16/R30 fraction. This paper refers to objectives 1 and 2.

Paper III contains results from different methods of weighting averages of fiber characteristics. The *BIN* model and the hydrocyclone fractionated pulps were used as references, and the prediction of tensile index for the long fiber fractions P16/R30 and P30/R50 was made for arithmetic, length weighted, wall volume weighted and length^2 weighted averages of cross-sectional fiber dimensions from the FiberLab analyzer. Length^2 weighed averages are sometimes used as a measure of weight weighted data when the fiber volume is not available, based on the assumption that the coarseness of a fiber is proportional to its length. It was found that length^2 weighted averages of cross-sectional fiber dimensions correlated poorly to wall volume weighted averages, at least when different pulp types were evaluated. Wall volume weighted averages of fiber wall thickness and fibrillation indices resulted in the most accurate prediction of long fiber tensile index in the *BIN* model. If the *BIN* model is used for predicting averages of tensile index, a model based on wall volume weighted averages is recommended. The length^2 weighted averages gave *BIN* models of poor correlation to long fiber tensile index due to too high dependency on fiber length. For two of the five pulps, the ranking in fiber width of the five hydrocyclone streams changed to the complete opposite when the averages were wall volume weighted compared to arithmetic. When fiber width was combined with fiber wall thickness into collapse resistance index,

no rankings changed. The *BIN* model was found to be more accurate when fiber width was not included as a single factor. This paper refers to objectives 1 and 2.

Paper IV shows results from evaluations of changes in sheet properties and fiber dimensions over a high (HC)- and a low consistency (LC) refiner. The evaluated LC refiner was placed in the main line after the primary stage HC refiner in a TMP process for news grade pulp. The tensile index increased both in HC and LC refining but the development of fiber characteristics as evaluated in a FiberLab analyzer was different. In HC refining, fiber wall thickness and fiber width indices decreased and fibrillation index increased which resulted in increased *BIN*. Over this LC refiner, fiber wall thickness and fiber width indices were unchanged or even increased, and fibrillation index was unchanged or decreased, quite the opposite to HC refining. As a result, *BIN* did not increase in LC refining despite the increased tensile index, the current *BIN* model was not applicable to LC refining. Fiber curl increased in HC refining but decreased in LC refining, hot disintegration prior to sheet forming resulted in the same decrease in curl index and increase in tensile index as in the LC refining. It is possible that the increased tensile index in LC refining may at least partly be a result of decreased curl. This paper also discussed the rather large variations in the results of physical testing of laboratory sheets. This paper refers to objectives 1 and 2.

Paper V shows that distributions of high resolution of *BIN* and other fiber characteristics can be made by applying a mathematical method (kernel density estimation, KDE, *via* diffusion mixing) to raw data from the FiberLab optical analyzer. These distributions can also be weighted by *e.g.* fiber length or wall volume without losing resolution. Distributions made with this method are easier to evaluate than histograms and also enables faster measurements, as fewer fibers are needed to reach sufficiently high resolution (10 000 fibers compared to 60 000). Distributions of fiber wall thickness from samples collected at different levels of specific energy in a commercial TMP process showed that the wall thickness of the latewood fibers was reduced with an increased specific energy input which could not be established from evaluations of averages values. Arithmetic and length weighted distributions revealed two peaks that represent early- and latewood fibers, whereas the earlywood peak quite naturally was diminished in wall volume weighted distributions. Until the influence of fiber width on the wall volume weighted distributions is fully evaluated, arithmetic or length weighted distributions are recommended. *BIN* distributions of non-fractionated mechanical pulps ranked the pulps in accordance with known process differences and the levels of specific energy consumption in producing the pulps. This paper refers to objective 3.

1.2.1 Outline of thesis

Section 1 contains an introduction to put the purpose of the study into a wider perspective and make it accessible also for scientists and engineers not familiar with the pulp and paper industry. A general background to wood fibers, mainly from Norwegian spruce, *Picea abies*, as a raw material, and brief introductions to the pulp and paper processes as well as a literature survey of relevant publications in the area of mechanical pulping are presented in **Section 2**. **Section 3** presents materials and methods used and evaluated in this work, for example the FiberLab optical analyzer which was used as the main equipment in the evaluation of geometrical fiber dimensions. **Section 4** contains a summary of the results of the five papers upon which this thesis is based as well as results that were not published elsewhere. Some results of the four-stage hydrocyclone fractionation that was used to broaden the range of the evaluated fiber characteristics are shown. This is followed by examples of how geometrical fiber dimensions influenced the tensile index of laboratory sheets differently for different pulp types but still resulted in a common model to predict tensile index based on fiber wall thickness and fibrillation. Distributions of analyzed and calculated fiber characteristics that to a higher extent than averages reveal how fibers develop in various process stages are shown, together with recommendations of how these distributions can be weighted. This section also contains discussions of the results as well as thoughts about the possibilities of using geometrical fiber dimensions to predict properties of sheets and final paper both off-line and on-line. **Section 5** contains conclusions for the areas in which this study was conducted. In **Section 6**, ideas and recommendations for future work are presented based on findings and thoughts that were outside the frames of this study but would be interesting to evaluate further.

Additional figures, tables and details of interest for the study are found in the **Appendices: Appendix A** contains results, process settings and calculations of the hydrocyclone fractionations, **Appendix B** contains different versions of the *BIN* model used to predict tensile index of laboratory sheets and **Appendix C** lists some statistics which were relevant in evaluating the methods used in this study.

2. BACKGROUND

2.1 Paper production

Paper is commonly produced from processed fibers. In manufacturing fiber based products, a diluted fiber-water dispersion (approximately 99% water), most often containing some additives, is sprayed upon the moving wire of the paper machine where the fibers form a network. The structure and character of the sheet is set already in the forming section. By different methods of pressing and drying, the dry content is increased to approximately 92% in the end of the paper machine. Figure 2.1 below shows an outline of a paper machine producing printing paper. The forming, pressing and drying sections of the paper machine are marked in the image.

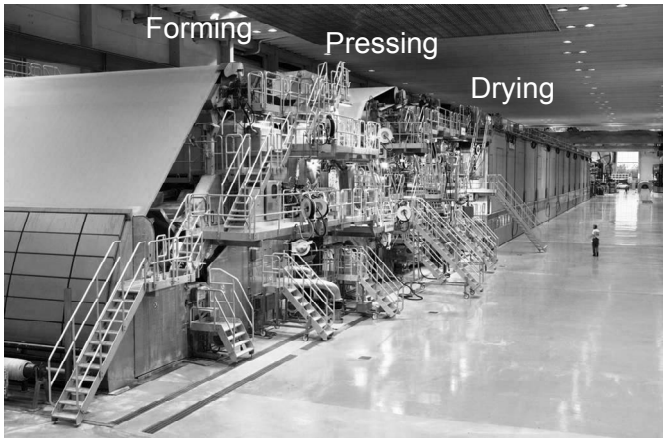

Figure 2.1. A paper machine producing printing paper with marked forming, pressing and drying sections. Photo: Lasse Arvidsson ©Stora Enso.

2.2 Mechanical pulping

Fibers need to be separated from each other and made suitable for making the final product. In chemical pulping, fibers are separated from each other by chemically dissolving the middle lamella which functions as a glue between fibers. In mechanical pulping; mechanical forces acting upon the wood chips (or roundwood) results in both separation of the fibers (defibration) and further treatment of the fibers, such as peeling of the fiber surfaces (fibrillation). Mechanical pulping results in a distribution of different particle sizes, from intact fibers to broken fibers and smaller fragments peeled off the fiber wall (fines) and a distribution in fiber wall thickness and fiber width. In producing mechanical pulp, nearly all components in the native wood except the bark are maintained in the pulp, with an overall yield of about 97%. As a comparison, the chemical pulping yield is typically 50%.

This study includes three mechanical pulp types: stone groundwood pulp, SGW, thermomechanical pulp, TMP, and chemithermomechanical pulp, CTMP, which is a chemically pretreated TMP. The SGW, TMP, and CTMP processes result in fibers of different characteristics which are exemplified in the following section by micrographs together with the general concept of each process.

2.2.1 Groundwood pulp, SGW

In the groundwood process, logs are pressed against a rotating grindstone together with hot water and pulp is formed by tearing the fibers from the logs. The SGW in this study was produced by grinding under atmospheric conditions in which the process water temperature is usually around 75 °C. Figure 2.2 below shows an outline of a grinder used in the groundwood process (Liimatainen *et al.* 1999, page 110).

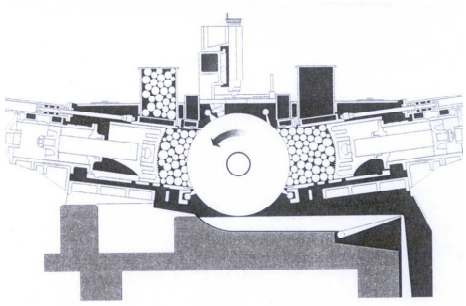

Figure 2.2. Outline of an atmospheric grinder (Liimatainen *et al.* 1999, page 110). Logs and hot water are pressed against a rotating grindstone which tears the fibers from the log.

Figures 2.3a-d show scanning electron microscope (SEM) images of groundwood fibers. The torn and broken fibers and the high content of fibrils are typical for SGW fibers, as are the fully collapsed fibers that the micrographs below illustrate.

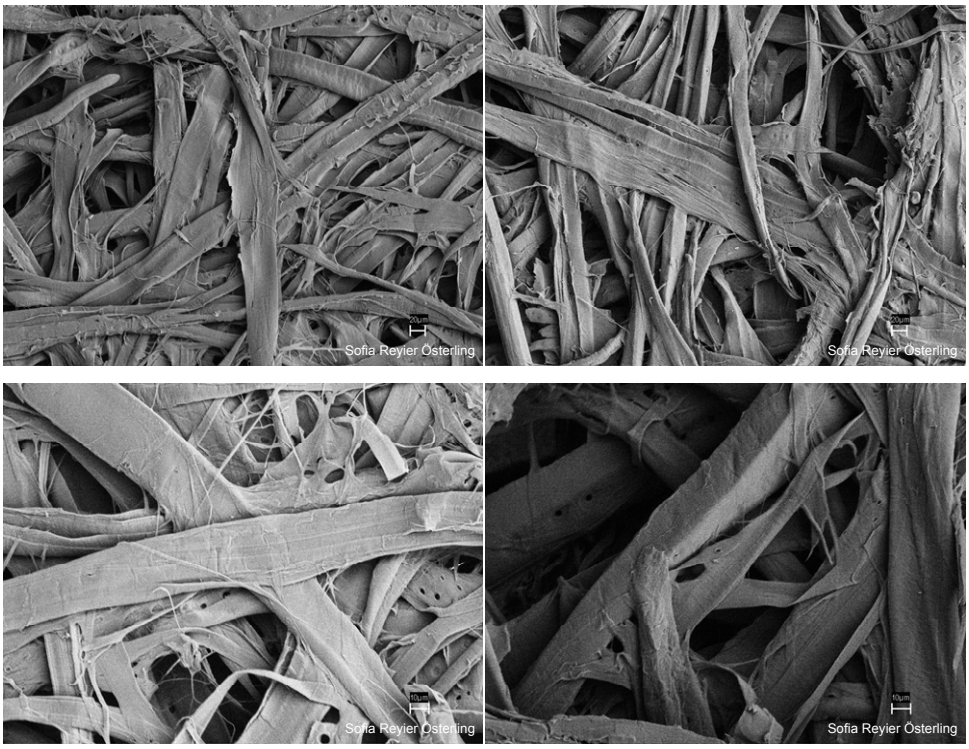

Figure 2.3a-d. SEM micrographs of SGW fibers from an atmospheric Tampella process. The micrographs are made from laboratory sheets of the long fiber fraction P16/R30. The high degree of fiber treatment is typical for groundwood pulps. The micrographs represent 600x (a-b) and 1500x (c-d) magnification.

2.2.2 Thermomechanical pulp, TMP

In the TMP process, washed and pre-steamed wood chips are refined between two metal discs with a pressurized, narrow space between them, one disc or both discs are rotating. On the refiner discs, steel segments with a grooved pattern are mounted, *cf.* Figure 2.4b. Chips are fed into the center of the refiner disc, into the breaker bar zone, from which the segments on the rotating disc(s) by means of steam dynamics feed fibers and steam produced in the refiner gap towards the periphery of the refiner. The refiner is pressurized by saturated steam, usually to 0.2 – 0.4 MPa, corresponding to a temperature of 130 – 150 °C. The high temperature softens the wood lignin, a polymer that is stiff at room temperature. The middle lamella which holds the fibers together in the wood have the highest lignin concentration of all layers of the fiber wall, around 70% according to Panshin and DeZeeuw (1970, page 91) and the softening of the lignin simplifies the release of fibers from the wood.

Either one [single disc (SD)] or both [double disc (DD), counter rotating] refiner discs rotate by the force of one (SD) or two (DD) motors. This study also contains results from a conical disc (CD) refiner process, in which a single disc refiner has both a flat and a conical zone. It has been reported that TMP produced from double disc refiners has higher density and tensile index at a given specific energy consumption and higher light scattering coefficient at a given tensile index than single disc refiners (Falk *et al.* 1987, Ferritsius *et al.* 1989, Wedin *et al.* 1992, Sundholm *et al.* 1987). Kure *et al.* (1999b) also found that double disc refiners resulted in fibers of thinner walls than single disc refiners, compared at a given specific energy consumption and rotational speed, and a higher degree of fiber splitting compared to single disc refiners. High fiber split is reportedly favorable for paper surface smoothness (Reme *et al.* 1998) and light scattering (Reme and Helle 2001).

The defibration mainly occurs in the refiner center and the development of the fiber wall, fibrillation, continues throughout the refiner when the fibers are sheared against other fibers and segment bars. At the refiner disc periphery, the pulp is emitted containing fibers and fragments of fibers of various lengths, geometry, flexibility and state of fibrillation as well as fines of different character. Some bundles of fibers may still remain in the pulp. These are called "shives" and are treated further in the process (Hill *et al.* 1975).

Refiners require large amounts of electrical energy, even if parts of the energy can be recovered as stream. A large conical disc refiner has for example a 26 MW motor to rotate the disc at 1800 rpm (Tienvieri *et al*. 1999, page 175) and a 68" double disc refiner can rotate its two discs at 1800 rpm in opposite directions with a total motor power of 25 MW (Tienvieri *et al*. 1999, page 179). Figure 2.4a below to the left shows a 68" double disc refiner and Figure 2.4b shows the grooved pattern of refiner plate segments. The pattern becomes finer towards the periphery.

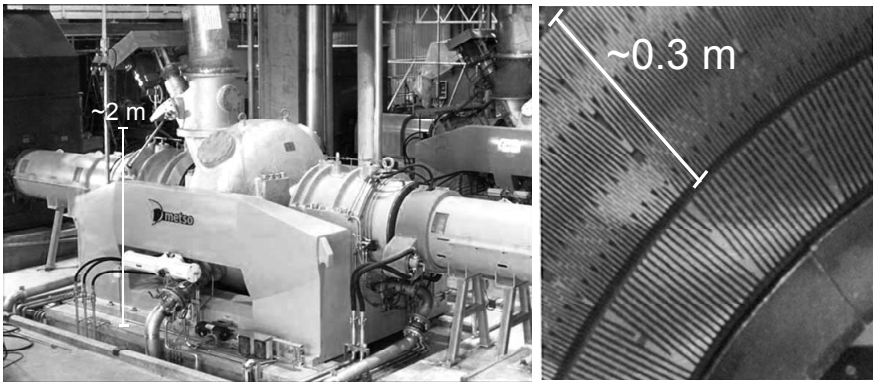

Figure 2.4a-b. A RGP DD68 refiner (left) and an example of the grooved pattern of refiner plate segments (right).

Figures 2.5a-d show SEM images of TMP fibers from a double disc refining process. Long, slender fibers with high fibrillation can be observed and the fibers retain their tubular shape to a higher degree than SGW fibers, *cf.* Figures 2.3a-d above.

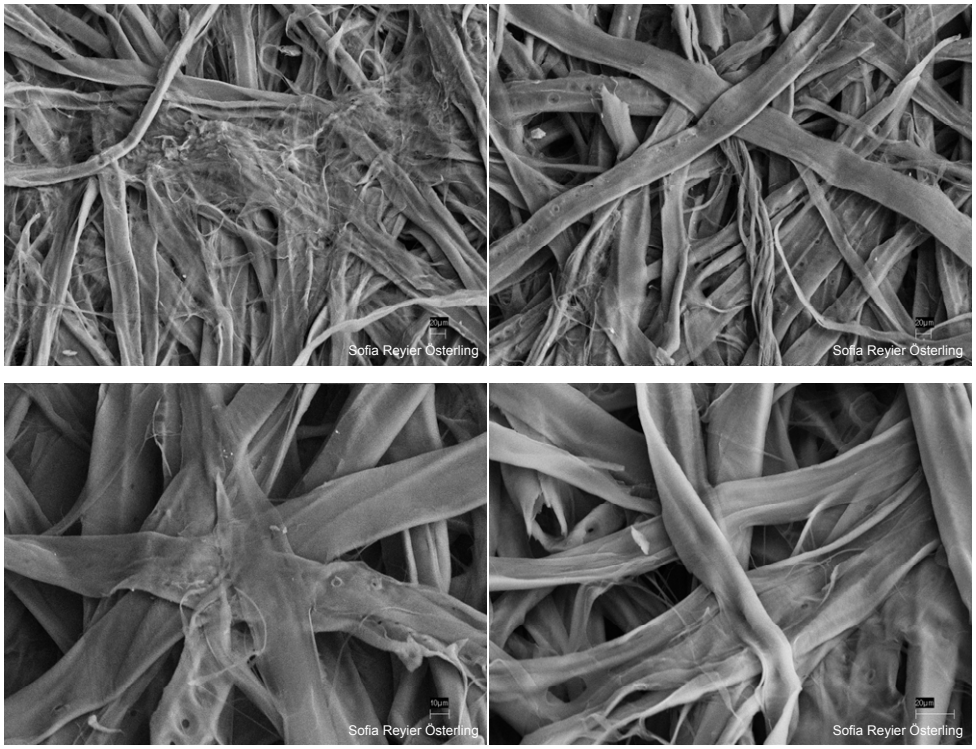

Figure 2.5a-d. SEM micrographs of TMP fibers from a double disc refining process. The micrographs are made from laboratory sheets of the long fiber fraction P16/R30. The high amount of long, yet flexible fibers with preserved cylinder shape compared to SGW fibers is typical for TMP. The micrographs represent 600x (a-b) and 1500x (c-d) magnification.

Pulp refining at low pulp consistency, LC refining, is performed at approximately 4%, compared to approximately 30% in high consistency refining. LC refining has been shown to increase the tensile index (see *e.g.* Musselman *et al.* 1966, Engstrand *et al.* 1988, Hammar *et al.* 1997, Hammar *et al.* 2010, Andersson *et al.* 2012) but does not seem to develop the fiber dimensions in the same way as high consistency refining (Lundin 2008, page 121).

2.2.3 Chemithermomechanical pulp, CTMP

Chemithermomechanical pulp, CTMP, is produced from chemically pretreated chips processed in refiners. The CTMP evaluated in this study was intended for the middle layer of paperboard, where a high bulk is desired.

Sodium sulfite is a common pretreatment chemical. The chemical softening of lignin by sulfonation makes the defibration occur to a higher extent in the primary wall and middle lamella rather than deeper in the fiber wall as for TMP (Franzén 1986; Htun *et al.* 1993). CTMP fiber surfaces are therefore generally smoother with less fibrils and broken parts of the fiber wall than TMP or SGW fibers. The low extent of torn and broken fibers in CTMP results in higher long fiber content of these grades as compared to TMP intended for printing paper. The chemical pretreatment also enables separation of the fibers from their wood matrix with lower electrical energy input compared to TMP.

Figures 2.6a-d below show some examples of SEM micrographs of CTMP fibers intended for the middle ply in paperboard. The chips were treated with sodium sulfite and refined in CD refiners. The bulky network of mainly unbroken fibers with smooth surfaces with a low degree of external fibrillation compared to TMP or SGW is typical for fibers manufactured in a CTMP process.

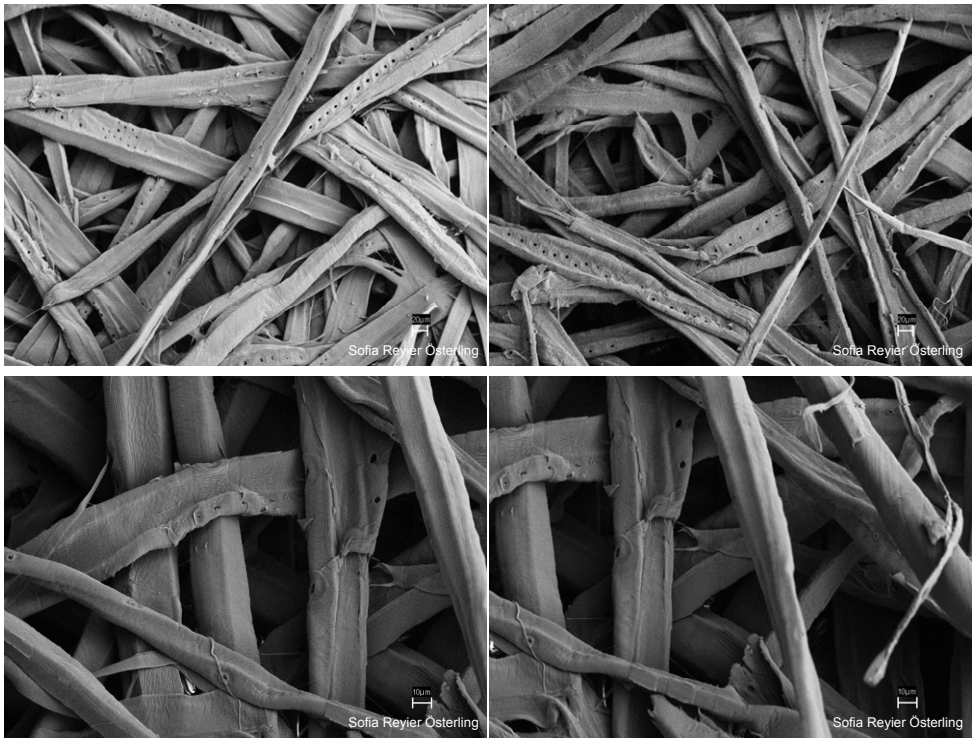

Figure 2.6a-d. SEM micrographs of CTMP fibers intended for the middle layer in paperboard, from a process of pre-treatment with sodium sulfite followed by refining in conical disc refiners. The micrographs are made from laboratory sheets of the long fiber fraction P16/R30. The high amount of unbroken fibers with smooth surfaces is typical of CTMP fibers intended for bulky products. The micrographs represent 600x (a-b) and 1500x (c-d) magnification.

2.2.4 Fiber development in mechanical pulping

In the refining process, the fiber wall of single fibers is peeled. As a consequence, the width and wall thickness of the fiber is reduced (Karnis 1994). This increases the flexibility of the fiber wall and often results in some shortening of the fibers. A refined pulp contains single fibers of different lengths and cross-sectional dimensions. Two or more fibers still attached to each other, shives, are non-beneficial for the strength- and surface characteristics of a sheet (MacMillan *et al.* 1965, Sears *et al.* 1965, Ferritsius and Rautio 2007). Gregersen *et al.* (2000) showed that the majority of the shives that induced cracks in a sheet were latewood shives oriented across the strain direction of the tested specimen.

Depending on how deep into the multi-layered fiber wall the peeling went, the surface characteristics of fibers can differ and various process types typically result in different fiber wall layers dominating the fiber surfaces (Franzén 1986; Htun *et al.* 1993). The material peeled off the fiber wall becomes either fine material that is separated from the fiber, fines, or fibrils that remain attached to the fiber surface. Fibrils still present on the fiber surface can be evaluated as the degree of external fibrillation. The nature of the pulping or grinding results in different character and shape of the peeled-off fiber wall material (Heikkurinen 1993, Fernando and Daniel 2004). A mechanical pulp intended for printing paper typically consists of about 30% fines which function as bridging material between the fibers and is important for optical properties such as light scattering (Lindholm 1980). Mohlin (1980) showed that fines and fibers interact so that the strength of a sheet made from a whole pulp is higher than the sheet strength of the various size fractions of the same pulp. Figure 2.7 below outlines the multi layered fiber wall and the fine material that is produced during refining (Rundlöf 2002, page 9).

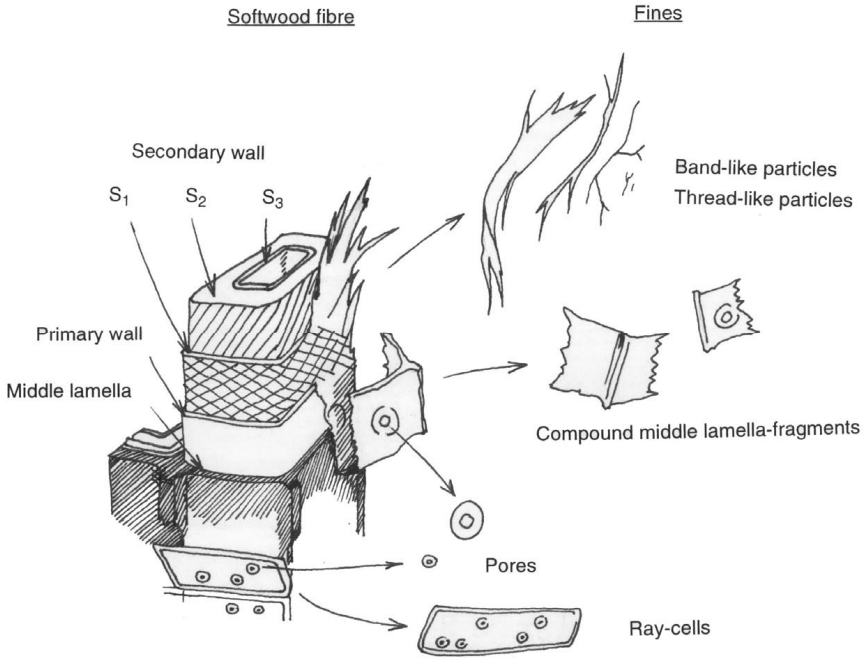

Figure 2.7. Fibers are held together in the wood by the middle lamella and the fiber wall consists of a primary wall and three layers of secondary wall; S1, S2 and S3. The figure shows an outline of the fiber wall layers and the peeling of the fiber wall that occurs in the refining process. The image is reproduced from Rundlöf (2002, page 9).

2.2.5 Quality assessment of mechanical pulps

The quality of mechanical pulps is traditionally evaluated by collecting pulp samples in selected positions along the process, and by making and testing handsheets in the laboratory. If focus is put on the characteristics of fibers of a particular length fraction, the pulp can be separated by screening before the sheets are made and tested. This traditional testing can provide an overview of the efficiency of the process and gives access to historical data which can be helpful in backtracking when and why changes in pulp quality began. The results of the testing of laboratory sheets can also be used for evaluating the effect of deliberate changes to the process.

The common testing of a laboratory sheet includes mainly measures of strength, structure and optical properties (including calculated light scattering and light absorption coefficients). Tensile index is one important measure used to characterize the strength of laboratory sheets and the final paper. It is generally established that increased refiner energy increases the tensile index of sheets made from mechanical pulps (Liimatainen *et al.* 1999, page 124). In order to produce a mechanical pulp of a given tensile index as energy efficiently as possible, an

increased knowledge is needed of which fiber characteristics that influence tensile index and how these fiber properties are influenced in different stages of the pulping process.

2.2.6 Demands on mechanical pulp

The final paper needs strength to withstand the large forces of the printing press, opacity to avoid print-through and sheet surfaces adjusted for the selected printing technique. One of the most important characteristics of mechanical pulps intended for printing paper is brightness and high opacity (evaluated as light scattering) at a given strength (Höglund 2002). Reme *et al.* (1999a) stated that pulp intended for calendered printing paper of high quality should contain easily collapsible fibers with thin walls and highly fibrillated surfaces. At the same time, the fiber length should be as well preserved as possible and the number of latewood shives should be kept low.

The high fiber stiffness and the high content of long fibers make mechanical pulp beneficial to be used as the middle layer in board (Fineman 1985, Bengtsson 2005). In using mechanical pulp for middle layer in paperboard, strength at a given bulk is one of the most important requirements. Höglund (2002) concluded that the best mechanical or chemimechanical pulp for the middle ply is one that gives the best combination of bulk and internal fiber – fiber bond strength. In practice, this would be evaluated as Scott-Bond strength at a given sheet density.

2.2.7 Characteristics of mechanical pulps

The mechanical pulp consists of both fines and fibers of various lengths and it has been reported that the characteristics of a mechanical pulp are to a large extent set by the character of the fibers. It has been shown that the fiber fractions set the ranking of various mechanical pulps with respect to light scattering coefficient and that the ranking remains when fines are added (Corson 1980, Lindholm 1980, Rundlöf *et al*. 1995, Rundlöf 2002, page 10). Rundlöf also showed that the tensile index increased with increasing proportions of fines but that the ranking of mechanical pulps with respect to tensile index was set by the fibers (Rundlöf 2002, page 14) as shown in Figure 2.8 below.

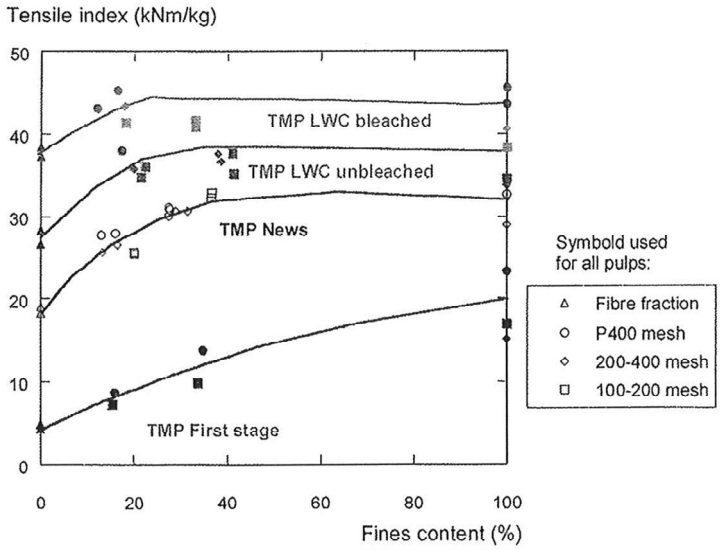

Figure 2.8. The internal ranking of various mechanical pulps with respect to tensile index remained when fines were added to the pulps. This showed that the character of the pulps was set by the fibers, not the fines. From Rundlöf (2002, page 14).

Mohlin (1989) concluded that at fines levels above 20-25%, the tensile index of a sheet becomes independent of average fiber length and depend only on fiber bonding ability (the notation "fiber bonding ability" is discussed in Section 2.4.3). Lindholm set this level to approximately 40% (Lindholm 1980) and concluded that the long fiber and fines fractions were the most important for changing the characteristics of mechanical pulps whereas the middle fraction did not change any rankings of sheet characteristics (Lindholm 1983). This is in line with results by Corson (1980) who showed that increased refining of the long fiber fraction increased the quality of the whole pulp. Jackson and Williams (1979) identified the long fiber fraction of TMP as the limiting factor for the strength of the whole pulp, and suggested that refining should be focused on this fraction.

2.3 Variations in the characteristics of the wood raw material

Wood can roughly be divided into two groups; softwoods (generally conifers) and hardwoods (generally deciduous trees). As the name suggests, most hardwoods have higher density than softwoods and structural and chemical differences make hardwood- and softwood fibers suitable for different end products. This study was based on conifers, more specifically Norway spruce, *Picea abies*. The correct denotation of a softwood fiber is tracheid but throughout this work, the more general term "fiber" is used.

2.3.1 Intrinsic geometrical fiber characteristics

Spruce fibers are typically cylinder shaped with a length to diameter ratio of about one to one hundred. The multi layered fiber wall encloses the cavernous lumen in the middle of the fiber (*cf.* Figure 2.7). Fibers have closed ends and liquid is transported between fibers through bordered pits. Apart from tracheids, other cell types are present in the wood, for example parenchyma cells and ray tracheids. These cell types were not further discussed or evaluated in this study. Table 2.1 shows mean values and natural variations of length, width, and wall thickness of fibers from Norway spruce, *Picea abies* (Trendelenburg and Mayer-Wegelin 1955, Höglund and Wilhemsson 1993, Sjöström 1993).

Table 2.1. Range of length, width and wall thickness of fibers from Norway spruce (*Picea abies*). The parentheses represent average values. Summarized from Trendelenburg and Mayer-Wegelin (1955), Höglund and Wilhemsson (1993) and Sjöström (1993).

Picea abies	Length, mm	Width, µm	Wall thickness, µm
Range[1]	1.1 – 6.0 (3.4)	21 – 40 (31)	
Range[2]		5 – 50	1 –8
Range[3]	2 – 4 (3.2)	20 – 40	2 – 4 (earlywood) 4 – 8 (latewood)

[1]*Trendelenburg and Mayer-Wegelin 1955, page 140*
[2]*Höglund and Wilhemsson 1993*
[3]*Sjöström 1993, page 9*

The seasonal differences of the northern hemisphere result in large variations in fiber growth and consequently variations in fiber geometry. Earlywood fibers grow in the early growth season of the tree and are designed to prioritize transport of fluids and nutrition. These fibers have a typical geometry of thin walls, large diameters and large lumens. Latewood fibers specialize in maintaining the tree structure and have thicker fiber walls, smaller diameters and smaller lumens than the earlywood fibers. The seasonal sequences of the bright earlywood fibers and the dark latewood fibers are seen as annual rings in a cross-section of a log, Figure 2.9. The fiber growth over a year can be followed from the left to the right in the micrograph in Figure 2.9 (micrograph from Ilvessalo-Pfäffli 1995, page 17) and clearly shows the differences between the geometry of fibers that grew early and late in the season.

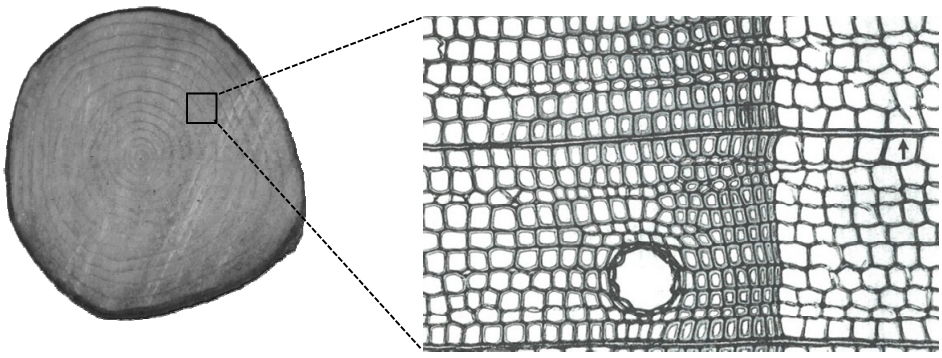

Figure 2.9. The cross-section of a Norway spruce (*Picea abies*) stem clearly shows the differences in fiber geometry between fibers that grew early and late in the growth season. The latewood fibers have a smaller diameter and thicker wall than the earlywood fibers and are seen as dark annual rings. The brighter wood consists of earlywood fibers with a larger diameter, thinner wall and larger lumen area compared to the latewood. The micrograph from Ilvessalo-Pfäffli (1995, page 17) is a magnification of one annual ring illustrating the growth from left to right over one year. Rays are seen horizontally across the micrograph and the cross-section of a circular resin canal is also included in the image.

The fiber wall thickness of earlywood fibers of Norway spruce is 2 - 4 μm compared to 4 - 8 μm for latewood (Sjöström 1993, page 9). Early- and latewood behaves differently during compression (Salmén *et al.* 1997) and sapwood specimen made from early- and latewood fibers of Norway spruce revealed differences in both compression and shear behavior (Svensson 2007, pages 66, 67). It has been shown that two pulps produced from early- and latewood fibers of the same wood but separately refined, resulted in different sheet properties (Huang *et al.* 2012) and that early- and latewood fibers respond differently to refining. For example, a higher degree of fiber splitting has been reported for earlywood fibers than for latewood fibers (Reme and Helle 2001).

The geometry of fibers grown in the transition period between early- and late growth can contain a mixture of characteristics typical for those of early- and latewood fibers, resulting in fibers of large diameters in combination with thick fiber walls. Due to their special geometry, the transition wood fibers were identified as the possible cause of moisture-induced "decollapse", spring-back of collapsed fibers, which can cause disturbances in the surface of printing papers (Norman and Höglund 2003).

The growth conditions of the tree affects the fiber morphology (see *e.g.* Tyrväinen 1995) and it is well established that the age of the tree, the position of the fiber in the tree, the tree's growth rate, surroundings and access to water and nutrition affects the geometrical characteristics of fibers. In addition to the differences in

fiber geometry induced by seasonal variations, this explains why the raw material used for producing mechanical pulps of wood from the northern hemisphere contains fibers of a wide range of geometrical characteristics.

2.4 Characterization of pulp fibers

2.4.1 The effect of fiber characteristics on sheet strength and structure

Forgacs (1963) stated that the cohesion in papers made from mechanical pulp is largely provided by cell wall fragments. He reasoned that the long fibers in papers made from mechanical pulps have the same function as steel reinforcements in concrete; to strengthen the structure of the material, and underlined the contribution the long fibers give to the total sheet strength. This is emphasized by the results shown in Figure 2.8 (Rundlöf 2002, page 14), where several samples had high tensile index already without added fines. Mohlin continues the same reasoning and concluded that the long fibers of intact walls had low strength, but contributed to the strength of the whole pulp by distributing the stresses in the sheet (Mohlin 1980). Forgacs (1963) identified the external surface of the fibers as important for inter-fiber bonding, and showed that the specific surface of different Bauer McNett fractions correlated to the strength of handsheets. The specific surface was derived from measurements of water permeability of pulp beds. Forgacs also concluded that the specific surface is closely related to the "bonding potential" of the mechanical pulp fractions.

Mohlin reasoned based on results from sheet testing and microscopic studies that fiber conformability, chemical character of the fiber surface, the degree of fibrillation and the degree of fiber collapse will influence the density of a handsheet (Mohlin 1980). Mohlin showed that pulps with a high tensile index of sheets made from long fibers (Bauer McNett P16/R30 fraction) had a lower surface roughness than pulps of lower long fiber tensile index. She also showed that pulp mixtures resulting in higher sheet density decreased the surface roughness. In 1997, Mohlin used the ratio between fiber perimeter and lumen perimeter as an indicator of the amount of latewood fibers and fiber collapsibility. In the same paper Mohlin showed that the tensile index of the P16/R30 fraction decreased with increasing fiber wall thickness, but could not explain all variations of tensile index of the samples included in the study (Mohlin 1997).

The production and testing of laboratory sheets is time consuming and the results are often influenced by the routines of the laboratory. Klinga *et al.* (2005) showed that different sheet forming methods and temperatures in forming laboratory sheets can affect the ranking of the strength of pulps, especially when evaluating high yield chemimechanical pulps. In contrast to distributions of fiber

characteristics, results from tensile testing will mainly reflect on the weakest point of the test specimen.

2.4.2 Quantification of fiber characteristics

This study focused mainly on the evaluation of fiber dimensions and external fibrillation as measured in the FiberLab optical analyzer, and these measures are discussed below. It is possible that measures of surface chemistry, bendability or fiber wall density of the analyzed fibers would provide additional information that may be useful in characterizing mechanical pulp fibers.

Fiber "flexibility"

Fiber flexibility has been referred to as one of the most important characteristics that contribute to tensile index and density of sheets of mechanical pulp fibers (Mohlin 1980). The influence of fiber flexibility on sheet density was shown by Steadman and Luner (1985). Fiber flexibility is sometimes used as a general expression referring to both fiber bendability (conformability) and cross-sectional fiber collapsibility. Methods for single fiber analysis of fiber flexibility are often time consuming, regrettably the results of the methods that take into account the single fiber flexibility often originate from too few measured fibers to be of statistical relevance (Tam Doo and Kerekes 1981, Steadman and Luner 1985, Tchepel *et al.* 2006).

One method that may indirectly evaluate the fiber flexibility is measures of what is denoted as the "relative bonded area" of the fiber. There are commercial analyzers available which are said to evaluate fiber flexibility and relative bonded area based on the method described by Steadman and Luner (1985), in which the contact area between glass and fibers that were individually dried onto a glass plate is compared to the total projected fiber area (Das *et al.* 1999). A trial to evaluate the relative bonded area was conducted within this study and the results are found in Section A10.2 in Appendix A.

External fibrillation

d'A Clark (1985, page 518) stated that cohesiveness of the fibers in paper is "caused by the microscopically visible fibrils on the fibers down to and including molecular fibrillation". External fibrillation is a denotation to describe the fiber wall parts that remain on the fibers in the form of fibrils when fines are peeled-off in the refiner process. Due to the earlier lack of analysis equipment in evaluating the external fibrillation of single fibers, indirect measures based on whole pulp or various pulp fractions have been used to characterize the degree of external fibrillation. One example of this is measurements of fibers' sedimentation time (Wakelin 2004) or water permeability through pulp beds (Forgacs 1963).

Fiber wall thickness

The wall thickness of fibers in pulp has traditionally been analyzed using different microscopic methods (see *e.g.* Höglund and Wilhemsson 1993, Mohlin 1997, Fjerdingen *et al.* 1997, Dickson *et al.* 2005). Microscopic analysis and the preparation for such analysis is time consuming and the results are consequently often based on a low number of analyzed fibers. Due to both the high cost and the long time from sampling to results, advanced microscopic methods are not suitable for daily mill control or to be used as the base for process steering.

Z-parameter

Reme *et al.* (1999b) introduced the use of the Z-parameter to group fibers into early- or latewood fibers. The Z-parameter was calculated based on the ratio between the cross-sectional area of fiber wall and fiber wall plus lumen, and indicates how large part of the total fiber cross-section that consists of fiber wall. The original calculation of Z-parameter was based on data from cross-sectional SEM micrographs but the equation was also applicable to FiberLab data. Some examples of averages and distributions of Z-parameter calculated for the pulps used in this study are found in Section A4.4 in Appendix A.

Fiber collapsibility

Fiber collapsibility of mechanical or chemimechanical pulp fibers is a theoretical calculation of how prone the fiber is to collapse, based on evaluations of cross-sectional fiber dimensions. Numerous methods of expressing fiber collapsibility have been presented (see *e.g.* Görres *et al.* 1993, Jang *et al.* 1995, Fjerdingen *et al.* 1997, Norman and Höglund 2003, Vesterlind and Höglund 2005, Norgren and Höglund 2007). In the major part of this study, the collapse resistance index suggested by Vesterlind and Höglund (2005) was selected to express the ability of the fibers to resist collapsing, using Equation 3.6a. The fiber outline shown in Figure 2.10 shows the principles of fibers of high and low collapse resistance index. The fiber of low collapse resistance index has a larger contact area available for interaction with other fibers, fibrils and fibrous material in a sheet structure whereas the contact area for the fiber of high collapse resistance index is smaller.

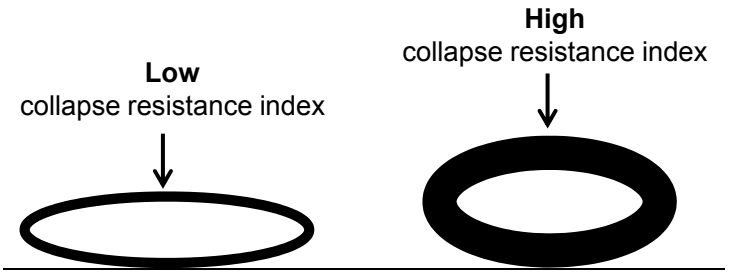

Figure 2.10. Outline of fibers of low and high collapse resistance index. The fiber of high collapse resistance index has a larger contact area available for interaction with other fibers, fibrils and fibrous material in a sheet structure than the fiber of low collapse resistance index, as seen from the different contact areas between the respective fiber and the flat "surface" in the illustration.

2.4.3 *BIN* – *B*onding ability *IN*fluence

This study resulted in a method to evaluate the propensity of single fibers to form dense sheets of high strength. The predicted tensile index was denoted *BIN*, which is an abbreviation for "*B*onding ability *IN*fluence".

The terms "fiber bonding", "fiber bonding ability" or "bonding properties of the long fiber fraction" has colloquially been used to describe fiber characteristics that influence the tensile index, burst or density of laboratory sheets made from long fiber fractions, for example by Mohlin (1979, 1980, 1989), Jackson and Williams (1979), Falk *et al.* (1987), Ferritsius (1996), Ferritsius and Ferritsius (1997). This was based on the formation of networks in sheets, where fibers of high "bonding ability" form a dense fiber network resulting in sheets of high strength and density.

In the context of this thesis, "fiber bonding ability" was seen as a consequence of measurable fiber dimensions which could be combined to predict *e.g.* the tensile index of laboratory sheets, referring to the dimensional prerequisites of the fibers to interact. The nature of the interactions which join together the mechanical pulp fibers in a sheet were outside the scope of this work and were not discussed.

2.5 Distributions of fiber characteristics and tensile index

Despite the large variations in fiber geometry in mechanical pulps, no rapid method has been available to make distributions of high precision of fiber characteristics. Distributions of high resolution compared to *e.g.* histograms, require large amounts of data, something that has been difficult or very time consuming to acquire before the relatively recent development of rapid optical analyzers that synchronize measurement data of single fibers. Histograms and normal distributions drawn based on a few points of data from microscopic

analyses have been used to illustrate the distribution of fiber wall thickness, fiber width and factors calculated from geometrical fiber dimensions in specific studies (see *e.g.* Mohlin 1989, 1995, 1997, Höglund and Wilhemsson 1993, Kure 1997, Reme *et al.* 1999a, Reme *et al*. 1999b, Rusu *et al.* 2011). Due to the long time required to prepare and analyze the cross-sectional wall dimensions of fibers using microscopic methods, these methods were not applied on daily process evaluations.

Höglund and Wilhemsson (1993) used distributions of fiber wall thickness and width to show that the character of the +30 fraction of different TMPs resembled the character of the distribution of the wood, and it was concluded that the wood type gave the character of the refined long fiber fraction. The data was based on microscopic analysis of 500 – 1000 fibers. Kure (1997) showed distributions of fiber wall thickness in pulp and in wood based on data from cross-sectional SEM analysis (pulp) and magnified images of parts of wood where the geometry of individual fibers was measured by a ruler. Also from this study, it was reported that the character of the fiber wall thickness distribution of a (primary refined) pulp resembled the character of the fiber wall thickness distribution of the wood.

Reme *et al.* (1999b) used distributions based on few points of the calculated factor "Z-parameter" (*cf.* Section 2.4.2) based on results from cross-sectional SEM images to illustrate the peaks representing the early- and latewood fibers in mechanical pulps. Mörseburg (2000, page 108) utilized FiberLab data to illustrate distributions of fiber wall thickness in pressurized groundwood. Mörseburg also used the raw data from FiberLab to be able to make distributions with higher accuracy than histograms.

Gavelin (1966, page 88) used distributions of tensile strength from a hundred tested sheet specimens to show that the tensile index was negatively affected by adding shives. He suggested a characterization method where the average, peak, and fifth lowest percentile of the strength distribution were reported. Gregersen (1998, pages 21-25) used Weibull statistics to predict the distribution of tensile index. The experimental data was based on laboratory analysis of tensile index of up to 1000 paper specimens and the fitted Weibull distributions showed high correlation to the experimental tensile index distributions.

Pulkkinen *et al.* (2006) used statistical high-order moments such as kurtosis and skewness to describe distributions of fiber characteristics in chemical and mechanical pulps. The distributions were made from normal distributions fitted to grouped data based on results from the FiberLab analyzer. Richardson *et al.* (2013) used the FiberLab data to make wall volume weighted distributions of fiber characteristics. Both the distributions and wall volume weighting was based on histograms which resulted in distributions of unnecessarily low resolution compared to weighting each fiber in the FiberLab raw data separately.

2.5 Prediction of sheet characteristics

Forgacs (1963) stated that at least two factors related to two different characteristics of fibers were needed to fully characterize a mechanical pulp; the L-factor, referring to fiber length, and the S-factor, related to fiber quality. The S-factor was defined as the specific surface area of the P48/R100 (P50/R100) fraction, evaluated from measurements of fiber bed permeability, and the L-factor was defined as the fiber length evaluated by microscopic analysis of fibers retained on a 48 (50) mesh screen. Forgacs showed that the use of linear regressions of the S- and L-factors could predict and explain bulk, tear, burst and wet web strength of 36 miniature grinders and commercial groundwoods. He found that for burst, bulk and wet web strength, the S-factor was the dominant factor, and changes in the L-factor did not affect the tensile properties. The equations resulting from the linear regressions were also evaluated on refiner pulps but with poor results.

Mohlin (1977) stated that the variation of properties in TMP is large, and that the L- and S factors were no longer sufficient for characterizing pulps, and wanted to include also measures of particle size and shape distribution, fiber flexibility/fiber collapse, and fiber surface character in models to characterize the quality of a pulp. In 1989, Mohlin defined the tensile index of laboratory sheets made from the P16/R30 fraction as "Bonding index".

Strand (1987) showed that it is possible to explain 92% of the variations in pulp properties by two factors, Factor 1 and 2, by multivariate data analysis. Factor 1 was referred to as "fiber quality" and Factor 2 was referred to as "fiber length". Factor 1 correlated to Forgacs' S-factor and Factor 2 to Forgacs' L-factor.

Ferritsius and Ferritsius (Ferritsius 1996, Ferritsius and Ferritsius 1997, 2001) applied the work of Strand on commercial mechanical pulp processes. They predicted the independent factors F1 and F2 to control the process in order to produce a stable pulp quality (Ferritsius *et al*. 1989). The F1 and F2 factors were calculated in similar ways as Factor 1 and Factor 2 by Strand, and were based on laboratory results from analysis of pulp- and sheet properties. It was for example shown that the factor F1 correlated well to variations in porosity of final paper of news grade (Ferritsius and Ferritsius 2001).

3. MATERIALS AND METHODS

The hypothesis behind this study was that it is possible to predict a major part of the tensile index of laboratory sheets of individual pulp fractions by utilizing fiber measurements based on image analysis.

In order to broaden the range of the average characteristics of the material used in the analyses, five mechanical pulps, three TMPs, one SGW and one CTMP, produced from Norway spruce (Picea abies), were fractionated both with respect to specific surface area and density by means of hydrocyclones and with respect to general fiber length by means of a Bauer McNett classifier. Fifty-eight samples were then analyzed both by laboratory sheet testing and measurements in a FiberLab™ image analyzer.

A way to test the hypothesis is to build a model that predicts tensile index based on the image analysis data from some of the fiber fractions. After this, it should be possible to validate the model by evaluating to what extent it can be used to predict the tensile index of the other pulp fractions. If the model shows potential of being applied on pulps that were not fractionated should also be evaluated.

3.1 Materials

Five mechanical pulps were selected to be fractionated in hydrocyclones. The pulps had different characteristics but were part of mechanical pulp types that all had a similar linear correlation between tensile index and density (Höglund and Wilhemsson 1993). The five mechanical pulps were all produced from Norway spruce (*Picea abies*) from growth areas of geographical proximity. The pulps were chosen to represent a broad range with respect to fiber quality and average fiber length and intended for various final products. The fiber quality was approximated as degree of fiber wall treatment based on knowledge of sheet strength and intensity and specific energy consumption of the different refining and grinding processes. Description and general quality of the five pulps is found in Table 3.1. In the earlier stages of this study (Paper I and Reyier 2008) and in some of the graphs and tables in the appendices, the pulps are denoted Pulps A-E.

Table 3.1. Overview of the five reference pulps that were fractionated in hydrocyclones.

Denotation	TMP1 (Pulp A)	TMP2 (Pulp B)	TMP3 (Pulp C)	SGW (Pulp D)	CTMP (Pulp E)
Pulp type	TMP News	TMP News	TMP SC	SGW SC	CTMP P. board mid. layer
Process[1]	CD refiner	DD refiner	DD refiner	Atm. grinder	Sulfite + CD refiner
Specific energy consumption, *kWh/ADMT*					
	~1900	~1900	~3000	~1900	~1000
Amount long fibers, *% of total pulp*					
R100[2]	70.5	66.6	62.2	46.1	79.6
P16/R30	30.7	28.4	26.9	18.5	34.8
P30/R50	12.7	10.9	10.7	13.2	12.8
Long fiber tensile index, *Nm/g*					
P16/R30	9.6	14.9	24.7	21.2	5.5
P30/R50	15.1	25.3	40.3	27.4	6.7

[1]*Conical disc refiner (CD) and double disc (counter rotating) refiner (DD)*

[2]*R100-fibers defined as fibers retained on a 100 mesh wire*

A general outline of the internal ranking of the hydrocyclone fractionated pulps with respect to general fiber quality and fiber length corresponding to F1 and F2 as described in the background section (Ferritsius 1996, Ferritsius and Ferritsius 1997, 2001) is shown in Figure 3.1 below.

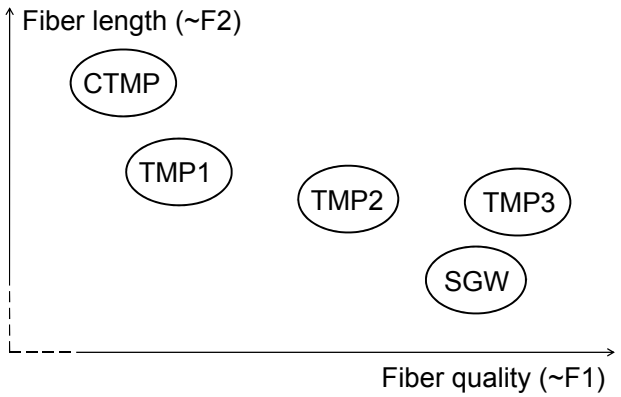

Figure 3.1. Imagined outline of the reference pulps' internal ranking of general fiber quality and fiber length influence, corresponding to the factors F1 and F2 respectively, as described by Ferritsius (1996) and Ferritsius and Ferritsius (1997, 2001).

Below are brief process descriptions of the commercial pulps that were used in the hydrocyclone fractionations. All pulps were final pulps, four of them bleached with either dithionite of hydrogen peroxide. The composition of each pulp with respect to Bauer McNett fractions is found in Paper II and in Section A2 in Appendix A.

TMP1. Dithionite bleached TMP intended for news grade printing paper produced by single stage conical disc refining followed by LC refining, about 1900 kWh/ADMT, Figure 3.2a.

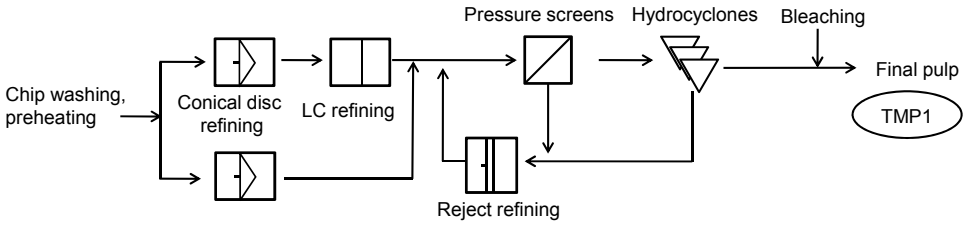

Figure 3.2a. Outline of TMP1 process.

TMP2. Unbleached TMP intended for news grade printing paper produced by single stage double disc refining, about 1900 kWh/ADMT, Figure 3.2b.

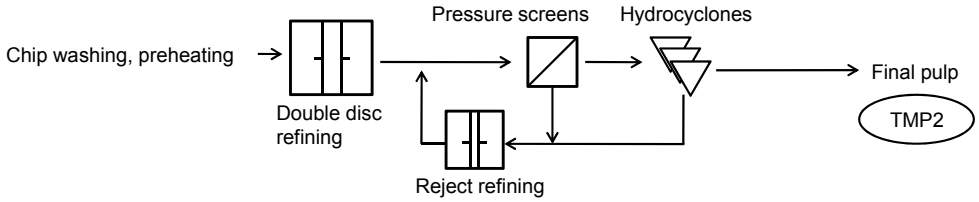

Figure 3.2b. Outline of TMP2 process.

TMP3. Hydrogen peroxide bleached TMP intended for SC grade printing paper produced by two-stage double disc refining, about 3000 kWh/ADMT, Figure 3.2c.

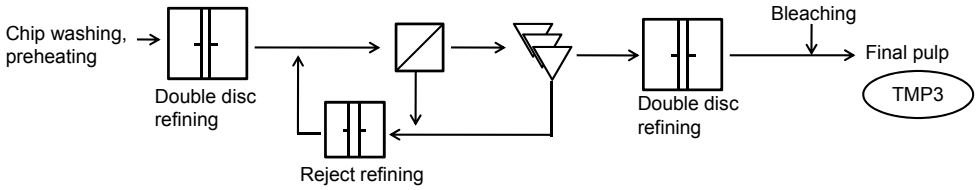

Figure 3.2c. Outline of TMP3 process.

SGW. Dithionite bleached atmospheric groundwood intended for SC grade printing paper, about 1900 kWh/ADMT, Figure 3.2d.

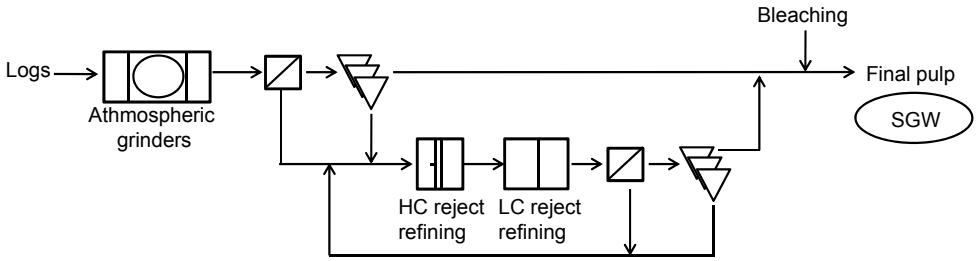

Figure 3.2d. Outline of SGW process.

CTMP. Hydrogen peroxide bleached CTMP intended for paperboard middle ply produced using sulfite pre-treatment at alkaline conditions and single stage conical disc refining, about 1000 kWh/ADMT, Figure 3.2e.

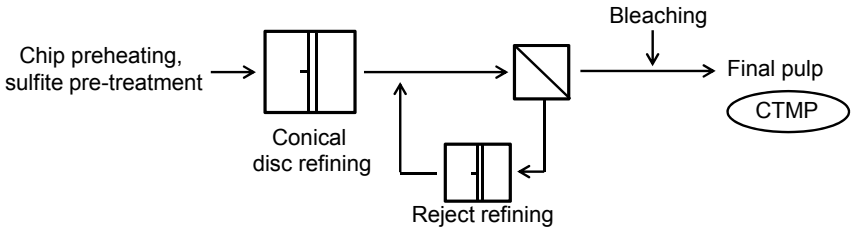

Figure 3.2e. Outline of CTMP process.

The level of bleaching was moderate to low for all the bleached pulps (TMP1, TMP3 SGW, CTMP). The volume of the pulp samples were 1 m^3 (TMP1, TMP2) and 2 m^3 (TMP3, SGW, CTMP) respectively, at approximately 4% consistency. For TMP3, the hydrocyclone fractionation required more pulp than was first approximated (1 m^3), and a second sample was required, sampled three days later. The pulps from the two sampling occasions of TMP3 were produced under similar process conditions and were mixed in the hydrocyclone trials; the results of the hydrocyclone fractionations should not have been affected by this. The characteristics of the other pulps included in this study are described in Paper IV and Paper V.

3.2 Methods

3.2.1 Hydrocyclone fractionation and pulp handling

Hydrocyclone fractionation

Hydrocyclones have been shown to separate fibers with respect to specific surface area (Wood and Karnis 1979) and by fiber wall thickness (Kure *et al.* 1999a) so that fibers in the accept stream has higher specific surface and thinner walls than the fibers in the reject stream. The purpose of the hydrocyclone fractionation was to separate the reference pulps with respect to fiber morphology and fiber dimensions to get a broad range of fiber characteristics upon which a model to predict the tensile index could be based.

The fractionation was performed in pilot scale but commercial size hydrocyclones were used. The hydrocyclone fractionations took place at Kadant Noss, Norrköping, Sweden, at five different occasions. The hydrocyclone fractionation was performed in four stages and resulted in five streams; accepts 1-4 ("Streams 1-4") and reject 4, denoted "Stream 5", *cf.* Figure 3.3.

For TMP1, the hydrocyclone process settings were adjusted so that approximately 20% of the R100 fraction (retained on a 100 mesh wire) went with each stream and the same settings were then used for the remaining four pulps. After hydrocyclone fractionation, each stream was also fractionated by general fiber length in a Bauer McNett classifier. Section A1.1 in Appendix A lists the reject rates of the hydrocyclone fractionations.

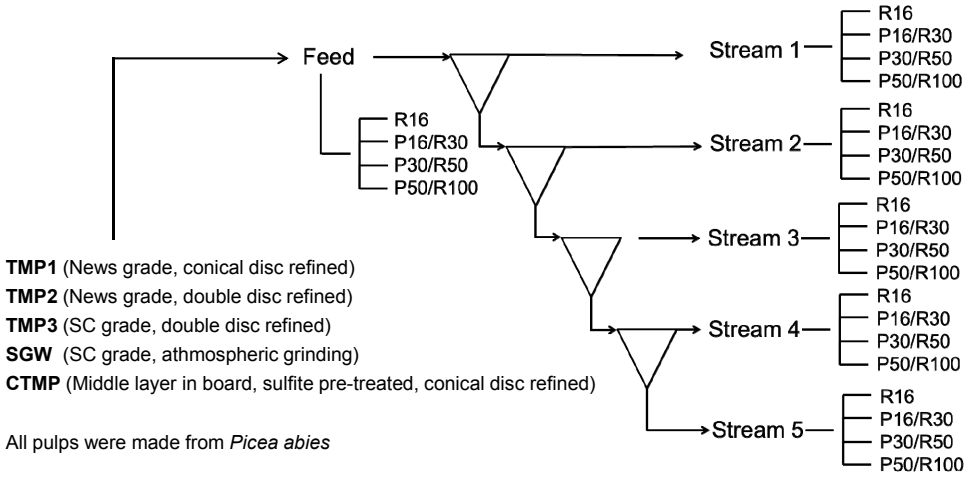

Figure 3.3. Outline of hydrocyclone fractionation of five mechanical pulps. Each of the hydrocyclone streams was also fractionated with respect to general fiber length in a Bauer McNett classifier.

Pulp handling

Each hydrocyclone accept, the final reject stream (Streams 1-5) and the feed (denoted Stream 0) were dewatered through a 200 mesh wire in 30 cm diameter cone directly after the fractionation. The filtrate was collected and recycled to the pulp until the water leaving the dewatering cone was clear as judged by the eye. Due to the large quantities of material, each stream was divided into smaller parts to enable dewatering. Samples were then packed in buckets and shipped to Stora Enso Research Centre in Falun, Sweden.

The pulp samples were then enclosed in a 200 mesh net before being centrifuged for 20 minutes in a standard laundry centrifuge. The outgoing water was collected and poured back to the centrifuge until it was free from fines, as judged by the eye. The centrifuged pulp became densely packed and was divided into coin-sized parts by a small rotating propeller in an apparatus designed specifically for that purpose. The dry content of the pulps were analyzed by double testing in a halogen heater dry content analyzer, and the samples were re-centrifuged until a dry content above 30% was reached. As expected, the first accept streams contained more fines and needed longer time for dewatering than the rejects.

After centrifugation, all portions of each sample were combined and carefully mixed and new double tests of dry content were made. Based on the dry content of each hydrocyclone stream, the pulps were divided in portions corresponding to 55 grams of dry material and packed in double plastic bags in carton boxes. The boxes were then stored in a pulp freezer at approximately -28 °C. Mechanical pulp starts decomposing if kept wet which is believed to affect the fiber characteristics. Continuously throughout the hydrocyclone fractionation and dewatering process, the pulp samples were treated with a preservative chemical (Spectrum PR3126 / RX6202 from Hercules), to avoid bacterial growth.

The dewatering and freezing of the pulps followed internal routines and was made to ensure that the large quantities of pulp would be evaluated under similar conditions. A comparison of fiber length and cross-sectional fiber dimensions of one pulp treated in two ways, frozen *etc.* according to normal procedures or analyzed directly, is found in Table A12.2 in Appendix A. Based on evaluations of this one pulp, the dewatered, frozen and hot disintegrated sample had lower fiber curl than the sample that was evaluated directly. This was expected based on other trials performed in this study, where the hot disintegration was found to reduce curl. Based on the result of the evaluation of the one sample, it is also possible that the fibrillation index was reduced by the dewatering – freezing – hot disintegration procedure, and that some fiber swelling occurred (indicated by slightly higher fiber wall thickness index and fiber width index). This would benefit from further evaluations. As results from evaluations of pulp samples in this study were only compared to samples that were handled by the same procedure, results and

internal rankings between the pulps should not have been affected by the pulp handling procedure.

3.2.2 Bauer McNett fractionation

To compare the fiber characteristics at similar fiber length levels, the pulps were fractionated in a Bauer McNett classifier, SCAN-P 88:01, with 16, 30, 50, and 100 mesh wires resulting in the fractions: R16 (retained fibers of a 16 mesh screen), P16/R30 (passed 16 mesh, retained 30 mesh), P30/R50 and R50/P100. Before fractionation, the frozen pulps were hot disintegrated according to ISO 5263-3:2004(E). It has been shown that the Bauer McNett fractionator separate fibers mainly with respect to fiber length but also to some extent by flexibility (Petit-Conil *et al.* 1994) and fractionations of different pulp types can result in different fiber lengths (Ullman *et al.* 1965). Results of the Bauer McNett fractionation are found in Section A2.1 in Appendix A.

The material in the R16 fraction was collected without an upper limit and could contain shives and untreated fiber material which affects the results from the sheet testing. The P50/R100 fraction contains short fibrous material which has little left of intact fiber characteristics. Most evaluations of fiber characteristics therefore focused on the P16/R30 and the P30/R50 fractions. It is likely that the P30/R50 fraction contains not only fibers but also ribbon-like lamella segments (Mohlin 1989). Sheets made from the P16/R30 and P30/R50 fractions of TMP and SGW follow a similar relation with respect to density and tensile index (Mohlin 1980). This enables a model based on these fibers to be focused on fiber characteristics that influences tensile index rather than differences in sheet densification.

3.2.3 Sheet forming and testing

Handsheets were made in accordance with ISO 5269-1 (earlier SCAN CM26:99) in a circular (177 cm^2) sheet former. All samples were hot disintegrated (ISO 5263-3) before sheets were made. Long fiber tensile index was tested in an Alwetron TH-1 according to SCAN-P 67:93. Sheets of the whole pulp were produced with white water recirculation according to SCAN-CM 64:00.

Studies of the repeatability of the laboratory which were summarized during the course of this work showed that the results of sheet testing can sometimes vary depending on differences in laboratory routines or sample preparation and also in repetitive testing in the same laboratory. In some cases, the variations in the results were as large as the variations between the parts of the process that were evaluated. To reduce experimental variation in this study, all sheets were prepared, produced and tested in the same laboratory by the same technician. The fractionation in hydrocyclones and its consistent ranking of the pulp fractions with respect to long fiber tensile index and fiber properties (such as fibrillation index

and fiber wall thickness index) also gave indications of possible outliers that may have been the results of testing errors.

In this study, the analysis of fiber characteristics of one sample was repeated up to three times due to re-calibrations of the apparatus (FiberLab). The results of the first two measurements in FiberLab showed a very consistent decrease in fibrillation index and increase in fiber wall thickness index from the first accept to the last reject for all 60 analyzed samples from the hydrocyclone fractionation. The third time the results were re-analyzed in FiberLab, the results correlated very well with the first two measurements for 58 of the samples, whereas two samples showed results at a very different level. Most likely, these two samples (TMP3 and CTMP Stream 3, P30/R50 fractions) were the mixtures of two pulp fractions due to a handling mistake. The two points were thereby identified as outliers and removed from the results.

The results from the physical testing of laboratory sheets are listed in Table A3.1 in Appendix A. Evaluations of light scattering and light absorption coefficients were performed using an Elrepho device according to ISO 9416 and STFI thickness (density) according to SCAN-P 88:01.

Long fiber sheets made for the acoustic emission analysis presented in Paper I were produced in a Formette Dynamic Sheet Former (DSF) from the P16/R30 fractions of TMP1 and TMP2, Streams 0-5. These sheets became anisotropic and the tensile strength in the machine direction (MD) was more than three times higher than the tensile strength in the cross direction (CD). The grammage of the sheets was aimed at 60 g/m^2. The drum operated at 1400 rpms and the fiber suspension of 3 g/L was sprayed onto the moving wire using a pump operated at 2.8 bars. The sheets were dried in a custom made dryer consisting of a Yankee cylinder nip through which the sheets were processed at 0.4 - 0.5 m/min at 107 °C, 20 kN. The sheets were manually fed through the drying nip, they were held at the edge and pulled with moderate force, to achieve a slightly restrained drying. Fracture toughness of the sheets was evaluated at PFI, Trondheim, Norway, according to SCAN-P 77:95.

3.2.4 Image analysis of cross-sectional SEM micrographs (Papers I, II)

For method comparisons regarding analysis of fiber wall thickness and fiber width, cross-sectional SEM images were prepared and analyzed using an internal, semi-automatic image analysis method based on methods based on Fjerdingen *et al.* (1997), Reme (2000, page 43), Reme and Helle (2001).

Fibers of the P16/R30 fraction were processed through a laboratory scale screen which aligned the fibers. Bundles of the aligned fibers were rapidly frozen by liquid nitrogen and treated in *vacuum* to preserve the wet fiber appearance. To

ensure less than 1% water content in the samples, the fiber bundles were kept at 60-70 °C in an oven for one hour, and then embedded in epoxy.

Thin cross-sectional slices were cut from the embedded fiber bundles and the slices were polished and processed to digital images in a SEM. Before the image analysis, individual fibers which were in contact with each other were separated by a one-pixel line and fine material, longitudinally aligned fibers and noise were removed from the SEM images. Shives were separately identified and digitally removed from the image, and pits seen as small ruptures in the fiber walls were filled to be able to analyze the fiber as to have an intact wall. Cross-sections of broken fibers were removed from the analysis image and fully collapsed fibers were given an "artificial lumen" by a one pixel line. From the SEM images, the perimeter and average fiber wall thickness of each fiber was analyzed. Based on this data, other fiber characteristics were calculated, for example the lumen area and fiber width. Results from the cross-sectional SEM image analysis presented in this study were based on 650 – 1200 fibers per sample.

3.2.5 FiberLab™ (Papers I-V)

Fiber dimensions in this study were mainly evaluated in a Kajaani FiberLab™ V3.5 optical analyzer. In this FiberLab device, values of fibrillation index, fiber wall thickness index, fiber width index, and two measures of fiber length are obtained through an image analysis system using two perpendicular cameras (Kauppinen 1998, Kajaani FiberLab™ Operating Manual W4230467 V3.5 2002). In addition, fiber characteristics based on these values are calculated in the FiberLab software.

FiberLab sample preparation and analysis

Before FiberLab analysis, the pulp samples were hot disintegrated (ISO 5263-3) and diluted to 0.16 g/L in a cylinder shaped 5000 mL container. From the highly diluted fiber-water solution, 50 mL samples were collected by a pipette after standardized stirring where the direction was altered perpendicularly.

In the measurement, diluted fiber samples are sucked from a measurement cup into a capillary, in which the fiber passes through a polarized laser beam. The light polarization changes when a fiber passes the beam and a detector registers the light with changed polarization. An image proportional to fiber length is formed and converted to digital form and an amplified detector signal then gives a value of fiber length.

When a fiber is in position to be analyzed, a xenon lamp flashes and a CCD (charged coupled device) camera takes a photo of the middle part of the fiber. Average fiber width and fiber wall thickness is calculated by grey level differences from 40 measurements along the middle 0.7 mm of each fiber which is considered statistically prevalent (Kauppinen 1998). The two cameras for measurements of

length and cross-sectional fiber dimensions respectively are positioned perpendicularly as seen in the FiberLab measurement chamber outlined in Figure 3.4 below by Kauppinen (1998).

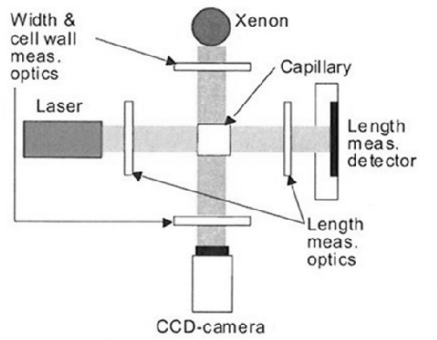

Figure 3.4. The FiberLab measurement principle is based on two perpendicular cameras for measurements of length and cross-sectional fiber dimensions. The results of the image analysis are synchronized for each fiber (Kauppinen 1998).

The result of the CCD camera image analysis is synchronized with the results of fiber length for each analyzed fiber and stored in a result file. Each FiberLab "run" (measurement of one pulp sample) produces both a raw data file and a default printout report of averages, where the averages are weighted in different ways. The default averages are also based on various numbers of fibers for different fiber characteristics. The raw data file has the format of a text file and both the raw data file and the default printout report provide data of fiber wall thickness, fiber width, fibrillation index and fiber length together with some calculated measures of for example cross-sectional area, fiber wall volume and curl (definition of curl such as used in the FiberLab analyzer is found below). Also data of for example the maximum length of straight segment for individual fibers is stored and by weighting the sample prior to analysis, the coarseness can also be evaluated. All cross-sectional fiber dimensions evaluated in the FiberLab device are indexes and not true fiber dimensions, but have proved equally valuable in rankings (see *e.g.* Mörseburg 2000, Lhotta *et al.* 2007, Norgren and Höglund 2007, Richardson *et al*. 2013).

Distributions of FiberLab data from the first part of this study (Reyier 2008) were based on 9-12 FiberLab runs per sample to ensure a high enough number of evaluated fibers (30 000 - 60 000). The high number of fibers was needed to reach a sufficiently high resolution in producing distributions of fiber data, to be able to distinguish and interpret differences between samples. High resolution is also needed to recognize characteristic features of the distributions. Statistical data analysis methods described in Paper V and Section 3.3.3 reduced the required

number of fibers to about 10 000 with preserved resolution of the results, which corresponded to triple runs for a news grade TMP. One sample ("run") is analyzed in less than 20 minutes, and the FiberLab device can be charged with six samples simultaneously. To be able to identify measurement disturbances, at least triple runs were analyzed for each sample. During analysis, the FiberLab default average of fibrillation index of each run was used as the primary indicator of acceptable measurement repeatability, and the default average of fiber wall thickness index as the second indicator.

Below are descriptions and equations of some of the analyzed and calculated fiber dimensions. Each of the Equations 3.1-3.6 below was applied on single fibers in calculations made in FiberLab and in calculations based on FiberLab raw data (Papers II-V).

Fiber length and curl

The length measurement settings used in the FiberLab analysis in this study ranges from 0.2 - 7.6 mm with a resolution of 10 μm. The results are given in the unit of millimeter. The two fiber length measures are "true" fiber length; fiber length along the fiber center, L_c, and projected fiber length, the shortest distance between the two fiber ends, L_p, Figure 3.5.

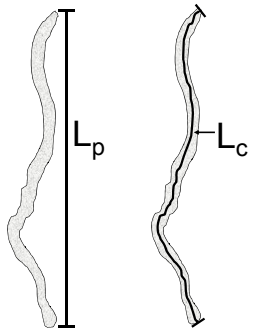

Figure 3.5. Outline of L_c, fiber length measured along the fiber center, and L_p, projected fiber length. The two measures of fiber length were used to calculate fiber curl.

Fiber curl was calculated according to Equation 3.1 (Kajaani FiberLab™ Operating Manual W4230467 V3.5 2002).

$$CURL = (\frac{Lc}{Lp} - 1) * 100 \qquad \text{Eq. 3.1}$$

Fiber wall thickness and fiber width

The results of the cross-sectional dimensions in the FiberLab are based on single fiber averages of fiber width index and fiber wall thickness index. The resolution of

the measurement of these cross-sectional dimensions in the used FiberLab device is 1.5 μm (Kajaani FiberLab™ Operating Manual W4230467 V3.5 2002). Continued software updates of the FiberLab device have improved the resolution of the fiber data, and the data used in Papers II-V had the resolution of 0.8 μm for fiber wall thickness and 0.001 μm for fiber width.

If the FiberLab software does not recognize a lumen in the image analysis of fiber width, no value of fiber width was saved and no data of fiber width or cross-sectional area was stored for that fiber. Fiber width and fiber wall thickness were evaluated as is seen in Figure 3.6 below.

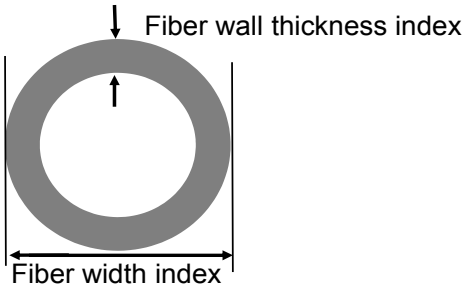

Figure 3.6. Outline of the evaluation of fiber width index and fiber wall thickness index.

From the average fiber wall thickness and fiber width of each fiber, the cross-sectional area and fiber wall volume (Figure 3.7) were calculated by the FiberLab software according to Equations 3.3 and 3.4. The cross-sectional wall area is given in the unit of μm^2, and the unit of the wall volume is μm^3 (Kajaani FiberLab™ Operating Manual W4230467 V3.5 2002) but as discussed above, the cross-sectional dimensions are indexes and not true fiber dimensions, and to avoid direct comparisons with "true" values, the results of the cross-sectional fiber dimensions of this study were shown without units.

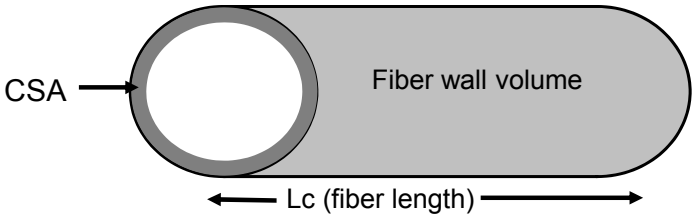

Figure 3.7. Outline of FiberLab calculations of cross-sectional wall area and fiber wall volume.

$$Cross-\sec tional\ fiber\ wall\ area\ (CSA) = A(total) - A(lumen) =$$
$$= \pi \left(\left(\frac{fiber\ width}{2} \right)^2 - \left(\frac{fiber\ width - (2 * fiber\ wall\ thickness)}{2} \right)^2 \right) \quad \text{Eq. 3.3}$$

$$Fiber\ wall\ volume = CSA * Lc \quad [\mu m] \quad \text{Eq. 3.4}$$

Based on the FiberLab data, more calculations were made, for example the collapse resistance index, CRI (see Equations 3.5a and 3.6a below), and the factor *BIN* which was one result from this study.

Collapse resistance index

In Paper I, the collapse resistance index was calculated according to the equation used by Norgren and Höglund (2007), Equation 3.5, and in Papers II-V by the equation suggested by Vesterlind and Höglund (2005), Equation 3.6.

$$CRI_{Norgren} = \frac{2 * fiber\ wall\ thickness^2}{fiber\ width - fiber\ wall\ thickness} \quad \text{Eq. 3.5}$$

$$CRI_{Vesterlind} = \frac{fiber\ wall\ thickness^2}{fiber\ width - fiber\ wall\ thickness} \quad \text{Eq. 3.6}$$

For results presented in Paper I, no raw data files but only FiberLab standard printout reports were available, and all averages of fiber characteristics were calculated from the default averages of the FiberLab software. The equation used to calculate the collapse resistance index, *CRI*, for data presented in Paper I, is found below, Equation 3.5a. Results presented in Papers II-IV are based on averages where the collapse resistance index was calculated for each fiber before the average collapse resistance index was calculated. This did not change any rankings between the hydrocyclone streams compared to the earlier data, but the level of collapse resistance index changed. The reason for this was the amplified effect of the non-linear scatter resulting from calculating combined factors from averages as opposed to on single fibers. Remarks about this are found in Section C1 in Appendix C. Average collapse resistance index in Papers II-IV were calculated according to Equation 3.6a below, for *N* fibers.

$$Average\ CRI_{Paper\ I} = \frac{2 * (average\ fiber\ wall\ thickness)^2}{average\ fiber\ width - average\ fiber\ wall\ thickness} \quad \text{Eq. 3.5a}$$

$$Average\ CRI_{Papers\ II-V} = \frac{1}{N}\sum_{i=1}^{N} CRI_i = \frac{1}{N}\sum_{i=1}^{N} \frac{fiber\ wall\ thickness_i^{\,2}}{fiber\ width_{\,i} - fiber\ wall\ thickness_{\,i}} \quad \text{Eq. 3.6a}$$

Fibrillation index

The fibrillation index of each fiber was calculated as the ratio between the area of fibrils and the area of fiber body plus fibrils, Equation 3.7. Grey scale sub-pixel calculations are used to define the area of fibrils with a resolution that is stated by the supplier to be <0.1 μm. The unit of fibrillation index is percent. Continuous FiberLab updates improved the resolution of the fibrillation index data, and data in Papers II-V had a data resolution for fibrillation index of 0.001 units. The optical measurement includes all fibrils in the measurement window in its calculations of fibril area, and the results can therefore in some cases contain data of fibrils which were not attached to the fiber body.

$$Fibrillation\,index = \frac{Area\,(fibrills)}{Area\,(fibrills + fiber)} * 100 \qquad \text{Eq. 3.7}$$

3.2.6 MorFi Lab (Paper II)

For comparisons of methods regarding fiber width, fiber samples analyzed in a FiberLab device were also processed through a MorFi Lab optical analyzer (Eymin Petot Tourtollet *et al.* 2003). The MorFi Lab analyzer is a fiber analyzer similar to FiberLab, but without the ability to measure fiber wall thickness or provide raw data of single fiber dimensions. The MorFi Lab results are default averages which were obtained without the data filtering that was often made for the FiberLab (*cf.* Section 3.3.1). MorFi Lab results were therefore compared to default averages from the FiberLab. Sample preparation prior to the MorFi Lab analysis was similar to the FiberLab analysis but the fibers were kept at the low concentrations used in measurements for approximately three weeks after hot disintegration, prior to the analysis. The MorFi Lab results included in this study were based on about 5 000 fibers per sample and evaluations were made for the P16/R30 fractions of TMP1, TMP2 and TMP3.

3.2.7 Acoustic emission (Paper I)

To evaluate if the sheets made from the hydrocyclone fractionated pulp streams showed different behavior during fracture, sheets from the P16/R30 fractions of TMP1 and TMP2 were evaluated using acoustic emission (Gradin *et al.* 1997, Gradin *et al.* 2008).

The acoustic emission testing was performed at as slow as 1 mm/minute displacement rate (compared to the 1.7 mm/s for SCAN-P 67:93) vertical tensile testing. Ten specimens per sample, 15*100 mm, cut along the MD direction were analyzed under controlled laboratory conditions (50% relative humidity, 23 °C). During loading, the numbers of acoustic events were recorded by a piezoelectric transducer attached to the specimen by using a small magnet. The load at 10% of

the cumulative number of recorded acoustic events at break was also used to calculate the factor Wc, critical strain energy density, which has been shown to correlate to fracture toughness for various paper products (Gradin *et al.* 2008). More details about the acoustic emission testing method are found in earlier publications (Gradin *et al.* 1997, Klinga *et al.* 2007, Gradin *et al.* 2008). Results from the acoustic emission are found in Paper I and discussions about the use of acoustic emission are found in Section 6. Section A11 in Appendix A contains data from the acoustic emission testing.

3.3 Methods of data evaluation

3.3.1 Filtering of raw data files from FiberLab (Papers II-V)

FiberLab analysis results in both a printout default report of averages and a raw data text file. For data in Papers II-V, the FiberLab raw data files were imported into a data base from which results were filtered to evaluate fiber properties without the influence of fines or fibrous material without intact walls. This was done by excluding fiber data that had no registered value of cross-sectional wall area. Exceptions to this are comparisons to averages of fiber width from the MorFi Lab analyzer (Paper II) from which raw data was not available and standard FiberLab printout reports were used. Paper IV also includes comparisons of averages from default printout reports and filtered data. When the measurements leading to the results of Paper I were made, only FiberLab standard printout reports were available and thus data in Paper I is based on averages of all analyzed material above 0.2 mm.

By default settings, fibrillation index was not analyzed for all fibers. For statistical validity only fibers with a measured fibrillation index were included in the results.

In the raw data, some fibers had a curl value of "-1". Negative curl is believed to indicate measurement disturbances or measurements outside the defined length range. In Papers II and IV, only data from fibers with a positive curl was included in the results. Later it was found that the inclusion of fibers of negative curl did not influence any rankings of average cross-sectional fiber dimensions between the pulp samples. The procedure was therefore changed and data in Papers III and V is based on results including fibers with all values of curl. FiberLab settings were set to measure fibers between 0.2 and 7.6 mm.

In comparing the correlation between predicted and measured tensile index in Paper I to the correlation between *BIN* and measured tensile index in Paper II, is was found that the raw data filtering had limited influence on the results in the FiberLab evaluations of long fiber fractions, but should be considered as a method of precaution. The data filtering could be done based on any of the fiber characteristics that were measured or calculated from the FiberLab instrument.

Figure 3.8 below outlines the principle of the raw data filtering.

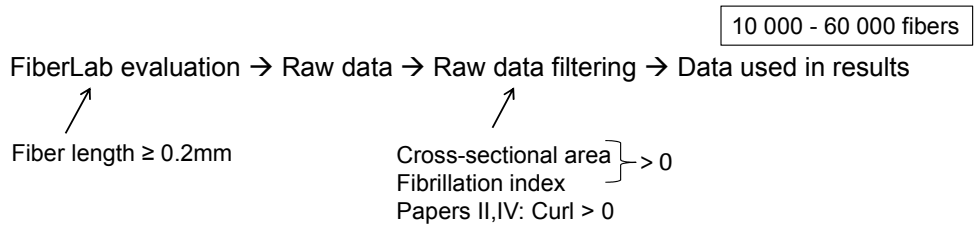

Figure 3.8. For results in Papers II-V, the FiberLab raw data was filtered to ensure that the results were based on fibers and not fines or fibrous material without intact fiber walls.

After data filtering, the result files consisted of 10 000 – 60 000 fibers, which required approximately nine FiberLab runs for TMPs. More runs were needed to reach the required number of fibers for pulps containing higher amounts of short fibers and fibers with broken walls, *e.g.* SGW. This is also discussed in Section 4.2.5. Averages which the *BIN* models were based on and validated against were usually calculated from approximately 30 000 fibers. In Section 3.3.3 it is described how it was possible to reduce the number of FiberLab runs from nine to three with preserved resolution in producing distributions of fiber characteristics.

The fiber length interval 0.7 to 2.3 mm was identified to cover the P16/R30 and P30/R50 fractions for which the *BIN* model was developed. The range of the fiber lengths for the P16/R30 and P30/R50 fractions can be seen in Paper IV (Figure 4). Paper V contains a comparison between distributions of fiber characteristics based on the whole fiber length interval and based on fibers between 0.7 and 2.3 mm, which shows that length- and wall volume weighted distributions of the two length intervals seem to have similar shapes and levels.

The 95% confidence intervals of averages of FiberLab analyses based on three and ten runs respectively are found below, Table 3.2. The confidence intervals were calculated according to Equation C2.6 (Appendix C).

Table 3.2. Example of 95% confidence intervals of three and ten FiberLab measurements per sample for a SC grade pulp with similar properties as TMP3. Based on fibers between 0.7 and 2.3 mm.

95% confidence intervals from ten FiberLab measurements

"Runs"	Fibrillation	Fiber wall thickness	Fiber width
3	0.11	0.04	0.09
10	0.03	0.08	0.08

3.3.2 Weighted averages (Paper III)

Fibers differ in length and volume and the influence that a single fiber has on the characteristics of a pressed sheet may be different for a fiber of large wall volume than for a fiber of small wall volume. In this study, the influence of fiber geometry on sheet properties was evaluated by comparing models where arithmetic, length weighted and wall volume weighted averages of fiber characteristics were used to predict the long fiber tensile index.

Also length^2 weighted averages of cross sectional fiber dimensions were analyzed, as the square fiber length is sometimes used to simulate weight weighted averages when the true fiber wall volume is not available. This is based on the assumption that the coarseness of a fiber is proportional to its length (d'A. Clark 1985, page 452, Pulkkinen *et al.* 2006). It was however stated by d'A Clark that if the true weight of each fiber can be analyzed, the results of weight weighted averages are more accurate than length^2 weighted averages (d'A Clark 1985, page 464) and Jang and Seth (2004) also showed that the assumption of constant coarseness along the length of a fiber is incorrect. If the weight and density of the fiber wall is assumed to be constant for all fibers included in a study, then wall volume weighted averages should give a relative figure of the weight of a fiber as the lumen area approaches zero, which may occur for some fibers in a pressed sheet.

All weighted averages were calculated based on *N* fibers from the filtered FiberLab raw data using Equations 3.8-3.11 below.

$$PROPERTY(arithmetic) = \frac{1}{N}\sum_{i=1}^{N} PROPERTY_i \qquad \text{Eq. 3.8}$$

$$PROPERTY(length-weighted) = \frac{\sum_{i=1}^{N}(PROPERTY * fiber\,length)_i}{\sum_{i=1}^{N} fiber\,length_i} \qquad \text{Eq. 3.9}$$

$$PROPERTY(wall\,volume-weighted) = \frac{\sum_{i=1}^{N}(PROPERTY * fiber\,wall\,volume)_i}{\sum_{i=1}^{N} fiber\,wall\,volume_i} \qquad \text{Eq. 3.10}$$

$$PROPERTY(length^2-weighted) = \frac{\sum_{i=1}^{N}(PROPERTY * fiber\,length^2)_i}{\sum_{i=1}^{N}(fiber\,length^2)_i} \qquad \text{Eq. 3.11}$$

3.3.3 Distributions from KDE *via* diffusion mixing (Paper V)

In the beginning of using raw data from the FiberLab, distributions of fiber dimensions were made by the use of histograms (Reyier 2008, Ferritsius *et al*. 2009). To reach high resolution in producing these distributions, the histogram intervals were made as narrow as possible, for example 110 histogram boxes were used for *BIN* distributions. To reach acceptable resolution in these distributions, 30 000 – 60 000 fibers were needed. It was found that the character and shape of the histogram was defined already from distributions of 10 000 fibers, but histograms based on only 10 000 fibers resulted in too low resolution to easily distinguish differences between samples or characteristics features of a given distribution.

To increase resolution in producing distributions of fiber characteristics, the method of KDE (Kernel Density Estimation) *via* diffusion mixing (Botev *et al*. 2010) was used. KDE *via* diffusion mixing uses an algorithm in which a given data point is influenced by surrounding data by a distance dependent "density", and each data point can be considered to be a distribution. These sub distributions add up and as a comparison, a *BIN* distribution results in more than 16 000 "boxes" of data.

The KDE *via* diffusion mixing method did not only result in increased resolution of a distribution, but also decreased the time required for performing the fiber analyses by a third, as fewer fibers were needed. Figure 3.9 below illustrates an example of *BIN* distributions made from histograms (grey) and made from KDE *via* diffusion mixing (black). Both distributions are based on the same data. Any peaks and features of the distribution were more easily recognized using the KDE *via* diffusion mixing method.

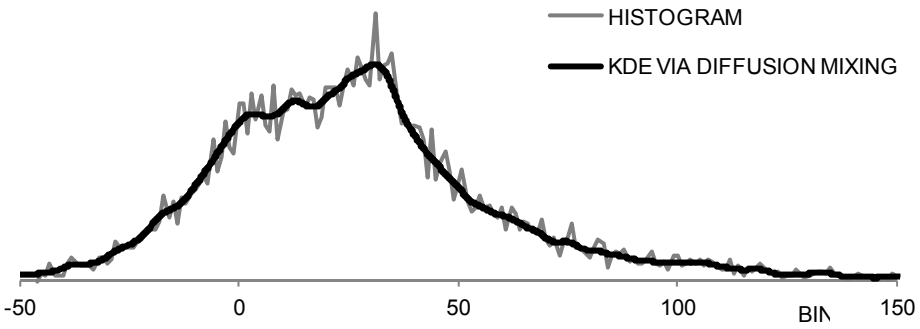

Figure 3.9. Distributions based on the same raw data made from histogram (grey) and Kernel Density Estimation (KDE) *via* diffusion mixing (black). Distributions made from KDE *via* diffusion mixing resulted in distributions in which features and peaks were more easily recognized than from histogram distributions.

In this study, the KDE *via* diffusion mixing method was used to determine the optimized bandwidth for distributions of different fiber characteristics, but a constant bandwidth was then consistently used for all distributions made of that property. Distributions in Paper V are made using the bandwidths 1.0 (fiber wall thickness index, fibrillation index) and 4.0 (*BIN*). To avoid extreme outliers, data exceeding 20σ, where σ is the standard deviation of the mean value of the data, were excluded. Less than ten such outliers were found in this study.

A width characteristic of a distribution was estimated as the difference between the percentile 0.95 and the percentile 0.05 according to Equation 3.12 below (Ferritsius *et al*. 2009).

$$Distribution\ width\ F0.90 = Percentile\ 0.95 - Percentile\ 0.05 \qquad \text{Eq. 3.12}$$

Weighted distributions

In forming weighted distributions, the fiber length or fiber wall volume was used as the base to convert every fiber to a number of replicate fibers, each with the dimensions of the original fiber. From these replicate fibers, distributions were made using KDE *via* diffusion mixing. Distributions presented in this study were arithmetic, length weighted or wall volume weighted but the same method can also be used in weighting distributions based on other fiber characteristics. The smallest repeating unit which was used in converting fibers to replicas was 0.001 for wall volume and 0.01 for fiber length.

3.4 Other methods of fiber characterization

In the search for a method to characterize the geometry of the fibers, some methods were tested which for various reasons were not practical for continued use. Some of the methods were used for comparisons with the FiberLab data, such as the cross-sectional scanning electron microscopic (SEM) image analysis or the MorFi Lab analyzer. These and some other methods to characterize fibers are presented below.

3.4.1 Simons' Stain

Simons' Stain has been reported to provide information about the fiber wall structure (Simons 1950). Simons' Stain was used to evaluate the P16/R30 fractions of Streams 0-5 of TMP1 at STFI-Packforsk (now Innventia) in Stockholm, Sweden. The fiber fraction was soaked in two colored reagents, pontamine sky blue and pontamine fast orange. The two dyes have different molecular size and consequently absorbs differently into the fiber wall, thus indicating the openness of the fiber wall structure. Yellow parts indicate an open fiber wall and blue parts indicate untreated fiber wall. A method which included three sublevels of blue and orange was used. The analysis was performed manually by microscopic analysis and color rankings were performed by visual ranking of 1 100 – 1 500 fibers per sample. The results showed that the amount of untreated fibers increased from Stream 1 to Stream 5 which was in line with the results from FiberLab and sheet testing of the same pulp fractions. However, the difficulty to interpret the results, the manual ranking in the methodology and the long time required for the analysis of each sample were the reasons why this method was not further utilized. Results from the analysis are found in Section A10.1 in Appendix A.

3.4.2 Relative bonded area with CyberBond™

Relative bonded area was evaluated in a CyberBond™ device (Das *et al*. 1999) at CTP, Grenoble, France. The P16/R30 fractions of Streams 0-5 of TMP1, TMP2 and TMP3 were analyzed. A diluted fiber solution was spread onto a glass plate and dried, and the total area of the fibers attached to the glass plate was compared to the total projected area. Results of the CyberBond™ evaluations included 500 fibers per sample and the result files contained a value of relative bonded area for each fiber. This method was therefore promising for use in distributions where the characteristics of each fiber is taken into consideration, but was rejected for further analysis in this study due to the low number of analyzed fibers (which could be improved by repeating the testing several times) and the influence that the manual handling in the preparation of the plates could have on the results.

The distributions of the relative bonded area showed that for all three evaluated pulps, the fibers of the first hydrocyclone accept, Stream 1, had higher relative

bonded area than the fibers in Stream 5, and the distribution of the relative bonded area was wider for the fibers in Stream 1 than 5. This was in line with the results of the physical testing of sheets made from the same pulp fractions as well as the FiberLab analysis. The analysis also showed that the relative bonded area of TMP3, the TMP of highest tensile index, was higher than for TMP1 and TMP2, as expected, and the average relative bonded area of the P16/R30 fractions of the three TMPs arranged as expected with respect to general fiber quality (*cf.* Figure 3.1). The average relative bonded area of the hydrocyclone streams did not arrange in the same consistent order as for tensile index, fiber wall thickness index or fibrillation index, which may have been due to the low number of analyzed fibers in the CyberBond™ analysis. Averages and distributions from the analysis are found in Section A10.2 in Appendix A.

3.4.3 Tam Doo and Kerekes method for fiber stiffness

Analysis of single fiber stiffness and flexibility was made using the Tam Doo and Kerekes method (Tam Doo and Kerekes 1981). The analysis was made for TMP1, P16/R30 fractions of Streams 0-5, at KCL (now Labtium) in Espoo, Finland. In the method, single fibers are picked with a pair of fine tweezers and put into a water filled capillary tube. When the water flow into the capillary tube is increased, the hydrodynamic drag force causes the fiber to bend and the maximum deflection in the middle of the fiber is measured. Collapsed, kinked or damaged fibers cannot be tested, neither fibers below 2 mm in length, nor fibers with large differences in diameter, or fibers with a high fibrillation. A good statistical average was reportedly found from measurements of 80 fibers, or less if the fibers were fractionated prior to testing. The method was rejected due to the very low number of analyzed fibers and the fact that only fibers of certain characteristics were measureable. Furthermore, the method is time consuming both in preparing and testing the samples. Results from the analysis are found in Section A10.3 in Appendix A. The results did not show consistent correlations to the results from testing of laboratory sheets or FiberLab.

4 RESULTS AND DISCUSSION

This section contains a summary of the results of the five papers. It also contains some complementary figures and discussions which were considered relevant. More figures and data are found in the appendices.

This study evaluates the relation between fiber dimensions and sheet properties. Cross-sectional fiber dimensions were mainly based on data from the FiberLab analyzer which is commercially available, and the results are naturally limited by the measurement technique of this particular analyzer. The FiberLab analyzer does not measure cross-sectional fiber dimensions of split fibers and the major part of the FiberLab averages shown in the following section are based on raw data which was digitally filtered to ensure that only fibers with intact walls were included in the data. The data of cross-sectional fiber dimensions from FiberLab are indexes and not true values, but have proven equally valuable in rankings. All references to fiber wall thickness, fiber width, fibrillation and collapse resistance as evaluated in the FiberLab analyzer therefore refer to indices.

A model was developed in which the average tensile index of laboratory sheets made from the long fiber fraction was predicted. In order to broaden the range of the model, various types of mechanical pulps were used. These pulps were bleached in different ways and one pulp was also pre-treated with sodium sulfite. The chemical treatments may have affected the strength of sheets made from these pulps, but were not considered apart from their possible effects on fiber dimensions. Instead, the chemical treatments were seen as part of the pulp characteristics.

The predicted tensile index was denoted "BIN", an abbreviation for "Bonding ability INfluence". The general term "fiber bonding ability" is referred to as the propensity of each fiber to form dense sheets of high strength, here mainly evaluated as tensile index of laboratory sheets of the long fiber fraction. The nature of the interactions which join together the fibers in a sheet were outside the scope of this study.

4.1 Hydrocyclone fractionation

The four-stage hydrocyclone fractionation was used as a tool to broaden the span of the average fiber dimensions before the influence of fiber geometry on sheet characteristics was evaluated. The fractionation successfully separated the fibers with respect to external fibrillation, fiber wall thickness, collapse resistance, curl and fiber width.

4.1.1 Partition of pulp in fractionation (Papers I, II)

The partition of the five pulps in the hydrocyclone fractionation was found to be an indication of the characteristics of the fractionated pulps. The TMP3 and SGW pulps were considered to have the highest general fiber quality of the five pulps

(*cf.* Figure 3.1). Almost 50% of the fibers of these two pulps went with the first accept stream. The CTMP intended for mid layer in paperboard which was designed to give high bulk products behaved differently in the fractionation; 75% of the CTMP fibers went with the last accept and reject, Stream 4 and Stream 5 (*cf.* Table A1.3.1a in Appendix A).

4.1.2 Characteristics of the hydrocyclone streams (Papers I, II)

The character of the fibers in each hydrocyclone stream was strongly influenced by the character of the fibers in the pulp that was fractionated. For all pulps in this study, the feed pulp's level of tensile index and density for the long fiber fractions did set the level of the tensile index and density of the long fiber fractions of Streams 1-5, seen in Table A3.1.1 in Appendix A. This was in line with the results reported by Kure *et al.* (1999a).

The long fiber fraction of mechanical pulps has been reported to set or follow the character of the whole pulp (Lindholm 1980, Lindholm 1983, Corson 1980, Mohlin 1989, Rundlöf 2002, page 14) which was also seen for the pulps in this study. Figures 4.1a-b below shows the tensile index and density of the Bauer McNett fractions R16, P16/R30, P30/R50 and P50/R100 in relation to the same property of the whole pulp. For all five pulps, the relation between the Bauer McNett fractions mirrored the relation between the whole pulps, for both tensile index and density.

The CTMP intended for middle layer in paperboard had the lowest tensile index and density, both for the whole pulp and the different Bauer McNett fractions, and the SC grade TMP, TMP3, had the highest. This strongly indicates that the fibers, fines and middle fraction material are all developed in the refining process. In order to evaluate the influence of fiber geometry on tensile index with limited influence of fiber length, this study mainly focused on the P16/R30 and P30/R50 fractions.

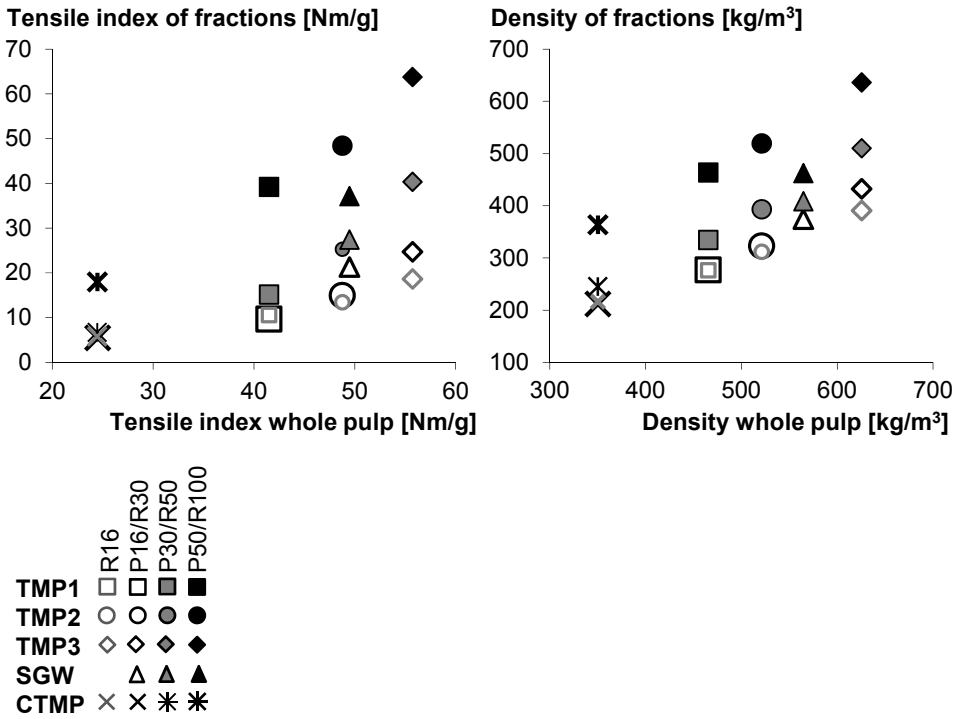

Figures 4.1a-b. The characteristics of the various Bauer McNett fractions mirror the characteristics of the whole pulp, both with respect to tensile index and density.

For all five pulps that were fractionated in the hydrocyclones, differences between Stream 1 (first accept) and Stream 5 (last reject) were larger in the P30/R50 fraction than in the P16/R30 fraction both for sheet- and fiber characteristics (*cf.* Tables A3.1.1 and A4.1.1 in Appendix A). Differences in sheet characteristics between Stream 1 and Stream 5 were also larger in the P16/R30 fraction than in the R16 fraction. This could either indicate that the hydrocyclones were more efficient in fractionating shorter fibers, and/or that the shorter fibers contained a larger range of fiber characteristics which were also reflected in sheet properties.

Fiber characteristics

The average fibrillation and curl indices were highest in the first accept, Stream 1, for all pulps and then decreased. The differences in average fibrillation index between the hydrocyclone streams were often numerically small but significant, repeatable and consistent even though the distributions of fibrillation were broad for all samples. Stream 1 had the lowest average fiber wall thickness index whereas Stream 5 had the highest. Collapse resistance index was calculated from fiber wall thickness and fiber width according to Equation 3.5a (Paper I) and Equation 3.6a (Papers II-IV) and had a high correlation to fiber wall thickness index.

The differences in fiber width were generally small between the hydrocyclone streams which was confirmed both by FiberLab and cross-sectional SEM micrograph analysis. Arithmetic averages of fiber width were lowest in the first accept stream and highest in the last reject for all evaluated pulp fractions whereas wall volume weighted averages of fiber width shifted the ranking between the streams for two of the five pulps. This is discussed in Section 4.1.5.

The results of the fractionation were in line with earlier publications for tensile index (Sandberg *et al.* 1997), fiber wall thickness (Kure *et al*. 1999a) and indirect measures of degree of external fibrillation (Wood and Karnis 1979, Karnis 1981, Shagaev and Bergström 2005). No consistent conclusions of the expected results of fiber width were available in the literature. In some of the two-stage fractionations made by Kure *et al.* (1999a), the accept stream had higher average fiber perimeter than the reject, and in some the average fiber perimeter was higher for the reject. Generally, the reported differences in fiber width were small between the accept- and reject streams. The average fiber perimeter presented by Kure *et al.* was based on cross-sectional SEM analysis of fibers from the Bauer McNett +50 fraction which may partly explain differences between the results of this study and their results.

TMP3 had the lowest fiber wall thickness of all evaluated pulp samples, and SGW the highest, for both the P16/R30 and P30/R50 fractions. SGW also had the highest fibrillation index and CTMP had the lowest. Both the TMP3 and the SGW pulp were intended for SC grade products, but the differences in fiber wall thickness and fibrillation were expected based on known differences between the process types, and are discussed more in detail in Section 4.1.4.

Sheet characteristics

For all evaluated Bauer McNett fractions, the highest tensile index was found in the first accept stream and the lowest in the last reject stream for all five pulps. Tensile index also decreased from one hydrocyclone stream to the following (*cf.* Papers I, II, Table A3.1.1 in Appendix A). The sheet density showed similar tendencies, but the decrease from one stream to another was not as consistent as for tensile index (*cf.* Table A3.1.1 in Appendix A). Figure 4.2 below shows the correlation between density and tensile index for the P16/R30 and P30/R50 fractions of the hydrocyclone streams.

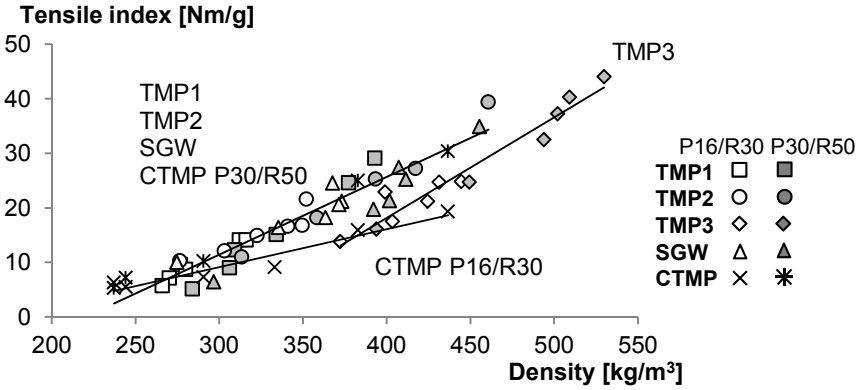

Figure 4.2. Tensile index increased linearly with increasing density but at slightly different levels for the various pulp fractions. TMP3 intended for SC grade products had higher density at a given tensile index than the news grade TMP. This may have been a result of the overall lower fiber wall thickness index of TMP3 compared to the other pulps. The P16/R30 and P30/R50 fractions of CTMP had different relations between density and tensile index which indicates different fiber characteristics for fibers of different lengths.

The correlation between tensile index and density was linearly grouped for all pulp fractions which showed that differences between the pulp fractions were mainly a result of fiber characteristics and not solely a densification of the sheet. TMP1, TMP2, SGW and the P30/R50 fraction of CTMP correlated on the same level, whereas TMP3 had higher density at a given tensile index. TMP3 had the overall lowest fiber wall thickness index of all pulps (*cf.* Table A4.1.1 in Appendix A) and it is possible that this resulted in a separate density level compared to the other four pulps. This may also have been an effect of the hydrogen peroxide bleaching.

The two Bauer McNett fractions P16/R30 and P30/R50 followed the same correlations between tensile index and density for the three TMPs and SGW whereas the two length fractions of CTMP correlated at different levels. The tensile index of the P30/R50 fraction of CTMP increased with increasing density at the same rate as for the TMPs and SGW, whereas the density of sheets from the P16/R30 fraction gave a lower increase in tensile index. It can be speculated that the fibers of the P16/R30 and P30/R50 fractions of the CTMP were differently sulfonated, something that would benefit from further evaluations.

A common level of sheet- and fiber characteristics in the last reject

For all five pulps, the tensile index of the hydrocyclone streams converged towards a value in the last reject which was common for all evaluated Bauer McNett fractions of each pulp, *cf.* Figures A3.2.1a-e in Appendix A. Also the fibrillation index and fiber wall thickness index converged towards a common lowest value in the last reject, *cf.* Appendix A, Figures A4.2.1a-j. Shives were not included in the

FiberLab data, and the level of fiber wall thickness and fibrillation was expected to be an effect of the fiber characteristics without disturbances of shives. This shows that each pulp had an inherent lowest level of fiber characteristics contributing to tensile index which was independent of fiber length.

In mechanical pulping it may be believed that strength properties of a sheet can be improved and a smoother surface achieved if fibers are "cut" to decrease the amount of long fibers. These results show that such actions are unnecessary for increasing the strength of a sheet, as the fiber characteristics that influenced the tensile index of the pulp fraction of lowest strength, were independent of fiber length. It is also possible that small pieces of cut, coarse fibers can increase the risk of linting and disturb the sheet structure.

The levels of the tensile index in Stream 5 for the five pulps appeared to follow known differences in process and specific energy consumption. The ranking of the lowest tensile index level of the TMPs and CTMP (Figures A3.2.1a-e, Appendix A) correlated to the estimated general fiber quality of each pulp (Table 3.1). The lowest tensile index level of the SGW intended for SC grade was at a similar level as TMP1, the news grade TMP, although the first accept streams of SGW reached higher levels of tensile index than those of TMP1, *i.e.* the distribution of the fiber characteristics of the SGW pulp was wider than for TMP1. This was also observed in *BIN* distributions (*cf.* Section 4.3.2 and Figure 7 in Paper V) where the lowest *BIN* level was similar for TMP1 and SGW but the SGW contained more fibers of high *BIN* (*cf.* Figure 4.13). In tensile testing, a sheet breaks at its weakest point and it is possible that the characterization of a pulp's lowest level of tensile index, or fiber characteristics that influence tensile index, would be a more useful measure than the average or highest value.

4.1.3 Acoustic emission (Paper I)

In Paper I, it was shown that the recording of acoustic events during slow tensile testing enabled the prediction of fracture toughness and fracture toughness index of laboratory sheets from the P16/R30 fractions. As a method for predicting fracture toughness, this had little interest since the time saved by using acoustic emission instead of standard fracture toughness testing was negligible in comparison to the time required for producing the test sheets. However, instead of only one figure representing the final breaking point of a sheet, the recording of acoustic events during tensile testing made it possible to follow the fracture behavior in new ways. This revealed interesting differences between the sheets made from the hydrocyclone streams of TMP1 and TMP2 that were not recognizable elsewhere (*cf.* Figures 9a-b in Paper I and Figures A11.4 a-f, A11.5a-f in Appendix A). For example, TMP2 showed a slower increase in the number of breaks, *i.e.* recorded events with time, than TMP1, which suggested that the sheets

made from TMP2 were tougher. Acoustic emission monitoring could enable novel, useful methods to characterize both laboratory sheets and final paper and is further discussed under recommendations for future work (Section 6).

4.1.4 Influence of fiber dimensions on long fiber sheet properties (Paper II)

Relations between fiber characteristics

It was found that the tensile index of both the P16/R30 and P30/R50 fractions could be predicted with high accuracy from fiber wall thickness and fibrillation index, Section 4.2.1. The relation between fiber wall thickness and fibrillation of the pulp fractions was helpful in explaining the differences between the pulp types and resulted in three groups; one for the TMPs, one for the CTMP and one for the SGW, Figure 4.3. For all three pulp types, the fibrillation increased linearly with decreasing fiber wall thickness.

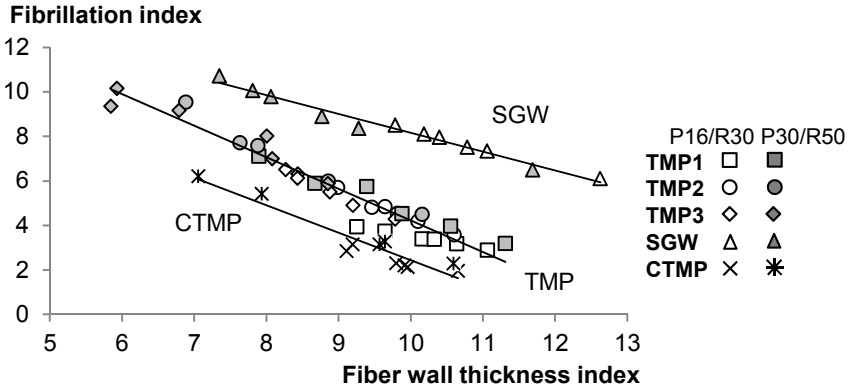

Figure 4.3. The relation between fibrillation index and fiber wall thickness index showed that the three pulp types TMP, SGW and CTMP had different internal correlations between fiber wall thickness and fibrillation. This was expected from process differences resulting in intact fiber walls of the chemically softened CTMP and torn and broken fiber walls for the SGW fibers.

The fibers of the SGW had a significantly higher fibrillation index at a given wall thickness index than fibers of the TMPs, and the CTMP fibers had a lower. This reflects the differences between the three process types where the broken walls of the SGW fibers resulted in high measures of fibrillation index and the chemical pre-treatment resulted in smooth surfaces of the CTMP fibers. Differences in fiber wall thickness index between the SGW and the TMPs also seemed to be larger at low fibrillation index levels, than at high. The fibrillation index of the longest fiber fraction (P16/R30) of TMP1 increased less with decreasing fiber wall thickness index than the rest of the TMPs and the P30/R50 fraction of TMP1. It is possible that this was related to differences between the conical and double disc refining processes, something that would benefit from further evaluations.

When comparing measured fiber dimensions with data from handsheets made of the Bauer McNett fractions, it was found that arithmetic averages of fibrillation index, fiber wall thickness index and collapse resistance index all gave linear correlations to tensile index, but on different levels. The fibrillation index had a positive influence, whereas fiber wall thickness and collapse resistance had a negative, Figures 4.4a–c. Collapse resistance index was calculated from fiber wall thickness and fiber width (Vesterlind and Höglund 2005), Equation 3.6a, and the strong correlation between fiber wall thickness index and collapse resistance index (Figure 4.6a) resulted in similar relations to tensile index for fiber wall thickness and collapse resistance index. Arithmetic averages of fiber width had a negative influence on tensile index but the data was scattered and the correlation resulted in two groups – one for the P16/R30 fraction and one for the P30/R50 fraction, Figure 4.4d. Correlations between fiber dimensions and sheet density are found in Section A6 in Appendix A and in Section A7.5 correlations between wall volume weighted averages of fiber dimensions and tensile index are found.

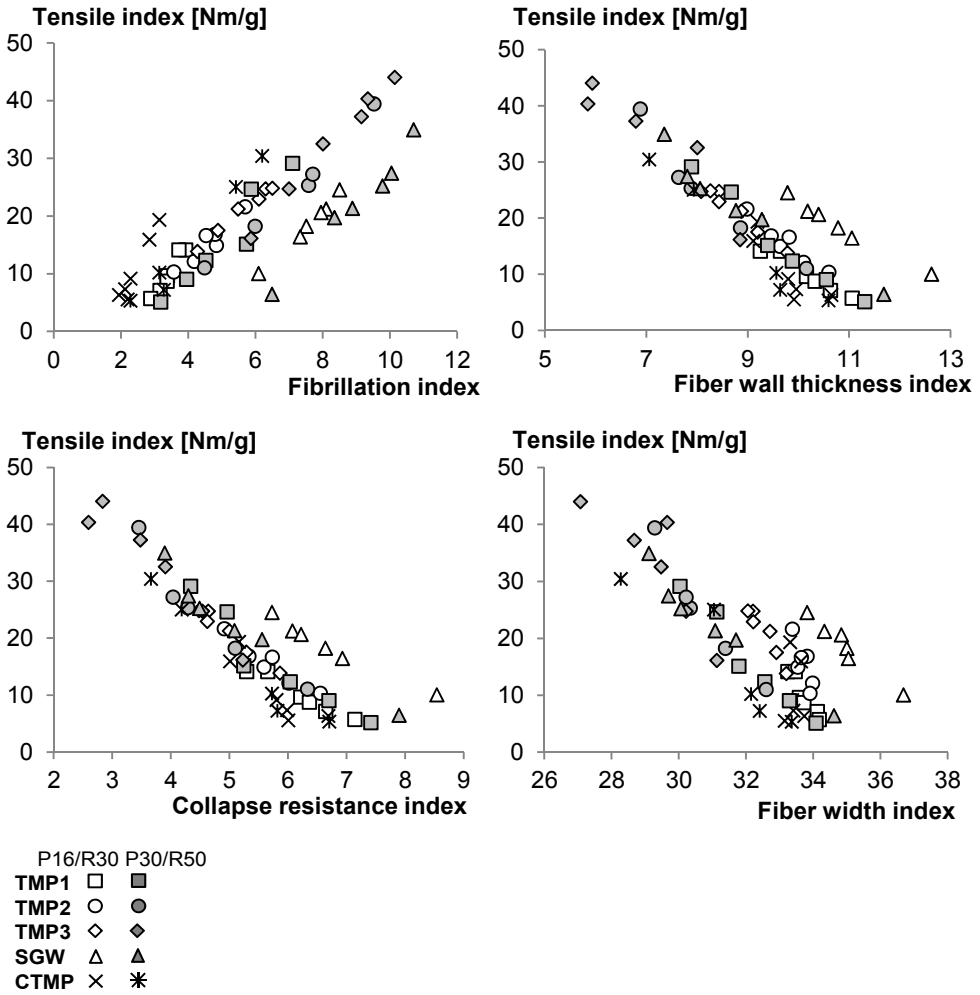

Figures 4.4a-d. The arithmetic averages of fibrillation index, fiber wall thickness index and collapse resistance showed linear correlations to tensile index. For fiber width, the data was scattered and the correlation resulted in two groups – one for the P16/R30 fraction and one for the P30/R50 fraction, Fibrillation index had a positive influence on the tensile index whereas the influence of arithmetic fiber wall thickness, collapse resistance and fiber width was negative.

The relation between tensile index and fibrillation (Figure 4.4a) was linear with the same slope for all pulp fractions but at three different levels that seemed to be process dependent. For all pulp samples, the fibrillation index was higher for the fibers in the P30/R50 fraction than in the P16/R30 fraction (see also Table A4.1.1 in Appendix A). The influence of wall thickness and collapse resistance on tensile index was similar for all fractions of the pulp streams except the longest SGW fibers, whereas there was a wide range of fiber widths at a given tensile index.

Process-induced differences in sheet- and fiber characteristics

TMP

The high temperature of the TMP process and the high frequency by which fiber material is hit by the refiner bars in refining gives a softening of the lignin, and the TMP fibers are therefore more easily separated from each other and less broken than SGW fibers. The wall thickness of the TMP fibers is continuously reduced from the initial defibration throughout the refining process, which results in lower wall thickness than for SGW fibers. As the fiber wall is peeled, parts of the fiber wall come off the fibers to form fines. At the same time, fibrils attached to the fibers are formed, and the area of measurable external fibrils increases.

For all three TMPs evaluated in this study, the degree of external fibrillation increased linearly with decreasing fiber wall thickness. The different refining energies resulted in different levels of fiber wall thickness and fibrillation, but all three TMPs followed the same relation, Figure 4.3. The fibers of the TMPs and the SGW with the lowest average fiber wall thickness had the same level of fibrillation index although the wall thickness of the SGW fibers was higher. The P30/R50 fraction of TMP3 had the highest fibrillation index and lowest fiber wall thickness index of the three TMPs. This was expected from the higher level of specific energy used in refining of this pulp compared to the news grade TMPs. The fibers of the longest Bauer McNett fraction, P16/R30, of TMP1 correlated at a level between TMP2/TMP3 and the CTMP, which showed that the fiber characteristics of some of the fibers of TMP1 and CTMP were similar. This was also reflected in the *BIN* distributions seen in Figure 4.13, which revealed some resemblance between TMP1 and CTMP.

The three TMPs were intended for different final products and the fibers of these pulps had different levels of wall treatment. The pulps were also bleached differently – TMP1 was dithionite bleached and TMP3 was bleached with hydrogen peroxide. Despite this, tensile index developed linearly with increasing fibrillation index and decreasing fiber wall thickness and collapse resistance for all three TMPs (Figures 4.4a-c). This shows that the fiber characteristics that resulted in a higher sheet density at a given tensile index of TMP3 (*cf.* Figure 4.2) were not recognizable in FiberLab measurements of fiber wall thickness and fibrillation index.

CTMP

In CTMP production, the separation of the fibers from the wood matrix is facilitated by chemical softening (sulfonation) of the wood chips. This results in a separation predominantly in the middle lamella/primary wall region and fibers with an intact fiber wall and with a low degree of fibrillation are produced, which was reflected in the low fibrillation index at a given fiber wall thickness index

(Figure 4.3) compared to the other pulp samples. The correlation between fiber wall thickness and fibrillation was similar for the P16/R30 and P30/R50 fractions of CTMP unlike the relation between density and tensile index (*cf.* Figure 4.2). This showed that the higher density at a given tensile index of the P16/R30 fraction of the CTMP was the result of other fiber characteristics than fiber wall thickness and fibrillation as measured in FiberLab.

Both Bauer McNett fractions of CTMP had a lower fibrillation index at a given tensile index than the SGW and the TMPs, which was expected from the intact, smooth fiber surfaces that are a result of the CTMP process. The fractionation of the CTMP resulted in very little pulp in the two first hydrocyclone streams (*cf.* Tables A1.3c-d in Appendix A) but the fibers of the P30/R50 fraction of these two streams had a rather high fibrillation index, 6.2 and 5.4 respectively (*cf.* Table A3.1.1 in Appendix A). This indicates that some of the fibers in the CTMP behaved more like fibers in a TMP process, in which the separation of the fibers from the wood matrix resulted in some fiber shortening, fiber wall thickness reduction and development of fibrils. The correlation between density and tensile index for the P30/R50 fraction of CTMP, Figure 4.2, support this.

The P16/R30 fraction of CTMP showed a steeper increase in tensile index with increasing fibrillation index than the other pulp fractions whereas the relation between fibrillation index and tensile index of the P30/R50 fraction followed the relation of the TMPs. It is possible that this can be explained by the influence of the chemical pre-treatment on the fiber wall and that fibers that were most affected by the pre-treatment were more easily released from the wood matrix; easier release from the wood matrix would have resulted in less fiber shortage compared to fibers that were harder attached. If so, the CTMP fibers of the longer Bauer McNett fraction (P16/R30) would be more influenced by the chemical pre-treatment than the fibers of the shorter P30/R50 fraction, which would explain the differences in fiber characteristics between the P16/R30 and P30/R50 fractions of this CTMP. This would benefit from further evaluations.

SGW

At a given tensile index and wall thickness, the SGW fibers had a higher fibrillation index than the TMPs and the CTMP. This was expected as the SGW process typically result in fibers of high fiber wall thickness and high fibrillation index. SGW fibers are torn from their wood matrix under atmospheric conditions at temperatures below the lignin softening temperature, which results in broken fibers. These fibers still have relatively untreated, thick, fiber walls. The large areas of broken fiber wall are recognized as fibrils by the optical analyzer and the level of fibrillation index was significantly higher for all SGW samples than for TMP and CTMP samples, *cf.* Figure 4.3 and Table A4.1.1 in Appendix A. SGW fibers in the lower range of fibrillation index also had a high fiber wall thickness. This implies

either that the thick-walled fibers were easier to pull from the wood than the thin-walled fibers, which resulted in less broken parts of fiber wall, or that the thin-walled fibers became more broken during the process.

With respect to fiber wall thickness (Figure 4.4b) and collapse resistance (Figure 4.4c), the two Bauer McNett fractions of the SGW behaved differently. The fiber wall thickness and collapse resistance indices of the P30/R50 fraction correlated to tensile index at the same level as the TMPs (Figures 4.4b-c) whereas the P16/R30 fraction had higher fiber wall thickness and collapse resistance than the TMPs at a given tensile index. Also the fiber width of the P16/R30 fraction was higher than the width of the other pulp fractions. The preserved fiber length of the fibers in the P16/R30 fraction indicates that the P16/R30 fibers of this groundwood sample were released from the wood matrix comparatively easy, which resulted in untreated, thick fiber walls. This was also supported by the degree of broken fiber surface (evaluated as fibrillation index) which was slightly lower for the P16/R30 than for the P30/R50 fraction (*cf.* Figure 4.4a and Table A4.1.1 in Appendix A).

Effect of fiber characteristics on predicted tensile index

The model to predict tensile index based on arithmetic averages of fibrillation and fiber wall thickness gave one single correlation between measured and predicted tensile index for all samples except the P30/R50 fraction of the SGW (*cf.* Figure 4.8). At a given measured tensile index, the predicted tensile index was too high for the six samples of this fraction.

Both Bauer McNett fractions P16/R30 and P30/R50 of the SGW had higher measured fibrillation index at a given tensile index than the other pulp fractions (Figure 4.4a) which had a positive influence on the predicted tensile index. The P16/R30 fraction had a slightly lower fibrillation index than the P30/R50 fraction but, above all, thicker fiber walls (Figure 4.4b) that compensated for the high fibrillation index in the prediction. This resulted in the same correlation between predicted and measured tensile index for the P16/R30 fraction of the SGW as for the majority of the pulp samples that were analyzed.

Wall volume weighted averages of fiber wall thickness and fibrillation resulted in correlations to tensile index at separate levels for the three pulp types (*cf.* Figures A7.5a-b in Appendix A). However, tensile index predicted from a combination of wall volume weighted averages of fiber wall thickness and fibrillation resulted in the same correlation to measured tensile index for all pulp fractions, also the P30/R50 fraction of the SGW (*cf.* Figure 7b in Paper III and Figure B1.2.1 in Appendix B). This shows that a model based on wall volume weighted averages is more accurate in predicting the characteristics of a sheet than a model based on arithmetic averages, which is further discussed in Section 4.2.1.

At a given tensile index, the CTMP had slightly lower fiber wall thickness and collapse resistance than the rest of the pulps (Figures 4.4b-c). This was beneficial to tensile index and was likely why the CTMP followed the same linear correlation between predicted and measured tensile index as the TMPs (Section 4.2.1) despite its lower level of fibrillation index.

Differences in fiber characteristics between the P16/R30 and P30/R50 fractions

The correlation between tensile index and fiber width index resulted in two separate groups for the two Bauer McNett fractions, Figure 4.4d. At a given tensile index, the range of fiber widths was quite broad and fibers from the P16/R30 fraction were wider than those from the P30/R50 fractions of all five pulps. Different relations for the P16/R30 and P30/R50 fractions were also observed in the relation between fiber width and fiber wall thickness (Figure 4.5) and fiber width and collapse resistance (Figure 4.6b). This means that fiber width has little and inconsistent influence on the tensile index of sheets made from long fiber fractions of mechanical pulps.

The geometry of the fibers in the P16/R30 and P30/R50 fractions differed slightly with respect to wall thickness and width. All pulp samples showed linear relations between fiber wall thickness and fiber width but on slightly different levels for the P16/R30 fraction compared to the P30/R50 fraction, Figure 4.5. For the P16/R30 fraction of the CTMP, the differences in average fiber width between the hydrocyclone streams were very small and this fraction was not included in the linear correlations seen in Figures 4.5 and 4.6b.

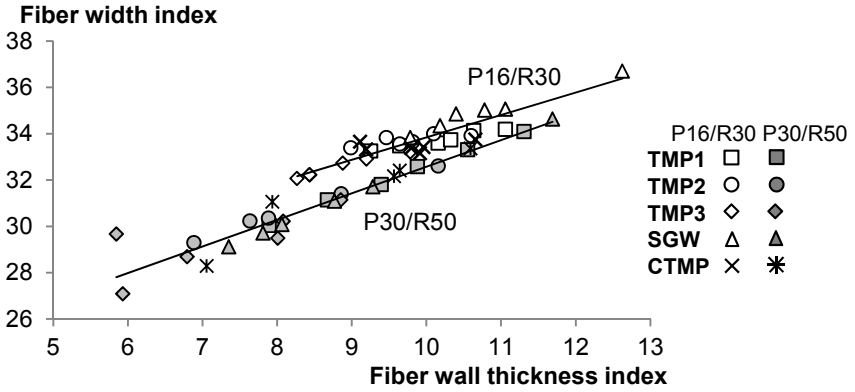

Figure 4.5. The correlation between fiber wall thickness and fiber width resulted in two linear relations for the P16/R30 and P30/R50 fractions respectively. The fibers of the P16/R30 fraction had thinner walls at a given fiber width index than the fibers of the P30/R50 fraction and can therefore be expected to have more flexible cross-sections.

Mechanical pulp fibers produced from Norway spruce include a wide range of both fiber width and fiber wall thickness. A fiber of a given width can have both thin and thick walls (Höglund 1997, Kure *et al.* 1999a). A high correlation between wall thickness and width can therefore not be expected. For the samples originating from the hydrocyclone fractionation, the fibers of the P16/R30 fraction had thinner walls at a given width than fibers of the P30/R50 fraction. It can be speculated if intrinsic differences in fiber characteristics were the reason for the differences between the two fiber length fractions. It is possible that the thin-walled fibers were more easily broken which resulted in higher amount of such fibers in the shorter P30/R50 fraction compared to the longer P16/R30 fraction. This was supported by conclusions made by Mohlin (1997) and Rusu *et al.* (2011). The fiber length range of the P16/R30 and P30/R50 fractions of each pulp is found in Table 3 in Paper II.

One common misconception in mechanical pulping is that long fibers are always coarse and should be removed from the pulp to avoid disturbances in the structure and surface of a sheet. At the same time, in producing high quality printing paper, costly kraft pulp is added to the mechanical pulp to increase the amount of long, slender fibers. These results show that long fibers can have more flexible cross-sections than shorter fibers and thereby be an asset in mechanical pulps. This would benefit from further evaluations. The correlation between fiber wall thickness and collapse resistance was linear for all evaluated pulp samples and the relation was the same for the P16/R30 and P30/R50 fractions. This was also true for volume weighted averages (Figure A7.4.1b in Appendix A). Collapse resistance and fiber width correlated linearly but at two levels – one for the P16/R30 fraction and one for the P30/R50 fraction, Figure 4.6b.

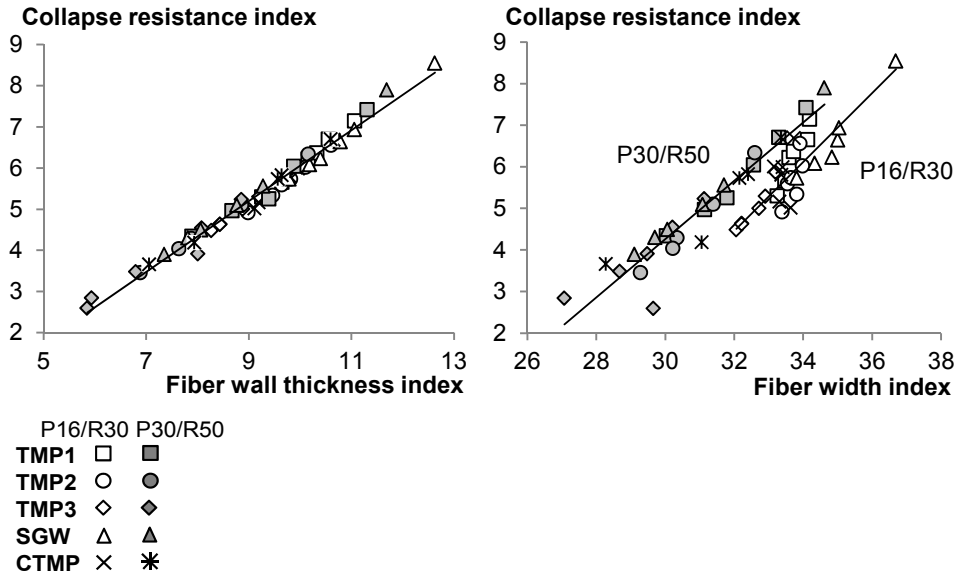

Figure 4.6a-b. Collapse resistance index correlated linearly to fiber wall thickness index for all evaluated pulp samples (left), but at a given collapse resistance, the fibers of the P30/R50 fraction had a smaller width than those of the P16/R30 fraction. This may have been caused by different behavior of various fiber types in the refining and grinding processes.

At a given collapse resistance index, all evaluated fiber fractions had the same wall thickness, but the fibers of the P30/R50 fraction had smaller diameters than the fibers from the P16/R30 fraction. This confirmed the earlier observation (*cf.* Figure 4.5) that fibers from the P30/R50 fraction had a lower fiber width index at a given fiber wall thickness than the P16/R30 fraction. Höglund (1997) showed in evaluations of fibers from the R30 fraction of TMP made from Norway spruce that there is a clear difference in fiber wall thickness between early- and latewood fibers, but a wide variation in fiber width for both fiber types. The fiber width is a poor measure for evaluation of the fiber's influence of sheet strength, as fibers of both large and small diameter can have high or low wall thickness and ability to form sheets of high strength.

4.1.5 Weighted averages of fiber characteristics (Paper III)

Fiber width

The fiber width index of the hydrocyclone streams was ranked differently depending on the method by which the fiber width averages were weighted. The arithmetic fiber width was lowest in Stream 1 and highest in Stream 5 for the P16/R30 and P30/R50 fractions of all five pulps. For the two pulps that originated from processes with double disc refiners, TMP2 and TMP3, the ranking between the hydrocyclone streams changed to the complete opposite when averages were wall volume weighted. For these pulp fractions, the highest fiber width index was that of Stream 1 and the lowest that of Stream 5. An example is shown in Figure 4.7. It is possible that the shifted rankings of average fiber width index originated from differences in fiber treatment between double disc refining and refining in single disc refiners or in grinders, but this was not investigated any further.

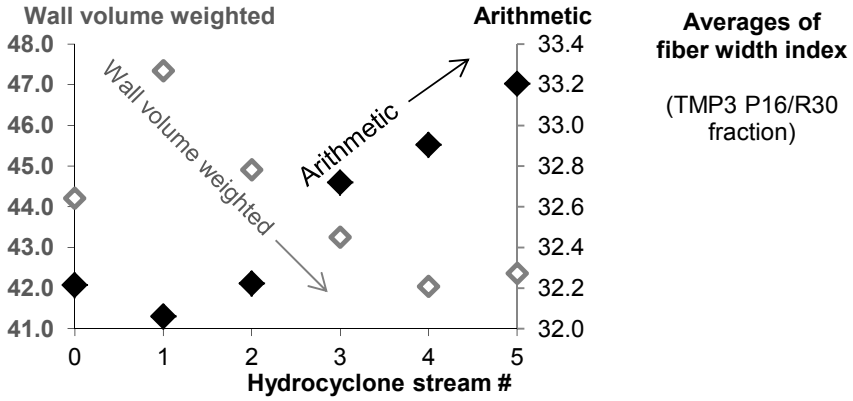

Figure 4.7. For the pulp samples that originated from processes with double disc refiners, TMP2 and TMP3, the ranking of the hydrocyclone streams with respect to fiber width changed to the complete opposite when averages were wall volume weighted instead of arithmetic.

The arithmetic and length weighted fiber width index of the filtered FiberLab data correlated well (*cf.* Figure 3b in Paper III) and the shifted ranking of fiber width originated from the cross-sectional geometry of the fiber, rather than fiber length. For the fibers of thinnest walls (fiber wall thickness index below 9.6), the variation in average fiber width between the streams was very small. As expected, the amounts of fibers with very high wall thickness (fiber wall thickness index above 25) were lowest in the first accept stream and highest in the last reject stream, between 0.2 and 5% of all fibers. Differences in wall volume weighted averages of fiber width between Stream 1 and Stream 5 were smaller when the fibers of very high wall thickness were removed from the data and it was clear that these few fibers influenced the results.

Fiber wall thickness, fibrillation, and collapse resistance

When averages of fiber wall thickness index were wall volume weighted compared to arithmetic, the curves representing the P16/R30 and P30/R50 fractions of the hydrocyclone streams of TMP3 were slightly altered into a U-shape, but the complete shift in ranking that was observed for fiber width index was not seen at all. The ranking of average fiber wall thickness index of the other pulp samples was not affected. Neither fibrillation index nor collapse resistance index showed any changes in ranking when averages were wall volume weighted compared to arithmetic. Wall volume weighted averages of fiber wall thickness, fiber width, fibrillation and collapse resistance indices are found in Table 1 in Appendix 1 of Paper III.

The collapse resistance index takes into consideration the relation between fiber width and wall thickness (Equation 3.6) and the correlation between fiber wall thickness and collapse resistance index is high (*cf.* Figure 4.6a). This may be the reason why the results of wall volume weighted collapse resistance index corresponded better to the expected results of hydrocyclone fractionation reported in the literature (Kure *et al.* 1999a) than fiber width.

4.2 Modelling strategies

This section describes how fiber dimensions from the FiberLab analyzer were used to predict the tensile index of the long fiber fractions P16/R30 and P30/R50 and motivates why certain modeling approaches were selected over others.

The denotation "bonding ability" is sometimes used to describe a fiber's effect on the strength and structure of laboratory sheets apart from fiber length, *cf.* Section 2.4.3, and the predicted tensile index was denoted *BIN*, short for *B*onding ability *IN*fluence.

4.2.1 *BIN* model as a tool to predict tensile index (Papers I-V)

Analysis of laboratory sheets is often used to get an indirect measure of the fiber characteristics in a mechanical pulp, despite the variations which are included in both making and testing laboratory sheets. If the refiner or other parts of the mechanical pulping process is adjusted based on the results of sheet testing, there is a risk that unnecessary variations are introduced which may result in increased electrical energy consumption and/or decreased pulp quality. With the ability to evaluate fiber characteristics directly, production and analysis of laboratory sheets becomes an unnecessary intermediate step.

Derivation of *BIN*

The original *BIN* model was based on fibrillation index and collapse resistance index (Paper I). The tensile index of laboratory sheets from the P16/R30 fraction of TMP1 and TMP2 was predicted with high accuracy by the use of linear regressions of fiber dimensions. It was found that the model was valid also for the P30/R50 fractions of these pulps and for the P16/R30 fractions of TMP3, SGW and CTMP as well as the P30/R50 fractions of TMP3 and CTMP. The exception to this was the P30/R50 fraction of the SGW which correlated linearly to tensile index but on a higher *BIN*-level than all the other pulp fractions. In total, 12 samples were used as a basis for the model and 46 for validating it. All data was based on measurements of the hydrocyclone streams. The correlation between *BIN* based on arithmetic averages of collapse resistance and fibrillation and tensile index are seen in Figure 24b in Paper II.

Various *BIN* models based on arithmetic averages were evaluated, the correlation between *BIN* and tensile index was found to be higher if fiber wall thickness index and fiber width index were combined into collapse resistance index before the linear regressions, than if fiber wall thickness and fiber width were used separately (Figures B1.1.1a-b in Appendix B). The use of fiber width as a separate factor in the *BIN* model even reduced the linearity between *BIN* and tensile index compared to a model without fiber width, *cf.* Figures 5b and 5c in Paper III.

***BIN* model based on wall volume weighted averages**

The *BIN* model was designed to account for the influence of the characteristics of fibers on the tensile index of a sheet consisting of these fibers. In a laboratory sheet that is pressed according to standard procedures, the lumen area may be approaching zero for some fibers. The volume of the laboratory sheet should then theoretically be composed mainly of the volume of the fiber wall and the spaces between the fibers. In order to evaluate if the *BIN* model became more accurate when wall volume weighted averages of fiber dimensions were used, the fibrillation, fiber wall thickness, fiber width and collapse resistance indices were wall volume weighted and the linear regressions were remade (Paper III). Linear regressions based on wall volume weighted averages of fiber wall thickness and fibrillation resulted in a single linear correlation between *BIN* and tensile index for all pulp fractions, also including the P30/R50 fraction of the SGW which correlated on another level then the rest of the pulp samples when the model was based on arithmetic averages. This is seen in Figure 7b in Paper III and in Figure B1.2.1 in Appendix B.

The shifted ranking of average fiber width index that occurred when fiber width was wall volume weighted instead of arithmetic (Section 4.1.5) influenced also the *BIN* model. Linear regressions made from wall volume weighted averages of fiber width resulted in a positive influence of fiber width on the tensile index, the opposite to arithmetic. The influence of fibrillation index, fiber wall thickness index and collapse resistance index did not change.

Current *BIN* model

The use of fiber width as a single factor reduced the accuracy of the *BIN* model. Until the influence of fiber width on tensile strength is fully established, also collapse resistance index which contained fiber width index was excluded from the model. There was a high correlation between collapse resistance index and fiber wall thickness (Figure 4.6a) and instead of collapse resistance index, only fiber wall thickness index and fibrillation index were used in *BIN* models.

The predicted tensile index was intended to be used for distributions based on single fiber characteristics in which the distributions themselves can be weighted. In order to produce these weighted distributions of predicted tensile index, the *BIN* model needed to be based upon arithmetic averages, as least as a first approach. If the *BIN* model is to be used to predict averages and not distributions, it is recommended to base the model on wall volume weighted averages.

Figure 4.8 shows the correlation between predicted and measured tensile index of the fifty-eight Bauer McNett fractions (P16/R30 and P30/R50) of the hydrocyclone fractionated samples. The tensile index was predicted using the *BIN* model based on arithmetic averages of fiber wall thickness and fibrillation.

The equation resulting from the linear regressions used to predict tensile index is found below, Equation 4.1.

$$BIN\,(arithmetic) = 29.95 - 3.09\,Wall + 3.36\,Fibrill \qquad \text{Eq. 4.1}$$

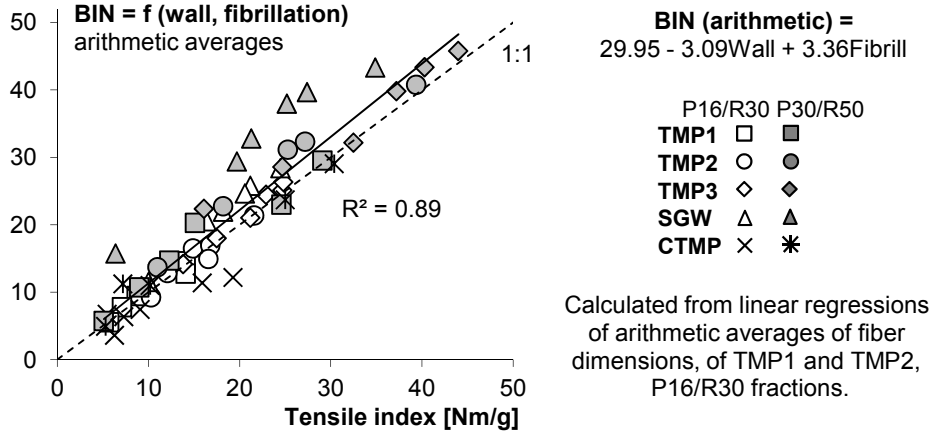

Figure 4.8. In order to use the predicted tensile index for weighted distributions, the *BIN* model needed to be based on arithmetic averages, at least as a first approach. Fiber width index reduced the accuracy of the *BIN* model and was excluded from the model until further evaluated. The current *BIN* model to predict tensile index from fiber dimensions was based on arithmetic averages of fiber wall thickness index and fibrillation index.

The higher fibrillation index of the SGW compared to the other pulps affected the *BIN* model which resulted in higher values of predicted tensile index than measured, for the SGW P30/R50 fraction. For the P16/R30 fraction of the SGW, the higher fibrillation index was compensated by the higher fiber wall thickness, which resulted in a correlation on the same level as the TMPs and the CTMP between predicted and measured tensile index. Figures B1.2.2a-d in Appendix B show that neither fibrillation index, fiber wall thickness index, collapse resistance index or fiber width index was enough to predict tensile index with acceptable accuracy when used as the single fiber characteristic in the *BIN* model.

The *BIN* model was valid for a surprisingly large range of pulp types. There were significant internal differences in the relation of fiber wall thickness and fibrillation for the evaluated samples of SGW, TMPs and CTMP, both for arithmetic (*cf.* Figure 4.3) and wall volume weighted averages (Figure A7.4.1a in Appendix A). Despite this, the combination of fiber wall thickness and fibrillation resulted in a linear correlation on the same level between predicted and measured tensile index for all pulp fractions except the P30/R50 fraction of the SGW for arithmetic averages, and for all pulp fractions for wall volume weighted averages.

It is noticeable that *BIN* based on fiber wall thickness index and fibrillation index gave the same correlation to tensile index for both the P16/R30 and P30/R50 fractions. This shows that fiber dimensions from both these fractions influenced tensile index in similar ways regardless of the differences in fiber length. The R16 fraction could not be analyzed in the FiberLab due to the size of the analyzer's measurement capillary. It is therefore still not known if also fibers that were longer than those of the P16/R30 fraction followed the same *BIN* model as fibers from the P16/R30 and P30/R50 fractions. This would benefit from further evaluations.

The approach of predicting sheet characteristics from fiber dimensions may also be applicable on final paper. This would enable faster feed-back from final product to refining operations and improve the ability of steering the refining process with respect to the fibers' performance on the paper machine to increase the final product quality. On-line analysis of fiber characteristics could also be helpful in continuously keeping the whole refining process within given operating windows and thereby optimizing the electrical energy input. Hopefully, technology will continue to develop so that on-line measurement of fiber wall thickness and fibrillation of unique fibers becomes available in the near future.

4.2.2 Effect of the exaggerated fiber wall thickness in FiberLab (Paper III)

The analysis of fiber dimensions such as fiber wall thickness and fiber width in optical analyzers is not standardized, and consequently the levels of the results differ between analyzers. The calibration of individual analyzers also affects the level of the results. For the FiberLab analyzer, the level of the fiber wall thickness index is 3-4 times higher than the true thickness of a fiber wall. Table 2.1 in Section 2 lists the range of fiber wall thickness for fibers in wood from Norway spruce (*Picea abies*). To evaluate if the exaggerated fiber wall thickness had any effect on the model to predict tensile index other than numerical, the fiber wall thickness was divided by four, and all calculations including weighting the average fiber dimensions were remade.

The equation (Equation 4.2a) for predicting tensile index from wall volume weighted averages of fiber wall thickness and fibrillation was (*cf.* Figure 7b in Paper III and Figure B1.2.1 in Appendix B):

BIN (wall volume weighted, **wall/1**, f(wall thickness, fibrillation)) =

$$= 29.29 - 2.46 \cdot \text{Wall thickness index} + 4.40 \cdot \text{Fibrillation index} \qquad \text{Eq. 4.2a}$$

By dividing the fiber wall thickness of all individual fibers by four and recalculating the weighted averages of fiber wall thickness and fibrillation, the following equation (Eq. 4.2b) was obtained:

BIN (wall volume weighted, **wall/4**, f(wall thickness, fibrillation)) =

= 27.37 - 9.06·Wall thickness index + 4.56·Fibrillation index Eq. 4.2b

In comparisons of Equations 4.2a and 4.2b it became apparent that the corrected fiber wall thickness index only resulted in numerical changes to the *BIN* equation and did not result in any changed rankings.

In Papers II and IV and related publications (Ferritsius *et al.* 2009, Reyier *et al.* 2011), results were published where *BIN* was predicted from multivariate analysis of fiber wall, fiber width and fibrillation indices, and tensile index and density. This *BIN* model resulted in numerically lower values of *BIN* than the model based on linear regressions, but rankings between the evaluated pulp fractions remained. More knowledge about which fiber dimensions that influence the structure of a sheet is needed before strength and density can be combined, and the *BIN* model made from multivariate analysis was temporarily discarded.

4.2.3 Application to LC-refining, identification of some model limits (Paper IV)

Evaluations of a main line low consistency (LC) refiner operating at approximately 100 kWh/ADMT showed that fiber wall thickness, fiber curl, fiber width and fibrillation developed differently than in high consistency (HC) refining. This affected the predicted *BIN*, which did not increase in LC refining despite the increased tensile index. This was expected, as the *BIN* model was developed for high consistency refining, and shows that one single model cannot be expected to cover any pulp sample, despite the fact that this model is applicable for a comparatively broad range of pulp samples from high consistency refining processes. A summary of the development of sheet- and fiber characteristics in high- and low consistency refining at an energy input of approximately 100 kWh/ADMT is found in Tables 4.1 and 4.2 below. The evaluation of fiber development focused on fibers between 0.7 and 2.3 mm and *BIN* was calculated as a function of arithmetic averages of fibrillation index and collapse resistance index (Table 4.2).

Table 4.1. Development of sheet properties in high (HC)- and low consistency (LC) refining at an energy input of ~100 kWh/ADMT.

	Tensile index	Stretch	Density	Z-strength	16-30 Tensile index	Light scattering
HC	↗	↗	↗	↗	↗	↗
LC	↗	↗→	↗	↗	↗	↗

Table 4.2. Development of fiber properties in high (HC)- and low (LC) consistency refining at an energy input of ~100 kWh/ADMT, fibers 0.7-2.3 mm.

	BIN	Fibrillation index	Fiber wall thickness index	Fiber width index	Fiber curl index
HC	↗	↗	↘	↘	↗
LC	↘→	→	↗→	↗→	↘

Fiber wall development is one of the main objectives for refining the fiber and the HC refining resulted in decreased fiber wall thickness and increased fibrillation. In LC refining, the fiber wall thickness and fiber width was unaffected or for some samples slightly increased, the opposite to HC refining. Fibrillation index as measured in FiberLab was also unaffected in LC refining whereas it increased in HC refining.

It can be speculated that there occurred some internal fibrillation or swelling of parts of the fiber wall in the LC refining, something that may have influenced the analysis of both the wall thickness and fibrillation in FiberLab. The resolution of the fibrillation measurement was <0.1 μm according to the supplier, Section 3.2.5, and it is possible that the LC refining resulted in fibrils that were thinner than the FiberLab could detect. Fibrils as thin as 0.06 μm have reportedly been detected for pulps refined in pilot scale LC refiners (Fernando *et al.* 2014). Very thin fibrils may still influence the tensile index but may not be recognized by the FiberLab analyzer. Neither degree of swelling nor the development of micro fibrils was possible to evaluate in the currently used optical analysis method but would benefit from further evaluations using other tools.

All evaluations of HC refined pulps made in this study showed that fiber curl increased with increased refining energy. In LC refining, the measured fiber curl decreased which indicated that the fibers became straighter. It is known from literature that fibers are straightened as a result of latency removal and that this increases the strength properties of sheets (Beath *et al.* 1966). In LC refining, no measurable cross-sectional fiber characteristics developed in the same way as in HC refining and it is possible that the increased tensile index was as least partly an effect of the decreased fiber curl. Figure 4.9 below shows the correlation between fiber curl and tensile index, for samples collected before and after LC refining. The samples were analyzed using hot, cold or no disintegration. The resulting decrease in fiber curl gave increased tensile index in a similar way for both disintegration and LC-refining. This was also confirmed in later studies (Ferritsius *et al.* 2014).

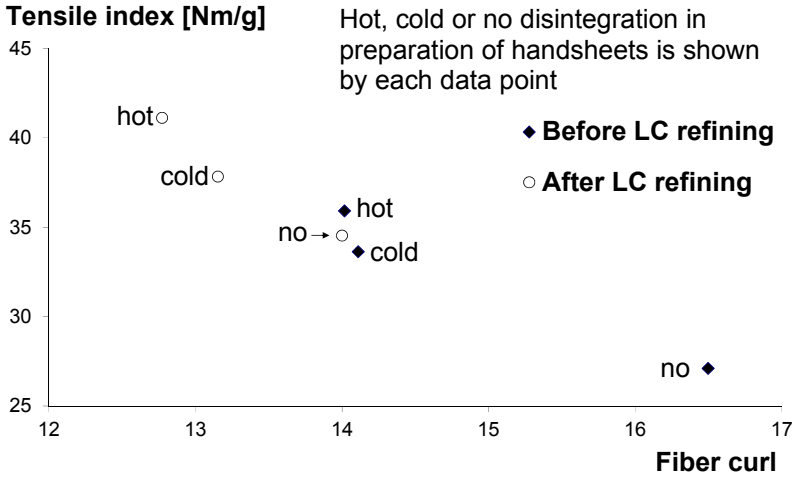

Figure 4.9. The samples collected before and after low consistency (LC) refining were prepared in three different ways – with no, cold or hot disintegration. For all three preparations, fiber curl decreased and tensile index increased. The disintegration method highly influenced the levels of both tensile index and fiber curl and the increased tensile index was as least partly an effect of the decreased fiber curl.

The effect LC refining has on mechanical pulp fibers and the LC refined fibers' effect on the final paper quality need to be further evaluated. It also needs to be established which testing methods that best reflect the potential and quality of the LC refined pulp. For all the hydrocyclone fractionated pulps, the fibers in Stream 1 had the highest fiber curl for both the P16/R30 and P30/R50 fractions and the fibers in Stream 5 had the lowest, Figures A4.3.1a-b and Table A4.1.1 in Appendix A. Average fiber curl ranked the hydrocyclone pulp fractions consistently and fiber curl as evaluated in the FiberLab optical analyzer should be further evaluated for the prospect of becoming an important measure in fiber characterization.

The present *BIN* model did not cover low consistency pulps. The same approach as for the high consistency *BIN* model can be used to predict the tensile strength of low consistency pulps, but most likely this model needs to include also other fiber characteristics. The results from this study showed that decreased fiber curl correlated well to increased tensile index for the low consistency refined pulps and fiber curl may be useful in a model that covers low consistency refining.

4.2.4 Fiber characteristics evaluated by other methods (Paper II)

Fiber width index of the P16/R30 fraction samples of TMP1, TMP2 and TMP3 was analyzed in a MorFi Lab optical analyzer. The MorFi Lab analyzer is an optical analyzer similar to the FiberLab instrument that analyzes fiber width but not fiber wall thickness (Eymin Petot Tourtollet *et al.* 2003). As does the FiberLab, the MorFi Lab gives relative values of fiber width. The fiber width index from the MorFi Lab correlated well with fiber width from the FiberLab (*cf.* Tables A5.1.1 and A4.2.1 in Appendix A and Figure 15 in Paper II).

Fiber wall thickness and fiber width were also evaluated by image analysis of cross-sectional SEM images. For all five pulps, the P16/R30 fractions of Feed, Streams 1 and 5 were analyzed. The SEM and FiberLab methods ranked the fiber wall thickness in the same way although at different levels (*cf.* Tables A5.1.1 and A4.1.1 in Appendix A and Figures 8a, 13a and 14a in Paper II). This was expected since the FiberLab evaluates fiber wall thickness as a relative value.

For the SGW and TMP3, the fiber width ranking using SEM of Feed, Streams 1 and 5 were consistent with the FiberLab rankings. For TMP1, TMP2 and CTMP; the differences in fiber width between Feed, Stream 1 and Stream 5 were very small. This was seen both in SEM- and FiberLab analysis (*cf.* Tables A5.1.1 and A4.1.1 in Appendix A and Figures 9a, 13b and 14b in Paper II) and for these pulp samples, the rankings of the SEM analysis did not follow FiberLab rankings. From these results, it seemed that FiberLab was more accurate in analyzing small differences in fiber width than the SEM image analysis. It is possible that a higher number of analyzed fibers and/or a more developed method may increase the accuracy of the SEM method.

4.2.5 Effect of exclusion of split fibers from FiberLab results

Completely split fibers, *i.e.* fibers with broken cross-sections, were not included in the results from the SEM- or FiberLab analysis. FiberLab data used in this study was digitally filtered (Section 3.3.1) before averages were calculated, to further ensure that fibers without measurable walls were excluded. No rankings changed compared to default printout averages (unfiltered data) as can be seen in comparisons of Tables A4.1.1 and A4.2.1 in Appendix A. This confirmed that the totally split fibers were not included in the unfiltered (unscreened) results of the

fiber analysis (default printout averages) which was also expected based on the FiberLab measurement principle (Kajaani FiberLab™ Operating Manual W4230467 V3.5 2002).

Reme *et al.* (1998) showed that the amount of split fibers in a mechanical pulp is large, up to 46% for the Bauer McNett +48 (+50) fraction for SGW and up to 10% for the analyzed TMP. Ferritsius and Rautio (2007) evaluated the amount of split fibers in five groundwood pulps and one TMP. The level of split fibers in the +50 fraction corresponded to 52-64% for the SGW and 38% for the TMP (recalculated from amount of split fibers in the total pulp, Figure 9, Ferritsius and Rautio 2007). Kure *et al.* (1999b) reported that 53% of the evaluated fibers in the +50 fraction of a pilot refined TMP (double disc refiner) were split fibers. If the amount of split fibers estimated by Reme *et al.*, Ferritsius and Rautio and Kure *et al.* are representative for a wide range of pulping processes, as expected, the FiberLab and SEM analysis of fiber wall thickness and fiber width were based on only parts of the analyzed fibers, possibly as little as half the fibers of the +50 fraction for groundwood. This was also confirmed during FiberLab analysis where the analyzed SGW samples required more FiberLab "runs" (repeated analyses) than the TMPs to acquire a given number of analyzed fibers with intact walls. The required number of FiberLab runs was also lower for CTMP than for TMP, which indicated a lower number of split fibers in the CTMP compared to TMP. This was also expected based on the requirements on the bulky CTMP fibers that were intended for use as the middle layer in paperboard.

It has been found that split fibers are more common for earlywood than for latewood (Reme and Helle 2001) and it is possible that a higher percentage of early wood fibers than late wood fibers were excluded from the FiberLab results. Despite this, it was evident that the tensile index of sheets could be calculated from fiber characteristics based only on fibers with intact walls, as shown in this study. It is possible that the fibers with intact fiber walls function as reinforcement in the sheet as suggested by Forgacs (1963) and later by Mohlin (1980) and that broken fibers and fines fill the sheet structure. Another possibility is that fibers with intact walls and fibers with split walls developed at the same rate which resulted in a model that covers both fiber types. This is supported by Corson (1980) who showed that if long fibers were separately refined and the original middle and fines fractions were then added to the long fibers, these fractions would decrease the quality of the pulp.

4.3 Distributions of fiber characteristics and *BIN* (Papers I, V)

A first approach to evaluating distributions of tensile index was presented in Paper I. The amount of fiber material in each hydrocyclone stream (*cf.* Section A1.3 in Appendix A) was combined with the measured or predicted tensile index of the same stream. Examples of these distributions were shown in Paper I and a more detailed description of the calculation of these distributions can be found in Section A8 in Appendix A. Already from these rather primitive distributions, it was obvious that the range of measured and predicted tensile indices for the hydrocyclone streams was wider for the shorter Bauer McNett fractions than for the longer.

4.3.1 Arithmetic, length weighted and wall volume weighted distributions (Paper V)

With the use of raw data from the FiberLab analyzer, high resolution distributions could be made. It was also possible to weigh the influence of each fiber on the distribution with any selected fiber characteristic as described in Section 3.3.3. This study evaluated arithmetic, length- and wall volume weighted distributions. Distributions were formed using the method of KDE *via* diffusion mixing. Figures 4.10a-c show the arithmetic, length weighted and wall volume weighted distributions of fiber wall thickness index from samples representing different levels of specific energy consumption of a 65" double disc refiner operated in a TMP line. Figure 4.10d shows the length weighted fibrillation index distributions of these pulps. As expected, the pulp which was sampled at the lowest specific energy consumption had the thickest fiber walls and the lowest fibrillation index. The highest specific energy consumption resulted in the thinnest fiber walls and highest fibrillation index.

The arithmetic and length weighted distributions revealed two peaks: one for thin-walled and one for thick-walled fibers. These two peaks were assumed to represent early- and latewood fibers. The latewood fiber peak became more apparent for length weighted than for arithmetic distributions which indicates that the thick-walled fibers also were longer. Wall volume weighted distributions of the same data diminished the earlywood fiber peak as expected. This was likely the result of the thin walls of the earlywood fibers which quite naturally have a much smaller wall volume compared to the thick-walled latewood fibers. For fibrillation index, the shape of the distributions was similar between arithmetic, length weighted and wall volume weighted distributions. Based on the results of the arithmetic and length weighted distributions of fiber wall thickness (Figures 4.10a-b) it was apparent that the wall thickness of the latewood fibers was reduced when the level of electrical energy input increased. This was expected but cannot be concluded by the use of standard testing or average values.

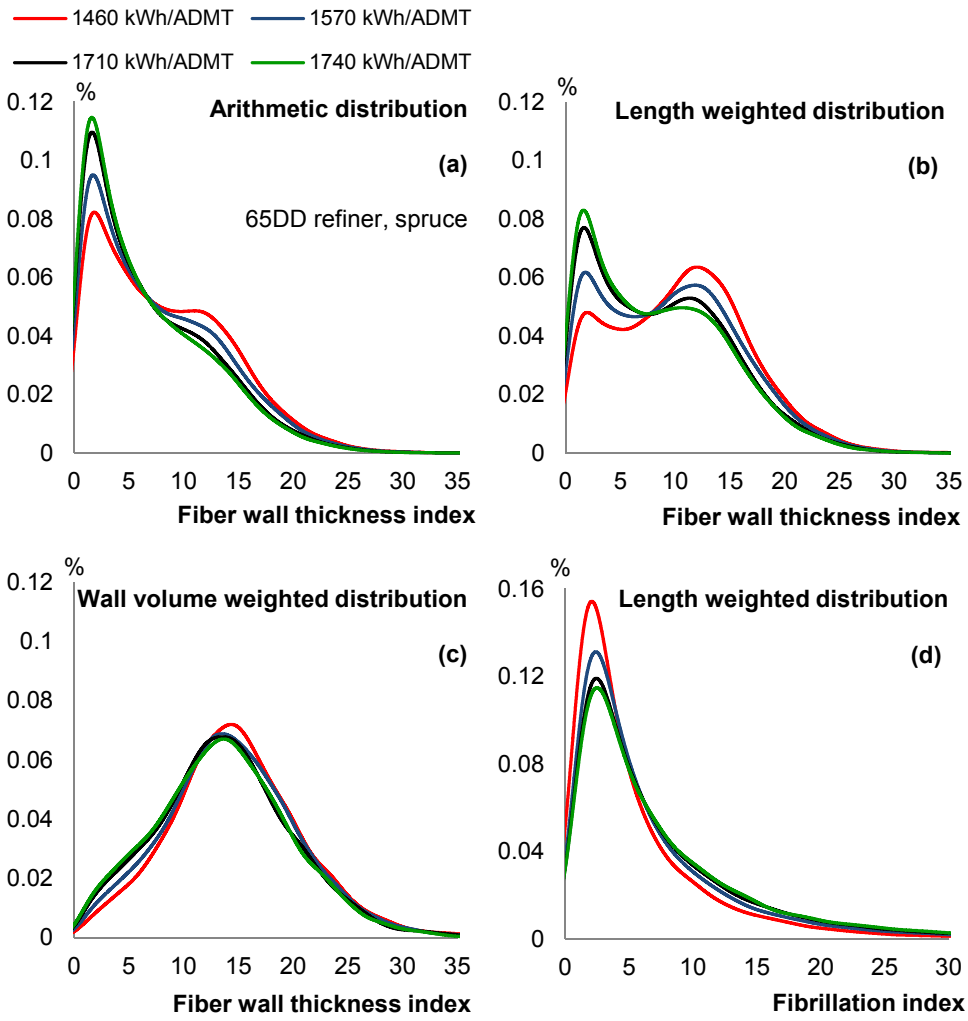

Figure 4.10a-d. Arithmetic and length weighted distributions of fiber wall thickness (a-b) revealed two peaks which were assumed to represent early- and latewood fibers. Wall volume weighted distributions of fiber wall thickness diminished the earlywood (c) due to the low wall volume of the thin-walled fibers. The shape and level were similar for arithmetic, length weighted (d) and wall volume weighted distributions of fibrillation index. For all three methods of weighting the distributions, the lowest refining energy resulted in the highest fiber wall thickness and lowest fibrillation whereas the highest refining energy gave pulps of the thinnest walls and highest fibrillation.

It is known that early- and latewood fibers influence sheets differently but surprisingly little is known about the optimum ratio between thick-walled and thin-walled fibers in the final product. It may never be possible to fractionate a mechanical pulp to contain only earlywood fibers, and it is doubtful whether that

would be desirable. Many suggestions have been made about how to best define the average ratio between early- and latewood fibers in pulps with one figure (for example Reme *et al.* (1999b), Mohlin (1995, 1997)). This may have been a useful intermediate step towards increased understanding of the fiber characteristics that influence the properties of a mechanical pulp, but offers limited information about the development of various fiber types. By using distributions of fiber wall thickness instead, the peaks of the early- and latewood fibers are distinguishable, and so is the effect of the refining process on the early- and latewood fibers respectively. Distributions also provide significantly higher resolution than only one value. The use of an average value to define the ratio between early- and latewood may however still be useful in some cases such as for characterizing the raw material, in order to sort and select the wood best suited for various end products.

Distributions of fiber characteristics enables evaluations of the effect of the refining process on all fibers, which makes it possible to optimize the mechanical pulping process with respect to the required fiber characteristics, and cut down on costly safety margins. The final paper is produced from all fibrous material in a pulp, and it would make more sense to optimize the operation and design of the refining process with respect to the development of all fibers rather than on an average "fiber". By using distributions to evaluate fiber characteristics of final pulps, it would also be possible to find out which composition of various fiber types, for example thick- and thin walled fibers that resulted in the most beneficial properties of the final product. This may for example differ depending on the printing technique that will be used.

4.3.2 *BIN* distributions (Paper V)

In order to form distributions of the predicted tensile index, the equation resulting from the linear regression of the *BIN* model was applied on each fiber in the raw data. Based on current knowledge, the range of the *BIN* model and present calibration levels of the FiberLab instrument, the predicted tensile index was calculated according to Equation 4.1 above.

Distributions of measured and predicted fiber characteristics are currently recommended to be either arithmetic or length weighted; predictions of the tensile index of long fiber sheets were based on fiber wall thickness and fibrillation indices. The fiber wall thickness was also included in calculations of wall volume (*cf.* Equation 3.4), and it is possible that the effect of the wall thickness becomes too enhanced in wall volume weighted distributions of *BIN*. The effect of, and true measurement of, fiber width which is included in calculations of fiber wall volume, also need more studies. Until these topics have been further evaluated, it was chosen to use arithmetic or length weighted *BIN* distributions.

Figure 4.11 shows the length weighted *BIN* distribution of the pulp samples from the refiner curves in Figures 4.10a-d. As expected, the samples of the refiner curve became arranged in order of specific energy consumption. The highest refining energy level resulted in the highest predicted tensile index (*BIN*), and the lowest refining energy level resulted in the lowest.

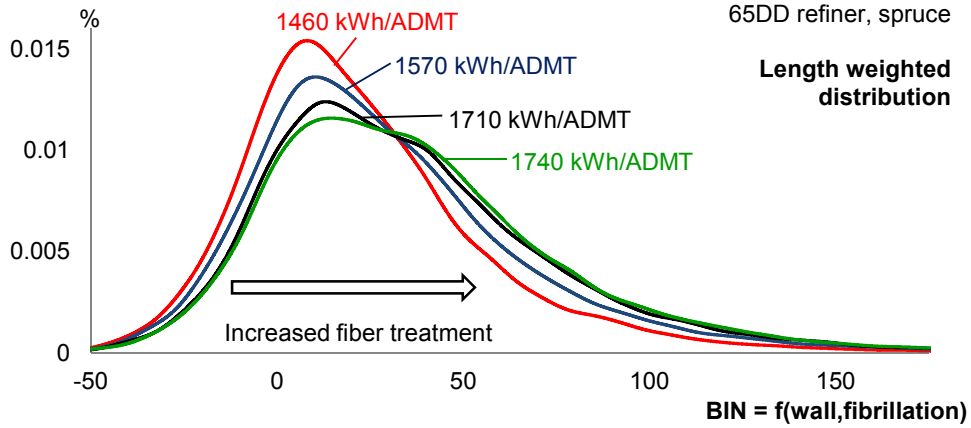

Figure 4.11. The *BIN* distributions were ranked in accordance with the specific energy consumption of the four samples in the refiner curve. The highest level of specific energy resulted in the highest *BIN* and the lowest energy level gave the lowest *BIN*. This was expected from the ranking of the fibrillation and fiber wall thickness seen in Figures 4.10a-d.

Various mathematical tools are available to describe a distribution with single numbers representing for example the kurtosis or skewness. The values resulting from these tools may be useful as input data in programming for process steering purposes and can be used as complements to distributions. For operators, technicians and engineers to fully understand the fiber characteristics that a distribution represents, it is important also to visualize the distribution as such. An example of how this could be transferred to an operator's screen is to combine a visual image of a distribution with the average value, kurtosis, skewness and percentage of fibers under a defined level critical for the fibers to form strong sheets.

***BIN* distributions from various fiber length intervals**

The *BIN* model was based on data from the Bauer McNett fractions P16/R30 and P30/R50. The fiber length interval representing these two fractions was identified to be 0.7 – 2.3 mm in the FiberLab analyzer which was graphically illustrated in Figure 4 of Paper IV. It was found that length- and wall volume weighted *BIN* distributions made from whole pulps and the fiber length interval 0.7 to 2.3 mm were very similar in shape and level. For arithmetic *BIN* distributions, the

differences were larger. Examples of *BIN* distributions of fibers of all lengths compared to fibers between 0.7 and 2.3 mm are found in Figures 5a-c in Paper V. When characterizing the fibers in a pulp, it is useful to be able to evaluate all the fibers as well as fibers of selected length fractions. The reasons for not using wall volume weighted *BIN* distributions until further evaluated were discussed above, and with current knowledge, length weighted *BIN* distributions are recommended.

Validation of *BIN* distributions by the use of pulp mixtures

Paper V contains *BIN* distributions of mixtures made of a news- and a SC grade TMP in different proportions. By increasing the amount of SC grade fibers, a higher *BIN* level was reached, Figure 4.12. This was expected based on the higher specific energy consumption of the SC grade TMP compared to the news grade TMP. The shapes of the *BIN* distributions of the mixed pulp samples also changed gradually. The fibers of the SC pulp had a flatter *BIN* distribution than the fibers intended for news. The mixtures came in between the shapes of the SC- and news grade TMPs, and resembled the *BIN* distribution which most of the fibers belonged to. With increasing amounts of SC grade TMP, a vague peak at a *BIN* level around 40 was also materializing. The peak seemed to be characteristic for the SC grade TMP, but was not further evaluated in this study.

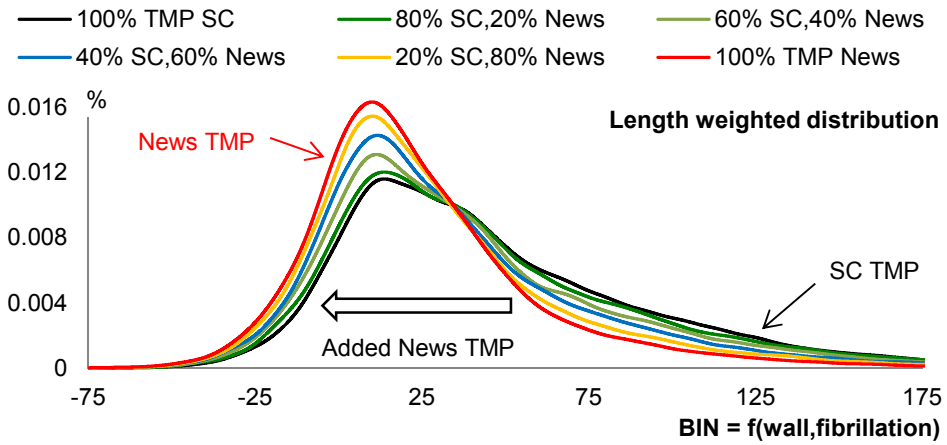

Figure 4.12. *BIN* distributions of mixtures of a news and a SC grade TMP. The mixtures were made in the laboratory based on weight. With added amounts of the SC grade TMP, the level of the *BIN* distributions increased and the distributions also became flatter. The fiber data is based on fibers between 0.7 and 2.3 mm.

Characteristic distribution width, F0.90

With increasing amounts of news grade TMP in the pulp mixtures, both the average *BIN* and width of the *BIN* distribution, F0.90, decreased, Figure 4.12 (see also Figures B1.3a-b in Appendix B). For all samples evaluated in this study, the width of a *BIN* distribution increased with increasing refining energy. Further studies are needed to establish if this is valid for a larger range of pulp processes and raw materials, for increasing the understanding of the underlying mechanisms resulting in the increased distribution width and for evaluating the application of such knowledge. Section A4.6 in Appendix A lists the development of the distribution width of some fiber characteristics for the hydrocyclone fractionated pulps.

In Appendix B, an example is found on how the averages and distributions of *BIN* can change throughout a TMP process (Figure B2.2.1 and Table B2.2.1) and over screening (Figures B2.1.1a-b). The results showed that *BIN* increased with main line and reject refining at high consistency over a process line, but that the post refining at low consistency did not influence *BIN*. These results were in line with the results presented in Papers IV and V and discussed above.

***BIN* distributions of the hydrocyclone fractionated pulps**

Figure 4.13 below shows the length weighted distributions of the five pulps that were hydrocyclone fractionated in the first part of this study. The pulps were intended for various end products but were made from a very similar raw material and the distributions and the shapes of the curves should therefore reveal process-related differences of the pulps.

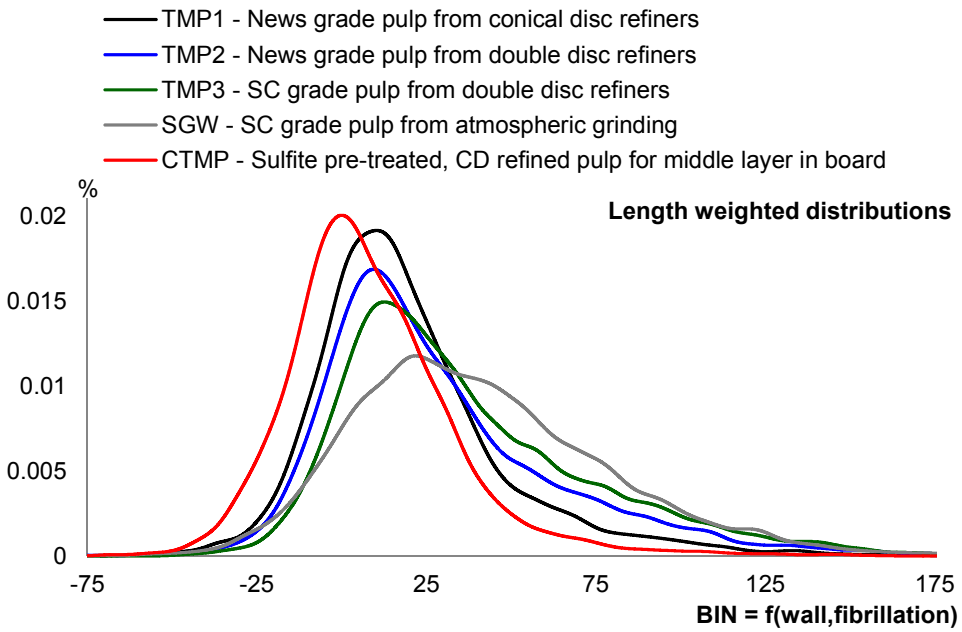

Figure 4.13. *BIN* distributions of the five pulps that were hydrocyclone fractionated. The pulps all originated from Norway spruce (*Picea abies)* which likely enhanced the resemblances of the five distributions. The various pulps were designed to fit different end products and were therefore tailored differently in the refining and grinding processes, resulting in *BIN* distributions of various levels and shapes.

All *BIN* distributions were arranged as expected: The *BIN* distribution of the SGW revealed high-*BIN* fibers, which was expected since these fibers were highly fibrillated (*cf.* Figures 4.3 and 4.4a). The distributions also revealed that the SGW contained as high amount of low-*BIN* fibers as TMP1. This was in line with the observations of the specific lowest level of tensile index in Stream 5 for each pulp discussed in Section 4.1.2 and shown in Figures A3.2.1a-d in Appendix A. The higher amount of low-*BIN* fibers of the SC grade SGW compared to the SC grade TMP (TMP3) may influence the final paper quality.

For the three TMPs and the CTMP, the specific energy consumption by which the pulps were produced in combination with differences in process design, for example single and double disc refiners, seemed to have set the order of the ranking:

The *BIN* distribution of the CTMP was located at a lower *BIN* level than the four other pulps. This was expected since these fibers had rather undamaged walls with low fibrillation compared to the other pulps, fiber characteristics that were a result of the chemical pre-treatment and desired for producing a bulky product.

The TMPs ranked according to the specific energy consumption in the refining process and expected fiber treatment: The TMP produced in conical disc refiners (TMP1) had a *BIN* distribution which was closer to the CTMP than the TMP produced at the same specific energy consumption as TMP1 but in double disc refiners (TMP2). This was expected as double disc refiners are known to give higher tensile index and density at a given specific energy consumption than single disc refiners (Falk *et al.* 1987, Ferritsius *et al.* 1989).

The SC grade TMP (TMP3) was produced in double disc refiners at a significantly higher specific energy consumption than TMP2. The shape of the curves of TMP2 and TMP3 showed some resemblance, but the *BIN* distribution of TMP3 revealed more fibers of higher *BIN* than TMP2. The SC grade SGW had a flatter distribution than the CTMP and TMPs with higher relative amount of fibers in the area of high *BIN* values.

There was an apparent resemblance between the *BIN* distributions of CTMP and TMP1, both produced in conical disc refiners but the CTMP with chemical pre-treatment and approximately half the specific energy consumption of TMP1. The difference between the *BIN* distributions of the SGW, the CTMP and the three TMPs were the most significant. This indicates that the influence of the pulping process on the fiber characteristics was mirrored in the *BIN* distributions.

4.4 Remarks on the applicability and use of the *BIN* model

Laboratory sheets made from long fiber fractions have been an important way to characterize a pulp. In today's reality, few mills have the resources to first fractionate pulps in a Bauer McNett classifier and then produce and test laboratory sheets for several process positions on a daily basis. To evaluate the whole pulp in a fiber analyzer either on-line or off-line and use the raw data to select the fiber fraction of interest for further analysis, is a much more rapid method. The access to single fiber characteristics also makes it possible to evaluate *which* fibers that are affected in various stages of the refining process, something that is useful in controlling, optimizing, re-designing or evaluating all parts of the mechanical pulping process. The ability to characterize fibers of a pulping process also enables increased flexibility in producing pulps intended for a wider range of final products. This may be helpful in quickly finding operating windows for the production of both pulps intended for *e.g.* printing papers and chemically pre-treated pulps intended for middle layer in paper board, should such mixtures of product portfolios become realized.

In this study, data from the FiberLab fiber analyzer was used, but the method would be applicable also for other analyzers that enable handling of single fiber data which is synchronized for measurements of fiber length, degree of external fibrillation and fiber wall thickness.

The approach of predicting tensile index from geometrical fiber characteristics of mechanical pulp fibers could be extended to include also the prediction of other sheet characteristics that are affected by fiber geometry and external fibrillation, for example light scattering or density. It is possible that this would require other analysis methods, but the approach would be similar.

The model which was developed for the pulp fractions evaluated in this study was applicable to a comparatively broad range of pulp samples. These pulp samples originated from the same wood species from but were the result of different pulping processes intended to treat the fibers for various end products. The pulps included in the model were also bleached in different ways and contained samples bleached both under oxidative (TMP3, CTMP) and reductive conditions (TMP1, SGW). However, one single model cannot be expected to cover any pulp sample, and other models need to be developed for specified parts of different process lines. These models may well be quite similar but their applicability needs to be considered in each case.

The use of geometrical fiber data to predict sheet properties is likely to require a new model for each process, in which new linear regressions or multivariate analysis needs to be performed. This is both to ensure that the *BIN* model is derived from and covers the process range for which it was intended, and because

most fiber analyzers use relative values of fiber characteristics instead of true values, which may change the relation by which fiber characteristics influence the sheet properties. To broaden the ranges of the *BIN* model, the linear regressions of multivariate analysis could for example be based on results from both primary and final pulps together with screening accepts and rejects.

If unscreened primary pulps are included in the model, it is recommended that shives are removed from the pulp before producing reference sheets. Shives are usually not included in the data from an optical analyzer, either the capillary is blocked and the analysis disrupted or data from shives are not stored due to the measurement algorithms of the analyzer. It is likely that a high amount of shives, such as expected in *e.g.* an unscreened primary pulp, influences the tensile index of laboratory sheets more than the geometry of the fibers. Basing a model upon a sheet with high amounts of shives would therefore result in a poor model, which would be based on other pulp properties than fiber geometry; the ability to follow the fiber development and the ability of the fibers to form sheets of high strength throughout the process would be lost.

The model has this far only been based on pulps produced from Norway spruce (*Picea abies*), and if pulp is to be produced from a mixture of raw materials, this naturally has to be taken into consideration in designing the model.

5 CONCLUSIONS

The tensile index of laboratory sheets made from long fiber fractions increases with increasing fibrillation index and decreasing fiber wall thickness index and collapse resistance index, a combination of fiber wall thickness and fiber width. Fiber width as evaluated in the FiberLab analyzer has little influence on tensile index.

Using wall volume weighted averages of fiber width instead of arithmetic, changes the ranking between the hydrocyclone streams of two of the five pulps studied to the complete opposite. None of the rankings of fibrillation, fiber wall thickness or collapse resistance indices was affected. This confirms both that the use of fiber width is questionable in evaluating mechanical pulps and that the results of fiber analysis may depend on how data is treated, and awareness of the manner of weighting averages is needed when fiber data are compared.

The propensity of each fiber to contribute to a sheet of high tensile index can be calculated from external fibrillation and wall thickness and was denoted *BIN*, *B*onding ability *IN*fluence. The tensile index of laboratory sheets from the Bauer McNett fractions P16/R30 and P30/R50 was predicted with high accuracy from fiber characteristics of 52 pulp fractions of TMP, SGW and CTMP using *BIN*. The exception was the P30/R50 fraction of the SGW which correlates linearly with the rest of the pulp samples but on another level for *BIN* based on arithmetic averages of fiber wall thickness and fibrillation. A *BIN* model based on fiber wall volume weighted averages resulted in more accurate predictions of the tensile index of laboratory sheets than arithmetic averages, and resulted in a single correlation between *BIN* and the measured tensile index for all (58) evaluated pulp samples, despite the fact that the pulps were intended for different end products and bleached both under oxidative and reductive conditions.

It is possible to illustrate the distribution of fiber characteristics quickly and with high resolution based on raw data from the FiberLab™ optical analyzer. Distributions of fiber wall thickness clearly show that the amount of thick-walled fibers was reduced when the specific energy consumption was increased in the double disc refiner used in these refining trials. This was expected but cannot be concluded from standards methods or from average values of fiber dimensions.

Distributions of *BIN* reveal expected differences between the evaluated pulp types from high consistency refiners. For example, SC grade pulps had a higher level of *BIN* values than pulps intended for news and the middle layer in paperboard; differences between pulps produced with various levels of specific energy were also distinguishable. The shape of a pulp's *BIN* distribution seems to be influenced by the process type. *BIN* distributions could be useful for identifying the right level of fiber treatment to minimize the electric energy consumption in mechanical pulping.

6 RECOMMENDATIONS FOR FUTURE WORK

This study was partly a methodology study and some of the suggestions for future work refer to the development of fiber analyzers, an important key for enabling energy-efficient production of mechanical pulps of the right quality.

Low consistency refined pulp did not fit the *BIN* model which was developed for high consistency pulps. It is possible that other means of characterizing the fibers are needed to describe fiber characteristics that influence the development of tensile index of low consistency pulps. In order to broaden the range of the model to predict sheet characteristics to also include pulps from low consistency refining processes, it is possible that access to data of the fiber wall density is necessary. For this, rapid methods of fiber wall density analysis need to be developed. It is also possible that increased resolution in the measurement of fibrils and the identification of thinner fibrils on the fiber surface would be helpful in characterizing pulps from low consistency refiners.

It should be possible to construct a model to predict sheet properties other than tensile index from fiber data for parts of a given process line. Since most fiber analyzers use relative values of fiber characteristics, this requires new linear regressions or multivariate analysis of fiber characteristics from the fiber analyzer to be used in predicting the sheet property. To broaden the ranges of the model, the linear regressions or multivariate analysis could for example be based on results from both primary and final pulps together with screening accept and reject. If using primary pulps, it is important that shives are removed before the model is made to avoid the influence that shives have on sheet characteristics as discussed in Section 4.4.

If fiber characteristics are to be used to predict surface characteristics of sheets, it may not be sufficient to analyze fibers with intact walls but also broken fibers may need to be included in the model. If so, one measure that defines if the fiber was broken or not (1/0) may be sufficient in combination with the full characteristics of the analyzed fiber.

In order to fully characterize a final paper, it is likely that other measures of sheet characteristics need to be taken into account, for example light scattering coefficient and measures of sheet toughness (*cf.* Section 4.1.3 about using acoustic emission analysis to characterize the toughness of a sheet). This study showed that fiber wall thickness and fibrillation indices of intact fibers of the Bauer McNett P16/R30 and P30/R50 fractions were enough to predict the tensile index of these fractions, which according to literature represent the level of the tensile index of the whole pulp. In order to predict the sheet characteristics of the final pulp or paper, measures and characteristics of also the fine material are likely needed and

if the pulp is coarse, the level and/or characteristics of shives and coarse fibers may need to be included in the prediction of the final pulp of paper quality. It is also possible that a separate factor is needed to account for the contribution of the surface chemistry of fibers or fines on the strength, structure or densification of the final paper.

Pulp samples collected from the same sampling position in a TMP line over two months showed remarkably small variations in length-weighted distributions of fiber wall thickness index and the shape and level of the wall thickness distributions seemed to be unique for various sampling positions. This would benefit from further evaluations as it may be helpful in identifying process variations and/or variations in the raw material.

Off-line quality control is important for ensuring that the right level of fiber treatment is maintained but on-line analysis of fiber wall thickness and measures of external fibrillation would enable steering of a HC refining process with respect to the tensile strength or other properties of the final product. The fiber analysis should be based on single fibers and also include measurements of fiber length. In order to make distributions of measured and predicted fiber characteristics and to characterize or follow the development of selected fiber types, the analysis tool should permit use of raw data handling. On-line fiber analyzers capable of this should be developed.

Software and measurement algorithms for fiber analyzers should be developed so that true values of fiber dimensions are used instead of relative values. This would simplify benchmarking and comparisons between processes.

Calibration of optical analyzers using reference fibers are currently based on average values. In order to improve the measurement stability and repeatability of both averages and distributions, distributions of fiber wall thickness and fibrillation is needed also for reference fibers. It is also recommended that developers of fiber analyzers spend some extra effort on methods for automatic calibration of the analyzer, in order to avoid drifting of the results.

The measure “fiber curl” as evaluated in the FiberLab analyzer showed high correlation to the specific energy consumption in high consistency refining. Fiber curl was also highest in the first hydrocyclone accept stream and decreased without exceptions for every stream to the last reject. For mills that are not yet able to continuously characterize the pulp with respect to fiber wall thickness but have access to fiber curl, this could be an alternative measure in evaluating if a process change had a desired effect on the fibers or not. It is however possible that the measure “fiber curl” differs between various fiber analyzers and before being used, the definition and measurement principles for fiber curl measurement should therefore be carefully studied.

The manner of weighting a distribution of predicted or measured fiber characteristics should be further evaluated. It is possible that process induced differences of some fiber characteristics would be easier to identify if distributions are arithmetic, whereas some should be length- or wall volume weighted. Also the preferred manner of weighting averages can be further investigated.

With a rapid tool to analyze the distribution of fiber characteristics, it would be interesting to evaluate the correlation between an average value and the width of a distribution for a given analyzed or predicted fiber property. What does it for example mean for the quality of the final pulp if the average fiber wall thickness is unchanged, but the width of the distribution of fiber wall thickness increases? That study would likely uncover some answers about the development of various fiber types in different process stages.

The R16 fraction could not be analyzed in the FiberLab due to the size of the measurement capillary and the enrichment of shives and non-treated fibers in the first Bauer McNett fraction. Therefore, it is still unknown if also fibers that were longer than the fibers in the P16/R30 fraction followed the same *BIN* model as fibers from the P16/R30 and P30/R50 fractions. To investigate this, the Bauer McNett fractionation could be remade with an added 12 mesh screen to collect the major part of shives and untreated fibers. After that, a model could be made in which the characteristics of the fibers in the P12/R16 fraction are evaluated together with fibers in the P16/R30 and P30/R50 fractions.

This study showed that fibers of the P30/R50 fractions had thicker fiber walls at a given fiber width than the fibers of the P16/R30 fraction. To increase the fundamental knowledge about the mechanical pulping process, it should be studied if this was related to the hydrocyclone fractionation or if it is a common relation. In evaluating this, it is recommended to use a wide range of mechanical pulp types.

In order to know how to design and optimize the refining process, it would be interesting to evaluate the effect of different distributions of fiber properties on the fiber network, *i.e.* to which extent fibers that have low propensity of forming strong sheets can be "helped" by fibers of high propensity to form strong sheets. Fracture toughness is a valuable measure of a sheet's ability to withstand an initiated rupture but the drawback is mainly the time consuming preparation of large quantities of laboratory sheets. If the structural differences that correlated to fracture toughness could be analyzed by acoustic emission during standard tensile testing as suggested by Gradin *et al.* (2008), the method could provide valuable information about the sheet structure without extra sample preparations. The recommendation of this study is to move away from the intermediate step of making and testing laboratory sheets and the acoustic emission method would also be valuable in characterizing final paper. The fiber characteristics needed to

acquire certain levels of fracture toughness and other measures of fractural behavior reveled by the acoustic emission testing of final paper could then be used for feed-back in steering the refining process.

The use of the acoustic emission method as a tool to characterize sheets will likely reveal more about the development of the fracture characteristics in a sheet. It may also be a helpful tool in evaluating the effect that various fiber types have on the fracture development in sheets. Prediction of the fracture behavior of the final paper by the use of fiber characteristics that were rapidly measured on-line would enhance the ability to steer the refiners as energy efficiently as possible.

ACKNOWLEDGEMENTS

This study was carried out at **Stora Enso** in cooperation with the **Mechanical Pulp Industrial Research College** at **Mid Sweden University**, **FSCN,** and I am grateful for the support from **both organizations** and for the opportunity to conduct my doctorate studies in the exciting interface between the university and a paper mill. **The Swedish Knowledge Foundation** (KK-stiftelsen) is acknowledged for financial support.

The group of supervisors who supported me in this project is acknowledged; **Olof Ferritsius**, the ideas and initiatives of you and Hans E were the start-up up this project and you have contributed with more ideas and inspiration. I've learnt a lot during these years from you and Rita and your seemingly never-ending driving force to optimize the refiner process is highly inspiring! **Rita Ferritsius**, with your vast knowledge of fibers and mechanical pulping, you have been an important resource in this project. Your ability to keep an open mind to fiber "truths" after so many years in this business is admirable. I am grateful for your genuine interest in this study, and also for participating in bringing the FiberLab to Falun, a prerequisite for this project. **Hans Ersson**, you managed to create a working environment with the ultimate mixture of mill operations, R&D and university connections. Without all those parts, this study would have haltered. Not only did you manage to do so in the hardest of time, you also always found the time for discussions. **Professor Per Engstrand** – the way you have implemented industrial views into the research of mechanical pulping has made mechanical pulping research both more industrially applicable and accessible. You were also helpful in widening the perspective of this study and contributed with both ideas end energy. **Professor Hans Höglund**, with your mechanical pulping expertise and experience you have contributed to this project from the beginning. I appreciate your involvement and support over these years and it has been a privilege to work with you! **Professor Per Gradin**, thanks for bringing a physicist's view on fibers and paper into this study. Your curiosity of the functions fibers have in sheets is inspiring! **Dr. Mats Rundlöf**, your support in the end of this study has been very valuable! Thanks for help with writing techniques, moral pep talks, discussions and insightful comments on the manuscript.

Adjunct Professor Magnus Paulsson and **Professor Myat Htun**, Mid Sweden University, FSCN, are acknowledged for valuable comments on the manuscript.

Anna Haeggström, **Anne Åhlin and Christina Olsson**, Mid Sweden University, Sundsvall, are acknowledged for assisting in all tasks related to administration and printing of this thesis. As is **Pethra Nordlund**, Stora Enso.

The personnel at the **libraries of Stora Enso, Mid Sweden University, Sundsvall, and Falun** are acknowledged for assistance in finding literature.

All participants of Mid Sweden University FSCN's Mechanical Pulp Industrial Research College are acknowledged for relevant and inspiring discussions, technical input and for contributing to a creative environment. Special thanks to my fellow PhD students **Mikael, Kristian, Dmitri, Karin, Erik, Sofia, Stefan, Marius, Lisa, Lisa, Jesper, Anette, Niklas, Kerstin, Dino, Mihaela and David**.

The staffs at **Kadant Noss** are acknowledged for skillfully carrying out the five hydrocyclone fractionations.

Staffan Nyström and **Professor Per Isaksson** are acknowledged for assisting with the acoustic emission measurements, data handling and evaluations.

Dr. Michel Petit-Conil and **Dr. Michael Lecourt** at CTP and FCBA, Grenoble, France, are acknowledged for supporting the MorFi Lab and CyberBond analyses.

Operators, engineers and **laboratory staffs** at the **involved mills** are acknowledged for kind assistance with sampling and for always doing more than was required. **Technicians and scientists** at **the laboratories at Stora Enso Kvarnsveden and Stora Enso Research Centre Falun** are acknowledged for skillful testing, helpful assistance and teaching of pulp testing methods. **Alf Gustavsson** is acknowledged for collecting pulp samples and performing FiberLab analyses in the later part of the study. **Ulf Ängsås** is acknowledged for carrying out the refiner curve trials and assisting in process related issues. For programming assistance and for help in setting up the database to store and filter fiber data, thanks to **Jakob Stångmyr, Patrik Joon** and **Christer A. Johansson**.

Everyone participating in the coffee breaks at Kvarnsveden development department over the years is acknowledged – the open atmosphere has been the rescue of several lost thoughts and the creation of many new ones – thanks to **Pethra, Jakob, Maria, Maria, Carl, Bitte, Anders, Emma, Rasmus, Åsa, Patrik, Mihaela, Eric, Jenny, Lars, Lars, Carola, Johan, Anna, Hans, Evelina, Håkan, Marit, Christer, Mahmoud, Mats, Matts, Fredrik, Marius, Jan-E, Andreas.**

Friends and family – thanks for your support and encouragement during these years! Extra thanks to **Hajer, Ylva, Susanna, Anna³, Emma, Karoline, Magnus, coach Björn and Björnligan**, **mamma and pappa, Henrik and Joel with families, mormor, farfar, Robert's parents and siblings with families** and my sister-in-law **Johanna,** who arranged the micrographs on the cover page of this thesis and provided me with boxes of tasty dinner during times of high work load.

Robert, my wonderful husband – Your perspective and down to earth approach to every challenge has helped me through many struggles, technical as well as non-technical. I am grateful that you are you and for the solid support you always provide. You and **Thor** are the most important people in my life. Jag älskar er!

REFERENCES

Andersson, S., Sandberg, C., Engstrand, P. (2012): "Comparison of mechanical pulps from two stage HC single disc and HC double disc – LC refining", Appita J. 65(1): 57-62.

Beath, L.R., Neill, M.T. and Masse, F.A. (1966): "Latency in mechanical wood pulps", Pulp Paper Can. 67(10): T423-430.

Bengtsson, G. (2005): "CTMP in production of high quality packaging board", Proc. Int. Mechanical Pulp. Conf., June 7 – 9, Oslo, Norway, pp. 7-13.

Botev, Z.I., Grotowski, J.F., Kroese, D.P. (2010): "Kernel density estimation via diffusion mixing", Ann. Stat., 38(5): 2916-2957.

d'A. Clark, J. (1985): "Fiber properties and tests", In: Pulp Technology and Treatment for Paper (ISBN 0-87930-164-3), Miller Freeman Publications Inc., San Francisco, USA, pp. 452-655.

Corson, S.R. (1980): "Fibre and fines fractions influence strength of TMP", Pulp Paper Can. 81(5): T108-T112.

Das, S., Cresson, T., Couture, R. (1999): "New pulp characterization from drainage, fibre flexibility and RBA", Proc. PAPTAC 85th Ann. Meeting, January 26 - 29, Montreal, Canada, pp. A345-A347.

Dickson, A., Corson, S., Dooley, N. (2005): "Fibre collapse and de-collapse determined by cross-sectional geometry", Proc. Int. Mechanical Pulp. Conf., June 7 - 9, Oslo, Norway, pp. 198-201.

Engstrand, P.O., Hammar, L.Å., Htun, M.T., Pettersson, R.L. and Svensson, B.N. (1988): "Framställning av mekanisk massa i två steg" (Two-step manufacture of mechanical pulp), Swedish patent 8801731-4, 461 103.

Eymin Petot Tourtollet G., Cottin, F., Cochaux, A., Petit-Conil, M. (2003): "The use of Morfi analyser to characterise mechanical pulps", Proc. Int. Mechanical Pulp. Conf., June 2 – 5, Quebec, Canada, pp. 225-232.

Falk, B., Jackson, M., Danielsson, O. (1987): "The use of single and double disc refiner configurations for the production of TMP for filled super calendered and light weight coated grades", Proc. Int. Mechanical Pulp. Conf., June 2 – 5, Vancouver, Canada, pp. 137-143.

Fernando, D., Daniel, G. (2004): "Micro-morphological observations on spruce TMP fibre fractions with emphasis on fibre cell wall fibrillation and splitting", Nord. Pulp Paper Res. J. 19(3): 278-285.

Fernando, D., Gorski, D., Daniel, G. (2014): "Exploring mechanisms of fibre development during HC- and LC refining of mechanical pulps that govern pulp and paper properties", Proc. Int. Mechanical Pulp. Conf., June 3 – 5, Helsinki, Finland, 7 pp.

Ferritsius, O. (1996): "Control of fundamental pulp parameters in TMP and SGW production by the use of factor analysis", 5th Int. Conf. New Available Technol., June 4 – 7, Stockholm, Sweden, pp. 245-255.

Ferritsius, O., Jämte, J., Ferritsius, R. (1989): "Single and double disc refining at Stora Kvarnsveden", Proc. Int. Mechanical Pulp. Conf., June 6 – 8, Helsinki, Finland, pp. 58-74.

Ferritsius, O., Ferritsius, R. (1997): "Improved quality control and process design in production of mechanical pulp by the use of factor analysis", Proc. Int. Mechanical Pulp. Conf., June 9 – 13, Stockholm, Sweden, pp. 111-125.

Ferritsius, O., Ferritsius, R. (2001): "Experiences from Stora Enso mills of using factor analysis for control of pulp and paper quality", Proc. Int. Mechanical Pulp. Conf., June 4 – 8, Helsinki, Finland, pp. 495-504.

Ferritsius, R., Rautio, M. (2007): "Differences on fibre level between GW and TMP for magazine grades", Proc. Int. Mechanical Pulp. Conf., May 6 – 9, Minneapolis, USA, CD-ROM, 10pp.

Ferritsius, O., Ferritsius, R., Reyier, S. (2009): "The influence of process design on the distribution of fundamental fibre parameters", Proc. Int. Mechanical Pulp. Conf., May 31 – June 4, Sundsvall, Sweden, pp. 160-168.

Ferritsius, R., Sandberg, C., Ferritsius, O. (2014): "LC-refining of mechanical pulps and its influence on fiber curl and handsheet strength properties", Proc. Int. Mechanical Pulp. Conf., June 3 – 5, Helsinki, Finland, 4 pp.

Fineman, I. (1985): "Let the paper product guide the choice of mechanical pulp", Proc. Int. Mechanical Pulp. Conf., May 6 – 10, Stockholm, Sweden, pp. 203-214.

Fjerdingen, H., Forseth, T.F., Gregersen, Ø.W., Heller, T., Johnsen, P.O., Kure, K.A., Reme, P. (1997): "Some mechanical pulp fibre characteristics, their process relationship and papermaking significance", Proc. 11th FRS: The Fundamentals of Papermaking Materials, September 21 - 26, Cambridge, Great Britain, pp. 547-605.

Forgacs, O.L. (1963): "The characterization of mechanical pulps", Pulp Paper Can. 64 (conv.): T89-T117.

Franzén, R. (1986): "General and selective upgrading of mechanical pulps", Nord. Pulp Paper Res. J. 3(1): 4-13.

Gavelin, N.G. (1966): "How to measure mechanical pulp quality", In: Science and Technology of Mechanical Pulp Manufacture, Lockwood Publishing Co., Inc. New York, USA, pp. 79-106.

Gradin P.A., Graham D., Nygård P., Vallen H. (2008): "The use of acoustic emission monitoring to rank paper materials with respect to their fracture toughness", Exp. Mech. 48(1): 133-137.

Gradin, P.A., Nyström, S., Flink, P., Forsberg, S., Stollmeier, F. (1997): "Acoustic emission monitoring of light-weight coated paper". J. Pulp Paper Sci. 23(3): J113-J118.

Gregersen, Ø.W. (1998): "On the assessment of effective paper web strength", Academic doctorate thesis (ISBN 82-471-0275-7), Norwegian University of Science and Technology, Trondheim, Norway, 75 pp.

Gregersen, Ø.W., Hansen, A., Tufa, L.D., Helle, T. (2000): "The influence of fibre shives on calender cuts in newsprint", J. Pulp Paper Sci. 26(5): 176-179.

Görres, J., Amiri, R., Grondin, M., Wood, J.R. (1993): "Fibre collapse and sheet structure", Proc. 10th FRS: The Fundamentals of Papermaking Materials, September 20 – 24, Oxford, Great Britain, pp. 285-310.

Hammar, L.Å., Htun, M., Svensson, B. (1997): "A two stage refining process to save energy for mechanical pulps", Proc. Int. Mechanical Pulp. Conf., June 9 – 13, Stockholm, Sweden, pp. 257-267.

Hammar, L.Å., Salmen, L., Sandberg, C. and Sundström, L. (2010): "The effect of process conditions on pulp quality development in low consistency refining of mechanical pulp – TMP", Appita J., 63(5): 257-262.

Heikkurinen, A. (1993): "Mechanical pulp fines – characterization and implications for defibration mechanisms", Proc. Int. Mechanical Pulp. Conf., June 15 - 17, Oslo, Norway, pp. 294-308.

Hill, J., Höglund, H., Johnsson, E. (1975): "Evaluation of screens by optical measurements", Proc. Int. Mechanical Pulp. Conf., June 16 – 20, San Francisco, USA, pp. 31-59.

Htun, M., Salmén, L., Eriksson, L. (1993): "A better understanding of wood as a material – a way to increased energy efficiency when making mechanical pulps?", In: Energy Efficiency in Process Technology (ISBN: 978-1-85861-019-1), P.A. Pilavachi (ed.), Elsevier Appl. Sci., London, Great Britain, pp. 1086-1095.

Huang, F., Lanouette, R., Law, K.-N. (2012): "Influence of Jack pine earlywood and latewood fbers on paper properties", Nord. Pulp Paper Res. J. 27(5): 924-929.

Höglund, H. (1997): "Tomorrow's challenges for mechanical pulps", Proc. Int. Mechanical Pulp. Conf., June 9 – 13, Stockholm, Sweden, pp. 29-36.

Höglund, H. (2002): "Mechanical pulp fibres for new and improved paper grades", Proc. 7th Int. Conf. New Available Technol., June 4 – 6, Stockholm, Sweden, pp. 158-163.

Höglund, H., Wilhemsson, K. (1993): "The product must determine the choice of wood type in mechanical pulping", Proc. Int. Mechanical Pulp. Conf., June 15 - 17, Oslo, Norway, pp. 1-22.

Ilvessalo-Pfäffli, M.-S. (1995): "Structure of Wood", In: Fiber Atlas: Identification of Papermaking Fibers, Part 1: Wood Fibers (ISBN 3-540-55392-4), T.E. Timell (ed.), Springer-Verlag, Berlin, Heidelberg, Germany, pp. 6-32.

Jackson, M., Williams, G.J. (1979): "Factors limiting the strength characteristics of thermomechanical pulp", Proc. Int. Mechanical Pulp. Conf., June 11 - 14, Toronto, Canada, pp. 37-48.

Jang, H.F., Amiri, R., Seth, R.S., Karnis, A. (1995): "Fibre characterization using confocal microscopy – collapse behaviour of mechanical pulp fibres", Proc. PAPTAC 81st Ann. Meeting, Jan 31 – Feb 3, Montreal, Canada, pp. B147-B154.

Jang, H.F., Seth, R.S. (2004): Determining the mean values for fibre physical properties, Nord. Pulp Paper Res. J. 19(3): 372-378.

Karnis, A. (1981): "Refining of mechanical pulp rejects", Proc. Int. Mechanical Pulp. Conf., June 16 – 19, Oslo, Norway, Session V, no. 6, pp. 1-32.

Karnis, A. (1994): "The mechanism in fibre development of mechanical pulping", J. Pulp Paper Sci. 22(10): J280-287.

Kauppinen, M. (1998): "Prediction and control of paper properties by fiber width and cell wall thickness measurement with fast image analysis", PTS Symposium: Image Analysis for Quality and Enhanced Productivity, Oct 12 – 13, Munich, Germany, 8 pp.

Klinga, N., Sandberg, C., Höglund, H. (2005): "Sheet properties of high yield pulps related to different pulping and drying conditions", Int. Mechanical Pulp. Conf., June 7 - 9, Oslo, Norway, pp. 344-348.

Klinga, N., Höglund, H., Sandberg, C. (2007): "Energy efficient high quality CTMP for paperboard", Proceedings, Int. Mechanical Pulp. Conf., May 6 - 9, Minneapolis, USA, CD-ROM, 11 pp.

Kure, K.-A. (1997): "The alteration of wood fibres in refining", Proc. Int. Mechanical Pulp. Conf., June 9 - 13, Stockholm, Sweden, pp. 137-150.

Kure, K.-A., Dahlqvist, G., Ekström, J., Helle, T. (1999a): "Hydrocyclone separation, and reject refining, of thick-walled mechanical fibres", Nord Pulp Paper Res. J. 14(2): 100-104.

Kure, K.-A., Dahlqvist, G., Helle, T. (1999b): "Morphological characteristics of TMP fibres as affected by the rotational speed of the refiner", Nord. Pulp Paper Res. J. 14(2): 105-110.

Lhotta, T., Villforth, K., Schabel, S. (2007): "Fibre classification – Advanced fibre analysis for quality control and process optimization in stock preparation", Int. Papwirtsch 3, pp. 50-53.

Liimatainen, H., Haikkala, P., Lucander, M., Karojärvi, R., Tuovinen, O. (1999): "Grinding and pressure grinding", in: Papermaking Science and Technology - Mechanical pulping (ISBN 952-5216-00-5), J. Sundholm (ed.), Fapet Oy, Helsinki, Finland, pp. 107-158.

Lindholm, C.A. (1980): "Comparison of some papermaking properties of groundwood and thermomechanical pulp by means of artificial blends of pulp fractions, Part 1. Primary results", Paperi Puu 62(10): 593-600, 603-605.

Lindholm, C.A. (1983): "Determining optimum combinations of mechanical pulp fractions, Part 2. Optimisation of the composition of SGW, PGW and TMP pulps", Paperi Puu 65(6-7): 404-409.

Lundin, T. (2008): "Tailoring pulp fiber properties in low consistency refining", Academic doctorate thesis (ISBN 978-952-12-2107-1), Åbo Akademi, Åbo, Finland, 259 pp.

MacMillan, F.A., Favrel, W.R., Booth, K.G. (1965): "Shives in newsprint: their detection, measurements and effects on paper quality", Pulp Paper. Can. 66(7): T361-T369.

Mohlin, U.-B. (1977): "The distinguishing character of thermomechanical pulp", Proc. CPPA 63rd Ann. Meeting, Februari, Canada, pp. A23-A28.

Mohlin, U.-B. (1979): "Properties of TMP fractions and their importance for the quality of printing papers", Proc. Int. Mechanical Pulp. Conf., June 11 – 14, Toronto, Canada, pp. 57-84.

Mohlin, U.-B. (1980): "Properties of TMP fractions and their importance for the quality of printing papers. Part 1: Large variations in properties within fractions are observed", Svensk Papperstidning 83(16): 461-466.

Mohlin, U.-B. (1989): "Fibre bonding ability – a key pulp parameter for mechanical pulps to be used in printing papers", Proc. Int. Mechanical Pulp. Conf., June 6 – 8, Helsinki, Finland, pp. 49-57.

Mohlin, U.-B. (1995): "Fibre development in mechanical pulp refining", Proc. Int. Mechanical Pulp. Conf., June 12 – 15, Ottawa, Canada, pp. 71-77.

Mohlin, U.-B. (1997): "Fibre development during mechanical pulp refining", J. Pulp Pap. Sci. 23(1): J28-J33.

Musselman, R., Letarte, D., Simard, R. and Lachance, C. (1966): "Third stage low consistency refining of TMP for newsprint/directory grades", Proc. Ann. Appita Conf., Auckland, New Zealand, pp. 363-368.

Mörseburg, K. (2000): "Development and characterization of Norway spruce pressure groundwood pulp fibres", Academic doctorate thesis (ISBN 952-12-0650-0), Åbo Akademi University, Åbo, Finland, 173 pp.

Norgren, S., Höglund, H. (2007): "Moisture-induced surface roughness in TMP sheets – Effects of coarse fibre decollapse and internal bond strength", Proc. Int. Mechanical Pulp. Conf., May 6 – 9, Minneapolis, USA, CD-ROM, 12 pp.

Norman, F., Höglund, H. (2003): "Moisture-induced surface roughness in TMP-based paper – The influence of fiber cross-section dimensions", Int. Mechanical Pulp. Conf., June 2 - 5, Quebec, Canada, pp. 409-415.

Panshin, A.J., DeZeeuw, C. (1970): "The Woody Plant Cell", In: Textbook of wood technology: Vol 1: Structure, identification, uses and properties of the commercial woods of the United States and Canada (ISBN: 0-07-048440-6), McGraw-Hill, New York, USA, pp. 67-109.

Petit-Conil, M., Cochaux, A., de Choudens, C. (1994): "Mechanical pulp characterization: a new and rapid method to evaluate fiber flexibility", Paperi Puu 76(10): 657-662.

Pulkkinen, I., Ala-Kaila, K., Aittamaa, J. (2006): "Characterization of wood fibers using fiber property distributions", Chem. Eng. Proc. 45(7): 546-554.

Reme, P.A. (2000): "Some effects of wood characteristics and the pulping process on mechanical pulp fibres", Academic doctorate thesis (ISBN 827-98-4042-7), Norwegian University of Science and Technology, Trondheim, Norway, 120 pp.

Reme, P.A., Helle, T., Johnsen, P.O. (1998): "Fibre characteristics of some mechanical pulp grades", Nord. Pulp Paper Res. J. 13(4): 8-13.

Reme, P.A., Kure, K.-A., Gregersen, Ø.W., Helle T. (1999a): "Optimal mechanical pulp fibres for improved publication paper: targets and treatments", Proc. Int. Mechanical Pulp. Conf., May 24 – 26, Houston, Texas, USA, pp. 171-182.

Reme, P.A., Johnsen, P.O., Helle, T. (1999b): "Changes induced in early- and latewood fibres by mechanical pulp refining", Nord. Pulp Paper Res. J. 14(3): 256-262.

Reme, P.A., Helle, T. (2001): "Quantitative assessment of mechanical fibre dimensions during defibration and fibre development", J. Pulp Paper Sci. 27(1): 1-7.

Reyier, S. (2008): "Bonding ability distribution of fibers in mechanical pulp furnishes", Academic licentiate of technology thesis (ISBN 978-91-85317-90-5), Mid Sweden University, Sundsvall, Sweden, 91 pp.

Reyier, S., Ferritsius, O., Ferritsius, R. (2011): "The development of fiber characteristic distributions in mechanical pulp refining", Proc. Int. Mechanical Pulp. Conf., Xi'an, China, June 27 – 29, pp. 40-43.

Richardson, J.D., Ridell, M.J.C., Burrelle, P. (2013): "Experience with the FiberLab™ V3.0 analyser for measuring fibre crosssection", Proc. 67th Appita Ann. Conf., May 8 – 10, Melbourne, Australia, pp. 315-322.

Rundlöf, M. (2002): "Interaction of dissolved and colloidal substances with fines of mechanical pulp – Influence on sheet properties and basic aspects of adhesion", Academic doctorate thesis (ISSN 1104-7003), Royal Institute of Technology, Stockholm, Sweden, 78 pp.

Rundlöf, M., Höglund, H., Htun, M., Wågberg, L. (1995): "Effect of fines quality on paper properties – New aspects", Proc. Int. Mechanical Pulp. Conf., June 12 – 15, Ottawa, Canada, pp. 109-118.

Rusu, M., Liukkonen, S., Gregersen, Ø.W., Sirviö, J. (2011): "The influence of fibre wall thickness and fibril angle on fibre development in the TMP process", Nord. Pulp Paper Res. J. 26(1): 6-12.

Salmén L., Dumail, J.F., Uhmeie, A. (1997): "Compression behaviour of wood in relation to mechanical pulping", Proc. Int. Mechanical Pulp. Conf., June 9 – 13, Stockholm, Sweden, pp. 207-211.

Sandberg C., Nilsson L., Nikko A. (1997): "Fibre fractionation – a way to improve paper quality", Proc. Int. Mechanical Pulp. Conf., June 9 – 13, Stockholm, Sweden, pp. 167-171.

Sears, G.R., Tyler, R.F., Denzer, C.W. (1965): "Shives in newsprint: The role of shives in paper web breaks", Pulp Paper Can. 66(7): T351-T360.

Shagaev, O., Bergström, B. (2005): "Advanced process for production of high quality mechanical pulps for value-added paper grades" Proc. Int. Mechanical Pulp. Conf., June 7 - 9, Oslo, Norway, pp. 169-179.

Simons, F.L. (1950): "A stain for use in the microscopy of beaten fibers", Tappi J. 33(7): 312-314.

Sjöström, E. (1993): "The structure of wood", In: Wood chemistry Fundamentals and Applications (ISBN 0-12-647481-8), Academic Press Inc., San Diego, USA, pp. 1-20.

Steadman, R., Luner. P. (1985): "The effect of wet fibre flexibility on sheet apparent density", Proc. Tappi Papermaking Raw Materials – 8th Fund. Res. Symp., Oxford, Great Britain, pp. 311-337.

Strand, B.C. (1987): "Factor analysis as applied to the characterization of high yield pulps", Proc. TAPPI Pulp. Conf., November 1 – 5, Washington D.C., USA, pp. 61-66.

Sundholm, J., Heikkurinen, A., Mannström, B. (1987): "The role of rate of rotation and frequency in refiner mechanical pulping", Proc. Int. Mechanical Pulp. Conf., June 2 – 5, Vancouver, Canada, pp. 45-51.

Svensson, B. (2007): "Frictional studies and high strain rate testing of wood under refining conditions", Academic doctorate thesis (ISBN 978-91-85317-64-6), Mid Sweden University, Sundsvall, Sweden, 88 pp.

Tam Doo, P.A., Kerekes, R.J. (1981): "A method to measure fibre flexibility", Tappi J. 64(3): 113-116.

Tchepel, M., McDonald, D.J., Dixon, T. (2006): "The effect of peroxide bleaching on the mechanical properties of black spruce fibres", Proc. PAPTAC 92nd Ann. Meeting, February 7 – 9, Montreal, Canada, pp. B193-B200.

Tienvieri, T., Huusari, E., Sundholm, J., Vuorio, P., Kortelainen, J., Nystedt, H., Artamo, A. (1999): "Thermomechanical pulping", In: Papermaking Science and Technology - Mechanical pulping (ISBN 952-5216-00-5), J. Sundholm (ed.), Fapet Oy, Helsinki, Finland, pp. 159-222.

Trendelenburg, R., Mayer-Wegelin, H. (1955): "Das Holz als Rohstoff", 2nd Ed. Carl Hanser Verlag, München, page 140.

Tyrväinen, J. (1995): "The influence of wood properties on the quality of TMP made from Norway spruce (*Picea abies*) – wood from old-growth forests, first-thinnings, and sawmill chips", Proc. Int. Mechanical Pulp Conf., June 12 – 15, Ottawa, Canada, pp. 23-33.

Ullman, U., Billing, O., Jonsson, A. (1965): "Fibre fractionation as a method of characterizing pulp", Svensk Papperstidning 68(7): 230-248.

Vesterlind, E.-L., Höglund, H. (2005): "Chemi-mechanical pulp made from birch at high temperature", Proc. SPCI Int. Conf., June 14 – 16, Stockholm, Sweden, 6 pp.

Wakelin, R.F. (2004): "Evaluation of pulp quality through sedimentation measurements", Proc. 58th Appita Ann. Conf., April 19 – 21, Canberra, Australia, pp. 357-365.

Wedin, P.-O., Falk, B., Fredriksson, B., Bäck, R., Höglund, H. (1992): "Double-disc refined TMP for LWC Paper", Proc. 4th Int. Conf. New Available Technol., May 19 – 22, Bologna, Italy, pp. 281-296.

Wood, J.R., Karnis, A. (1979): "Distribution of fibre specific surface of papermaking pulps", Pulp Paper Can. 80(4): T116-121.

Wood, J.R., Karnis, A. (1991): "Future furnish requirements for newsprint and mechanical printing papers", Pulp Paper Can. 92(1): 72-76.

Abbreviations:

CPPA: Technical section of Canadian Pulp and Paper Association (before 1998)
PAPTAC: Pulp and Paper technical Association of Canada (from 1998)
SPCI: Swedish Association of Pulp and Paper Engineers
Appita: Australian and New Zealand Pulp and Paper Technical Association
FRS: Fundamental Research Symposium
PTS: Papiertechnische Stiftung (Germany)

Other references

Statistics about mechanical pulp production in Sweden (*cf.* Abstract and Section 1) was found in the document **Branschstatistik 2013** (2014/09/19), downloaded from **skogsindustrierna.org**.

The approximate sieve sizes of the 16, 30, 50 and 100 mesh screens used in Bauer McNett fractionation (*cf.* Table A2.1.1 in Appendix A) were found under the heading "Particle Size - US Sieve Series and Tyler Mesh Size Equivalents" at **azom.com** (2014/09/19).

Published papers are included in the printed version of this thesis with the kind permission of the journals.

Where nothing else is stated or referenced, images and micrographs published in this thesis were taken by the author.

APPENDICES

The appendices contain results that were not included in any papers but were still considered important for the general outcome of this study. In the appendices, the notations "Pulps A-E" are sometimes used to describe the five pulps that were fractionated in hydrocyclones; TMP1 (Pulp A), TMP2 (Pulp B), TMP3 (Pulp C), SGW (Pulp D) and CTMP (Pulp E).

APPENDIX A

A1. Hydrocyclone fractionation

A1.1 Reject rate Rm

The reject rate, Rm, was calculated according to Equation A.1.1 below.

$$m_{out} = m_{feed}\left(1 - \frac{R_{m(n)}}{100}\right) \qquad \text{Eq. A1.1.1}$$

where $m_{feed\,(n)}$ = weight of pulp into fractionation stage *n*
$m_{out(n)}$ = weight out of hydrocyclone accept stream *n*
$R_{m(n)}$ = reject quote of fractionation stage *n*

Table A1.1.1. Reject rates for the pilot hydrocyclone fractionation.

Stage		Rm		Rm		Rm		Rm		Rm
1	PulpA	67	PulpB	62	PulpC	46	PulpD	43	PulpE	88
2	PulpA	68	PulpB	61	PulpC	40	PulpD	36	PulpE	88
3	PulpA	56	PulpB	62	PulpC	40	PulpD	47	PulpE	93
4	PulpA	50	PulpB	60	PulpC	44	PulpD	61	PulpE	52
5	PulpA	50	PulpB	60	PulpC	44	PulpD	61	PulpE	52

A1.2 Calculations of pulp partition per stream for tensile index distributions

In order to evaluate how much of the feed pulps' fibers that went with each stream, some calculations were needed. The calculation example below is based on the amount of R100 fibers for Pulp A. The same calculations were made with the Bauer McNett fractions R16, P16/R30, P30/R50 and P50/R100 for all pulps A-E.

Calculation example R100 fibers, Pulp A;

Calculate how many grams pulp that went with each accept stream n.

$$m_{out(n)} = m_{feed(n)} * \left(1 - \frac{R_{m(n)}}{100}\right) \qquad \text{Eq. A1.2.1}$$

Calculation base: 100 g.

Stage 1:
$m_{feed\ (1)}$ = 100.00 g
Rm_1 = 67 (*cf.* Table A1.1.1)
Stream 1: 100.00 g * (1 – 0.67) = 33.00g
Apex 1: 100.00 g *Rm_1=100.00 * 67 = 67.00 g (= $m_{feed\ (2)}$)

Eq. A1.2.1 → 67 weight % of the feed goes into the apex (reject) and the rest (1-Rm) to the base (taken out as Stream 1).

Stage 2:
$m_{feed\ (2)}$ = 67.00 g
Rm_2 = 68
Stream 2: 67.00 g * (1-0.68) = 21.44 g
Apex 2: 67.00 g * 0.68 = 45.56 g

Stage 3:
$m_{feed\ (3)}$ = 45.56 g
Rm_3 = 56
Stream 3: 45.56 g * (1 – 0.56) = 20.05 g
Apex 3: 45.56 g * 0.56 = 25.51 g

Stage 4:
$m_{feed\ (4)}$ = 25.51 g
Rm_4 = 50
Stream 4: 25.51 g * (1 – 0.50) = 12.76 g
Apex 4 (= Stream 5): 25.51 g * 0.50 = 12.76 g

Amount of R100 per stream:

$$Percent\ of\ R100\ stream\ n = \frac{Percent\ R100\ in\ stream\ n}{Percent\ R100\ \ in\ feed} \qquad \text{Eq. A1.2.2}$$

Eq. A1.2.2 →
70.5% R100 (*cf.* Table A2.1.2)
Weight of fiber fraction per stream was calculated above.

Stream 1: 46.9% R100 → (46.9 / 70.5) * 33.00 g = 22.0% of R100
Stream 2: 65.5% R100 → (65.5 / 70.5) * 21.44 g = 19.9% of R100
Stream 3: 84.9% R100 → (84.9 / 70.5) * 20.05 g = 24.1% of R100
Stream 4: 90.6% R100 → (90.6 / 70.5) * 12.76 g = 16.4% of R100
Stream 5: 93.2% R100 → (93.2 / 70.5) * 12.76 g = 16.9% of R100

SUM: 99.3%

The sum of the R100 should be 100%. The error was approximated to be the same for each stream and to compensate for small deviations in the Bauer McNett fractionation and in weighing the Bauer McNett samples, an adjustment was made according to Equation 1.2.3.

$$Percent\ of\ R100\ in\ stream\ n\_adjusted = \frac{Percent\ of\ R100\ in\ stream\ n}{total\ R100\ including\ fault} \qquad \text{Eq. A1.2.3}$$

Eq. 1.2.3 → The adjusted R100 for each stream then becomes:

Stream 1: 22.0% R100 → (22.0 / 93.3) * 100 = 22.2% of R100 (adjusted)
Stream 2: 19.9% R100 → (19.9 / 99.3) * 100 = 20.0% of R100 (adjusted)
Stream 3: 24.1% R100 → (24.1 / 99.3) * 100 = 24.3% of R100 (adjusted)
Stream 4: 16.4% R100 → (16.4 / 99.3) * 100 = 16.5% of R100 (adjusted)
Stream 5: 16.9% R100 → (16.9 / 99.3) * 100 = 17.0% of R100 (adjusted)

The result of the partition of the fibers from various Bauer McNett fractions is found in Section A1.3.

A1.3 Fiber partition in hydrocyclone streams

Table A1.3.1a. Partition of fibers per hydrocyclone stream with respect to the R100 fraction. The correlation between the amount of R100 fibers (fibers retained on a 100 mesh screen) and the amount of pulp in specific Bauer McNett fractions in each hydrocyclone stream was very high for the P16/R30 and P30/R50 fractions.

	Pulp A	Pulp B	Pulp C	Pulp D	Pulp E
Stream 1	22.1	29.8	48.5	49.3	8.7
Stream 2	20.0	24.2	29.2	30.3	9.9
Stream 3	24.3	16.6	12.9	10.7	5.2
Stream 4	16.5	11.5	5.3	3.9	36.4
Stream 5	17.0	17.9	4.0	5.9	39.7

Table A1.3.1b. Partition of fibers per hydrocyclone stream with respect to the R16 fraction.

	Pulp A	Pulp B	Pulp C	Pulp D	Pulp E
Stream 1	17.9	25.2	43.9	56.6	1.3
Stream 2	20.4	23.6	30.3	30.3	4.6
Stream 3	33.4	17.7	14.9	14.9	5.6
Stream 4	10.0	13.9	6.3	6.3	44.3
Stream 5	18.4	19.6	4.6	4.6	44.2

Table A1.3.1c. Partition of fibers per hydrocyclone stream with respect to the P16/R30 fraction.

	Pulp A	Pulp B	Pulp C	Pulp D	Pulp E
Stream 1	22.4	29.1	47.2	49.5	4.2
Stream 2	20.6	24.3	29.1	31.5	9.0
Stream 3	23.3	16.9	13.3	10.4	5.2
Stream 4	16.5	10.7	5.8	4.0	39.6
Stream 5	17.1	19.1	4.6	4.7	41.9

Table A1.3.1d. Partition of fibers per hydrocyclone stream with respect to the P30/R50 fraction.

	Pulp A	Pulp B	Pulp C	Pulp D	Pulp E
Stream 1	24.5	31.8	50.5	49.4	6.7
Stream 2	19.7	24.6	28.6	31.4	8.5
Stream 3	21.8	15.5	12.1	9.7	6.3
Stream 4	14.9	11.4	4.9	3.5	36.0
Stream 5	19.1	16.7	3.9	6.0	42.5

A2. Bauer McNett fractionation

A2.1 Results from Bauer McNett fractionation

Table A2.1.1. Approximate sieve size of the Bauer McNett screens (azom.com)

Sieve size (approx)	**US standard**	*Taylor Standard*
1.190 mm	16 mesh	*14 mesh*
0.595 mm	30 mesh	*28 mesh*
0.297 mm	50 mesh	*48 mesh*
0.149 mm	100 mesh	*100 mesh*

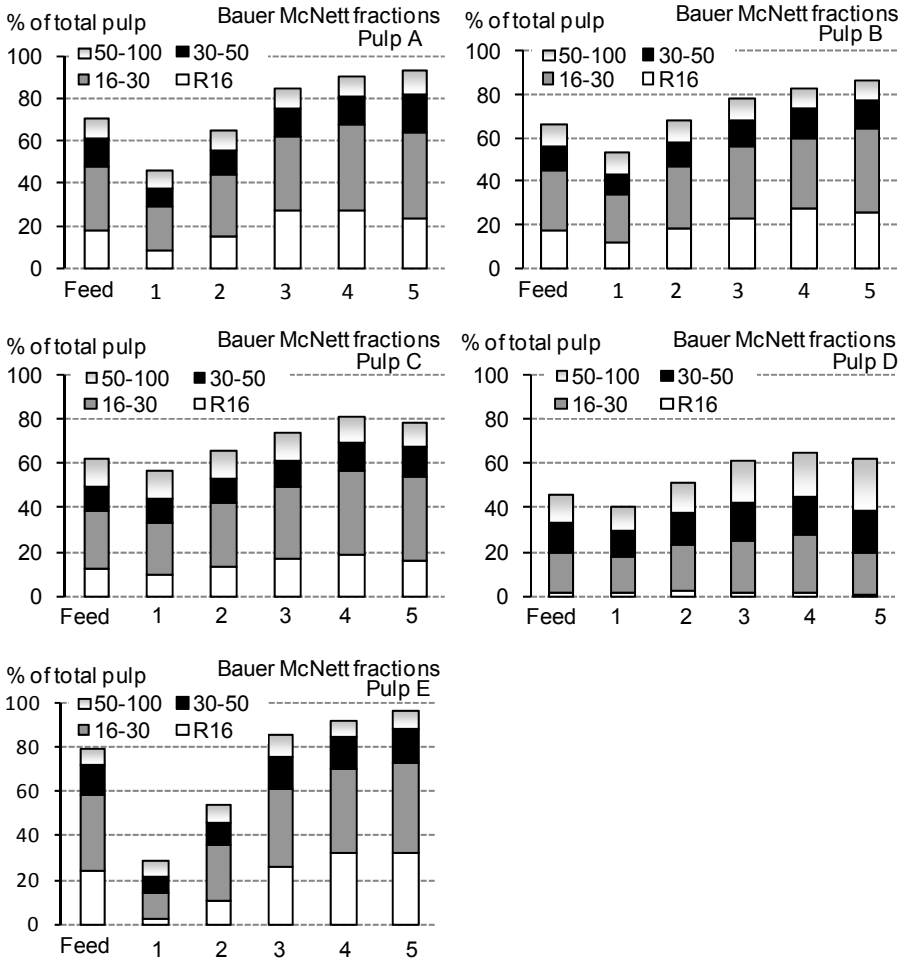

Figures A2.1.1a-e. Graphic results of Bauer McNett classification for the five reference pulps A-E. The height of each graphic blocks represent the R100 fraction.

Table A2.1.2. Results of Bauer McNett fractionation.

Pulp	Fraction	Feed	Stream 1	Stream 2	Stream 3	Stream 4	Stream 5
PulpA	R16	18.1	8.9	15.5	27.3	28.1	23.5
	16-30	30.7	20.8	29.5	35.6	39.6	41.1
	30-50	12.7	8.8	10.9	12.9	13.8	17.8
	50-100	9.0	8.5	9.7	9.2	9.2	10.8
	R100	70.5	46.9	65.5	84.9	90.6	93.2
PulpB	R16	17.4	12.6	18.5	23.4	28.0	26.5
	16-30	28.4	21.7	28.4	33.3	32.5	38.4
	30-50	10.9	9.2	11.2	11.8	13.4	13.0
	50-100	9.9	10.2	10.5	10.1	9.5	9.2
	R100	66.6	53.6	68.5	78.6	83.4	87.0
PulpC	R16	12.5	10.2	13.8	17.0	19.2	16.8
	16-30	26.9	23.6	28.5	32.6	37.7	37.9
	30-50	10.7	10.3	11.4	12.1	13.0	13.1
	50-100	12.2	12.6	12.9	12.3	11.9	10.9
	R100	62.2	56.6	66.6	73.9	81.6	78.6
PulpD	R16	1.9	1.9	2.6	2.0	2.0	0.7
	16-30	18.5	16.2	21.4	23.7	25.9	19.6
	30-50	13.2	12.1	14.5	16.5	17.4	18.8
	50-100	12.5	10.6	13.3	19.2	20.2	23.5
	R100	46.1	40.7	51.7	61.3	65.4	62.5
PulpE	R16	24.6	2.7	11.1	26.4	32.7	32.7
	16-30	34.8	11.7	24.9	35.3	38.4	40.8
	30-50	12.8	7.1	10.2	14.6	14.0	15.7
	50-100	7.5	7.6	8.6	10.3	7.9	7.9
	R100	79.6	29.1	54.7	86.5	92.9	97.0

A3. Physical testing of long fiber laboratory sheets

A3.1 Sheet testing results

Table A3.1.1. Results from physical testing of long fiber laboratory sheets.

Pulp	Stream	Fraction	Tensile index [Nm/g]	Density STFI [kg/m3]	Density single sheet [kg/m3]	Tensile stiffness index [kNm/g]	Strain at failure [%]	Tensile energy absorption index [J/g]	Light scattering coefficient Ry C/2° S1 Ry [m2/kg]
PulpA	0	R16	10.52	276.0	225.3	1.7708	0.8202	0.05166	24.89
PulpA	1	R16	11.85	278.0	213.0	1.8598	0.8910	0.06317	28.68
PulpA	2	R16	11.78	293.3	227.1	1.9544	0.8398	0.05982	26.83
PulpA	3	R16	9.12	280.1	211.9	1.6263	0.7993	0.04431	25.15
PulpA	4	R16	8.41	273.2	217.1	1.5881	0.7313	0.03667	23.90
PulpA	5	R16	5.87	262.8	194.3	0.0000	0.8040	0.02745	22.47
PulpA	0	P16/R30	9.60	276.9	223.7	1.6102	0.8171	0.04685	28.46
PulpA	1	P16/R30	14.08	312.0	234.2	2.1447	0.9367	0.08017	31.60
PulpA	2	P16/R30	14.07	316.1	246.4	2.1851	0.9218	0.07919	31.16
PulpA	3	P16/R30	8.65	280.0	219.4	1.4908	0.8414	0.04433	28.61
PulpA	4	P16/R30	7.14	270.2	205.1	0.0000	0.7860	0.03381	27.44
PulpA	5	P16/R30	5.68	266.0	199.9	0.0000	0.8450	0.02659	25.94
PulpA	0	P30/R50	15.14	334.0	280.2	2.2168	1.1560	0.11327	35.49
PulpA	1	P30/R50	29.14	392.9	338.8	3.5192	1.6692	0.32594	41.15
PulpA	2	P30/R50	24.55	377.3	335.4	3.2002	1.3699	0.22075	38.96
PulpA	3	P30/R50	12.27	309.3	261.3	1.9115	1.0412	0.08190	34.27
PulpA	4	P30/R50	9.00	306.2	234.7	1.5036	0.8903	0.04945	33.29
PulpA	5	P30/R50	5.08	284.0	235.1	0.0000	0.6270	0.02150	29.59
PulpB	0	R16	13.40	311.4	238.3	2.2188	0.8968	0.07348	27.37
PulpB	1	R16	16.59	343.1	255.8	2.4019	1.1192	0.11768	28.03
PulpB	2	R16	13.72	297.7	239.1	2.2669	0.9178	0.07782	28.61
PulpB	3	R16	14.70	303.2	235.5	2.4549	0.8697	0.07797	27.77
PulpB	4	R16	11.52	302.6	235.3	1.9239	0.8704	0.06120	25.37
PulpB	5	R16	10.20	313.4	244.3	1.8435	0.8118	0.05068	25.74
PulpB	0	P16/R30	14.87	322.5	256.4	2.2738	1.0023	0.09280	31.81
PulpB	1	P16/R30	21.63	352.0	292.0	2.9171	1.2553	0.17423	33.27

PulpB	2	P16/R30	16.78	349.5	285.6	2.6142	1.0021	0.10539	32.36
PulpB	3	P16/R30	16.63	340.9	277.5	2.5362	1.0559	0.11134	30.92
PulpB	4	P16/R30	12.08	303.2	239.5	2.2014	0.7951	0.05863	31.26
PulpB	5	P16/R30	10.25	276.5	227.1	1.8045	0.8416	0.05380	27.81
PulpB	0	P30/R50	25.26	393.2	330.1	3.0269	1.7000	0.29180	40.90
PulpB	1	P30/R50	39.44	460.6	398.4	4.0033	2.3602	0.65039	44.24
PulpB	2	P30/R50	27.24	417.1	365.5	3.3326	1.7191	0.32087	42.00
PulpB	3	P30/R50	24.41	404.1	340.3	3.0105	1.5993	0.26344	39.69
PulpB	4	P30/R50	18.22	358.4	313.3	2.5633	1.3105	0.15856	36.95
PulpB	5	P30/R50	10.97	313.5	266.6	1.8707	0.9469	0.06529	32.59
PulpC	0	R16	18.62	390.2	321.1	3.1218	0.8659	0.09873	28.62
PulpC	1	R16	17.22	410.2	208.2	3.0941	0.8384	0.08998	30.62
PulpC	2	R16	16.25	372.8	218.9	2.8931	0.8610	0.08774	28.15
PulpC	3	R16	17.00	369.3	192.5	2.9673	0.8955	0.09598	26.30
PulpC	4	R16	14.16	377.1	220.7	2.6279	0.8221	0.07311	26.17
PulpC	5	R16	13.68	356.8	223.7	2.8784	0.6731	0.05663	27.04
PulpC	0	P16/R30	24.66	431.3	370.6	3.6255	1.1136	0.17378	32.68
PulpC	1	P16/R30	24.84	444.5	172.7	3.9345	1.1108	0.18004	34.47
PulpC	2	P16/R30	22.91	399.1	183.9	3.6053	1.1050	0.16504	33.70
PulpC	3	P16/R30	21.22	424.6	179.0	3.4772	1.0556	0.14580	32.72
PulpC	4	P16/R30	17.49	403.4	198.0	2.9593	0.9624	0.10792	31.28
PulpC	5	P16/R30	13.80	372.3	216.0	2.6015	0.7933	0.06868	29.53
PulpC	0	P30/R50	40.31	509.1	452.3	4.7018	1.9902	0.56212	43.42
PulpC	1	P30/R50	43.97	529.8	134.9	5.1619	2.0333	0.62908	47.18
PulpC	2	P30/R50	37.25	502.1	146.9	4.6106	1.8820	0.49356	44.69
PulpC	3	P30/R50	32.53	493.9	150.2	4.2208	1.7159	0.38903	41.85
PulpC	4	P30/R50	24.68	449.3	164.8	3.5591	1.3875	0.23219	39.20
PulpC	5	P30/R50	16.06	393.9	189.4	2.6361	1.0873	0.11593	35.07
PulpD	0	P16/R30	21.24	373.2	302.3	2.9518	1.3397	0.18724	37.09
PulpD	1	P16/R30	24.50	367.7	195.6	3.2507	1.4610	0.23641	37.34
PulpD	2	P16/R30	20.55	371.6	217.7	3.0754	1.2200	0.16393	37.16
PulpD	3	P16/R30	18.24	363.5	218.9	2.6910	1.1922	0.14124	36.21
PulpD	4	P16/R30	16.37	335.4	219.1	2.5391	1.1322	0.12112	34.97
PulpD	5	P16/R30	9.96	274.9	292.9	1.6288	1.0260	0.06552	31.96
PulpD	0	P30/R50	27.36	407.4	359.3	3.2655	1.8541	0.34705	45.69
PulpD	1	P30/R50	34.93	455.4	162.0	3.9282	2.0189	0.48159	48.27
PulpD	2	P30/R50	25.23	411.5	180.1	3.3416	1.6758	0.29094	46.48

PulpD	3	P30/R50	21.28	401.6	190.6	2.9376	1.4483	0.20637	43.83
PulpD	4	P30/R50	19.66	392.1	191.4	2.6961	1.6023	0.21667	43.43
PulpD	5	P30/R50	6.43	296.9	277.8	1.1114	1.2488	0.04892	35.36
PulpD	0	P50/R100	37.11	461.5	430.2	3.8226	2.3164	0.59448	57.47
PulpD	1	P50/R100	46.47	524.8	134.4	4.5666	2.4105	0.76780	60.02
PulpD	2	P50/R100	33.25	470.8	154.4	3.6993	2.0978	0.48245	57.84
PulpD	3	P50/R100	29.15	457.9	160.6	3.4801	2.0337	0.41741	54.92
PulpD	4	P50/R100	21.73	429.2	177.8	2.8421	1.6703	0.25085	48.57
PulpD	5	P50/R100	4.66	332.4	236.5	0.0000	1.0140	0.03715	35.31
PulpE	0	R16	5.76	216.1	170.7	0.0000	1.0422	0.03072	26.27
PulpE	1	R16	10.82	260.8	195.9	1.9755	0.8015	0.05336	28.93
PulpE	2	R16	13.25	261.2	190.1	2.4733	0.7624	0.06148	31.88
PulpE	3	R16	6.94	231.9	179.3	0.0000	0.7740	0.03185	25.32
PulpE	4	R16	6.28	248.5	212.9	0.0000	0.6980	0.02435	23.41
PulpE	5	R16	5.99	224.8	195.6	0.0000	0.7978	0.02518	22.00
PulpE	0	P16/R30	5.47	211.5	170.9	0.0000	0.7380	0.02247	29.36
PulpE	1	P16/R30	19.27	266.5	235.2	3.2486	0.8714	0.10349	35.32
PulpE	2	P16/R30	15.94	290.3	237.1	2.7436	0.8309	0.08050	33.58
PulpE	3	P16/R30	9.13	229.5	191.1	2.0053	0.6557	0.03616	32.64
PulpE	4	P16/R30	7.29	248.4	193.6	0.0000	0.5840	0.02437	29.39
PulpE	5	P16/R30	6.30	226.7	177.6	0.0000	0.7070	0.02486	28.84
PulpE	0	P30/R50	6.71	244.2	206.5	1.2690	0.8186	0.03276	33.94
PulpE	1	P30/R50	30.38	436.6	377.6	3.7343	1.6649	0.34319	39.96
PulpE	2	P30/R50	25.01	382.7	332.6	3.4689	1.2423	0.20113	40.88
PulpE	3	P30/R50	15.08	333.1	284.3	2.3946	1.0524	0.10257	36.78
PulpE	4	P30/R50	10.15	290.7	236.7	1.8879	0.7757	0.04834	35.14
PulpE	5	P30/R50	5.33	237.1	194.8	0.0000	0.6450	0.01761	32.30
PulpE	0	P50/R100	17.94	362.9	322.9	2.6281	1.2381	0.14621	40.70
PulpE	1	P50/R100	53.16	606.8	551.1	5.3050	2.5111	0.93511	48.98
PulpE	2	P50/R100	43.84	494.5	477.4	4.6538	2.1369	0.64924	48.52
PulpE	3	P50/R100	29.42	499.6	441.0	3.9318	1.7324	0.35599	45.63
PulpE	4	P50/R100	17.14	375.5	330.1	2.5759	1.2357	0.14188	41.84
PulpE	5	P50/R100	7.74	309.1	262.3	1.4543	0.8309	0.03996	36.47

Table A3.1.2. Average coefficient of variation of measurements of physical testing of long fiber laboratory sheets*.

Measured long fiber sheet property	Average CV*
Tensile index	6.8%
Density STFI	raw data not available
Density (single sheet)	4.7%
Tensile Energy Absorption Index	13.6%
Tensile Stiffness Index	6.5%
Strain at failure	9.0%
Light scattering coefficient Ry	3.7%

**confidence intervals, repeatability reports and deviations are based upon evaluations from this work and do not provide a general description of any method repeatability.*

A3.2 Characteristics of each hydrocyclone stream – Tensile index

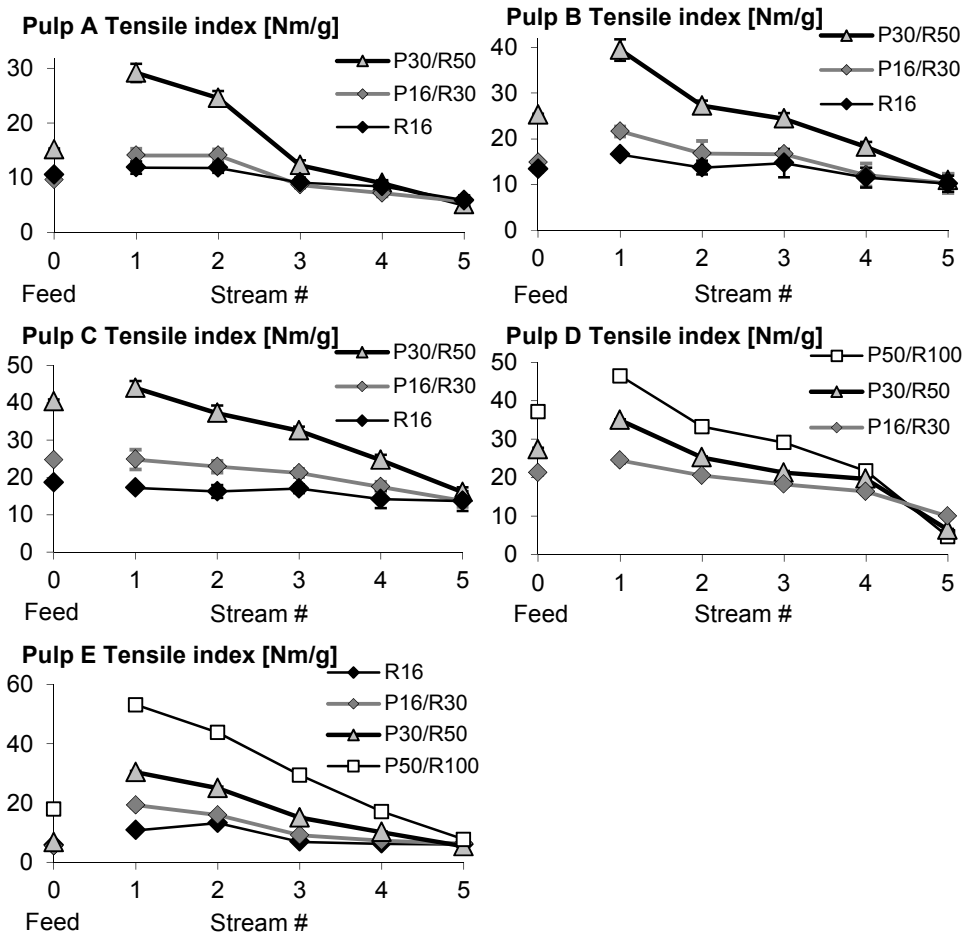

Figures A3.2.1a-e. For all five evaluated pulps, the tensile index of each Bauer McNett fraction of the reference pulps was converging towards a lowest value in Stream 5 which was independent of fiber length. Also the density converged towards a common value in Stream 5 for all Bauer McNett fractions, but the density of Stream 5 was not consistently similar as for tensile index. The level of the lowest tensile index can be derived from specific energy consumption and known process differences. It is possible that a pulp's lowest level of tensile index is a more valuable measure of characterization than the highest.

A4. FiberLab™

A4.1 FiberLab averages

Table A4.1.1. Arithmetic averages of fiber characteristics from the FiberLab optical analyzer for P16/R30, P30/R50 fraction, 0.7-2.3 mm fraction and all fibers. Figures are based on data which was screened to include fibers of cross-sectional fiber wall area, fibrillation index and curl index > 0.

Pulp	Stream	Fraction	Lc	Lp	CSA	Volume	Curl	Fibrillation	Width	Wall	CRI	BIN =f(CRI,fibrill.)
PulpA	0	P16/R30	1.87	1.73	747.83	1.38	7.87	3.39	33.59	10.16	6.22	9.89
PulpA	1	P16/R30	1.96	1.80	686.55	1.36	9.03	3.93	33.25	9.25	5.30	14.59
PulpA	2	P16/R30	1.86	1.71	717.29	1.33	8.54	3.73	33.47	9.65	5.66	12.80
PulpA	3	P16/R30	1.83	1.70	757.94	1.37	7.68	3.37	33.73	10.33	6.37	9.35
PulpA	4	P16/R30	1.83	1.70	789.17	1.42	7.31	3.16	34.13	10.64	6.65	7.79
PulpA	5	P16/R30	1.84	1.72	818.83	1.46	6.64	2.89	34.19	11.06	7.14	5.32
PulpA	0	P30/R50	1.09	0.99	663.87	0.73	10.15	5.09	31.79	9.39	5.67	16.81
PulpA	1	P30/R50	1.11	0.99	553.61	0.63	13.06	7.11	30.04	7.90	4.34	27.31
PulpA	2	P30/R50	1.09	0.98	614.64	0.68	11.50	5.88	31.14	8.67	4.96	21.56
PulpA	3	P30/R50	1.09	1.00	707.03	0.77	9.10	4.53	32.57	9.88	6.04	13.90
PulpA	4	P30/R50	1.11	1.03	754.68	0.84	8.07	3.96	33.29	10.55	6.70	9.98
PulpA	5	P30/R50	1.13	1.06	818.98	0.91	6.75	3.18	34.09	11.31	7.42	5.29
PulpA	0	0.7-2.3mm	1.26	1.15	676.18	0.88	11.08	6.25	32.21	9.40	5.60	20.52
PulpA	1	0.7-2.3mm	1.24	1.10	570.91	0.74	14.04	8.14	30.41	8.10	4.49	29.89
PulpA	2	0.7-2.3mm	1.25	1.13	634.53	0.82	12.42	6.77	31.60	8.82	5.05	23.92
PulpA	3	0.7-2.3mm	1.27	1.17	704.11	0.91	9.56	4.90	32.53	9.83	5.97	15.26
PulpA	4	0.7-2.3mm	1.27	1.18	751.49	0.97	8.39	4.20	33.33	10.34	6.42	11.65
PulpA	5	0.7-2.3mm	1.26	1.18	792.26	1.00	7.31	3.49	33.66	11.06	7.18	6.99
PulpA	0	all fibers	1.21	1.10	602.20	0.82	10.45	6.72	30.22	8.70	5.09	23.64
PulpA	1	all fibers	1.16	1.03	510.82	0.68	13.03	8.59	28.57	7.53	4.08	32.63
PulpA	2	all fibers	1.21	1.09	575.02	0.79	11.43	6.87	29.85	8.27	4.65	25.56
PulpA	3	all fibers	1.24	1.15	644.58	0.89	9.09	4.91	30.87	9.29	5.58	16.60
PulpA	4	all fibers	1.24	1.15	687.48	0.92	7.96	4.12	31.64	9.81	6.04	12.69
PulpA	5	all fibers	1.17	1.09	725.08	0.89	6.62	3.33	31.95	10.57	6.88	7.52
PulpB	0	P16/R30	1.86	1.66	733.69	1.40	12.52	4.84	33.55	9.64	5.59	16.35
PulpB	1	P16/R30	1.89	1.66	704.15	1.39	14.17	5.70	33.39	8.99	4.91	21.18
PulpB	2	P16/R30	1.87	1.67	733.97	1.41	12.56	4.80	33.82	9.47	5.34	17.08
PulpB	3	P16/R30	1.82	1.63	743.56	1.37	11.70	4.54	33.65	9.82	5.73	14.97

PulpB	4	P16/R30	1.79	1.62	766.59	1.38	10.96	4.18	33.99	10.10	6.02	12.94
PulpB	5	P16/R30	1.86	1.69	785.41	1.45	9.61	3.57	33.91	10.60	6.56	9.33
PulpB	0	P30/R50	1.09	0.94	578.36	0.65	16.65	7.58	30.34	7.88	4.29	28.89
PulpB	1	P30/R50	1.13	0.94	513.11	0.61	19.89	9.53	29.28	6.88	3.45	37.51
PulpB	2	P30/R50	1.09	0.93	561.70	0.64	16.93	7.71	30.22	7.64	4.04	30.11
PulpB	4	P30/R50	1.08	0.95	641.72	0.71	13.69	5.99	31.40	8.86	5.10	21.42
PulpB	5	P30/R50	1.12	1.01	724.79	0.82	11.00	4.49	32.60	10.16	6.33	12.81
PulpB	0	0.7-2.3mm	1.25	1.08	605.83	0.80	16.74	8.12	30.69	8.27	4.62	29.42
PulpB	1	0.7-2.3mm	1.24	1.04	528.98	0.70	20.53	10.38	29.44	7.16	3.68	39.31
PulpB	2	0.7-2.3mm	1.25	1.08	587.13	0.78	17.26	8.32	30.76	7.88	4.21	31.36
PulpB	3	0.7-2.3mm	1.26	1.10	639.81	0.84	15.38	6.96	31.59	8.64	4.86	25.12
PulpB	4	0.7-2.3mm	1.11	0.97	617.91	0.70	15.08	6.61	31.22	8.44	4.72	24.54
PulpB	5	0.7-2.3mm	1.26	1.14	732.29	0.94	11.30	4.59	32.65	10.21	6.36	13.01
PulpB	0	all fibers	1.20	1.05	550.90	0.79	15.43	7.92	29.04	7.80	4.32	29.83
PulpB	1	all fibers	1.19	1.01	481.52	0.71	18.60	10.26	27.76	6.75	3.44	39.74
PulpB	2	all fibers	1.21	1.05	533.02	0.77	15.84	8.04	29.04	7.41	3.92	31.53
PulpB	3	all fibers	1.22	1.08	582.38	0.83	14.07	6.58	29.89	8.16	4.55	25.05
PulpB	4	all fibers	1.07	0.93	602.56	0.67	14.91	6.72	30.78	8.28	4.61	25.26
PulpB	5	all fibers	1.19	1.08	663.89	0.86	10.07	4.21	30.85	9.71	6.06	12.89
PulpC	0	P16/R30	1.82	1.59	643.56	1.23	14.54	6.31	32.22	8.44	4.64	23.91
PulpC	1	P16/R30	1.83	1.59	636.33	1.25	15.37	6.51	32.06	8.27	4.48	25.03
PulpC	2	P16/R30	1.80	1.58	643.37	1.22	14.36	6.11	32.22	8.44	4.62	23.37
PulpC	3	P16/R30	1.78	1.57	674.58	1.23	13.72	5.49	32.72	8.88	5.00	20.27
PulpC	4	P16/R30	1.78	1.59	688.97	1.24	12.04	4.89	32.91	9.20	5.29	17.49
PulpC	5	P16/R30	1.79	1.62	724.75	1.30	11.20	4.28	33.20	9.78	5.86	13.76
PulpC	0	P30/R50	1.20	0.98	467.23	0.65	20.89	9.34	29.66	5.85	2.60	39.83
PulpC	1	P30/R50	(0.98)	0.81	431.05	0.47	19.81	10.14	27.08	5.93	2.84	41.41
PulpC	2	P30/R50	1.05	0.89	495.58	0.55	17.97	9.16	28.68	6.79	3.48	36.31
PulpC	3	P30/R50	1.04	0.89	536.67	0.58	16.77	8.01	29.48	7.36	3.91	31.44
PulpC	4	P30/R50	1.05	0.91	580.55	0.63	14.91	7.00	30.22	8.08	4.54	26.30
PulpC	5	P30/R50	1.07	0.94	630.60	0.68	13.02	5.87	31.14	8.85	5.23	20.63
PulpC	0	0.7-2.3mm	1.24	1.06	531.40	0.70	18.61	9.58	29.59	7.24	3.82	36.42
PulpC	1	0.7-2.3mm	1.24	1.04	493.31	0.65	20.68	10.62	28.91	6.63	3.33	41.16
PulpC	2	0.7-2.3mm	1.24	1.06	547.09	0.72	17.98	9.08	29.81	7.33	3.87	34.79
PulpC	3	0.7-2.3mm	1.24	1.08	572.58	0.75	16.75	7.87	30.41	7.81	4.26	29.88
PulpC	4	0.7-2.3mm	1.26	1.11	619.35	0.81	14.51	6.87	31.32	8.47	4.81	25.02

PulpC	5	0.7-2.3mm	1.27	1.13	651.12	0.85	12.88	5.66	31.46	9.17	5.49	19.11
PulpC	0	all fibers	1.20	1.03	484.55	0.68	16.79	9.27	27.93	6.88	3.60	36.25
PulpC	1	all fibers	1.17	0.99	445.68	0.63	19.05	10.38	27.13	6.25	3.12	41.19
PulpC	2	all fibers	1.18	1.02	490.35	0.68	16.60	8.79	27.98	6.91	3.62	34.74
PulpC	3	all fibers	1.17	1.02	511.33	0.69	15.34	7.48	28.44	7.33	3.96	29.68
PulpC	4	all fibers	1.19	1.05	559.04	0.75	13.17	6.32	29.45	8.01	4.52	24.34
PulpC	5	all fibers	1.20	1.07	603.91	0.80	11.59	5.10	29.90	8.87	5.36	17.89
PulpD	0	P16/R30	1.86	1.56	824.36	1.58	18.84	8.10	34.33	10.19	6.08	24.47
PulpD	1	P16/R30	1.87	1.56	788.91	1.56	19.53	8.51	33.82	9.79	5.73	26.84
PulpD	2	P16/R30	1.86	1.57	851.35	1.64	18.22	7.96	34.84	10.40	6.23	23.55
PulpD	3	P16/R30	1.81	1.54	871.02	1.59	17.53	7.51	35.01	10.78	6.64	20.83
PulpD	4	P16/R30	1.79	1.53	889.45	1.62	17.08	7.34	35.05	11.06	6.93	19.33
PulpD	5	P16/R30	1.90	1.65	1037.95	1.90	14.83	6.10	36.69	12.63	8.55	10.24
PulpD	0	P30/R50	1.08	0.89	586.80	0.66	20.86	10.05	29.70	7.81	4.30	36.24
PulpD	1	P30/R50	1.09	0.89	549.02	0.63	21.69	10.71	29.11	7.35	3.89	39.58
PulpD	2	P30/R50	1.07	0.89	607.76	0.68	20.31	9.78	30.07	8.07	4.49	34.80
PulpD	3	P30/R50	1.06	0.89	663.17	0.72	18.94	8.89	31.08	8.77	5.09	30.14
PulpD	4	P30/R50	1.05	0.89	706.94	0.76	17.69	8.35	31.71	9.28	5.56	26.96
PulpD	5	P30/R50	1.09	0.95	907.26	0.98	14.77	6.49	34.62	11.69	7.90	13.57
PulpD	0	0.7-2.3mm	1.16	0.95	590.05	0.73	22.93	11.11	29.65	7.92	4.45	38.94
PulpD	1	0.7-2.3mm	1.16	0.94	537.23	0.68	24.01	12.06	28.75	7.23	3.83	43.81
PulpD	2	0.7-2.3mm	1.16	0.95	604.08	0.75	22.56	11.08	29.81	7.95	4.40	38.99
PulpD	3	0.7-2.3mm	1.17	0.97	654.64	0.82	21.68	10.21	30.78	8.59	4.92	34.65
PulpD	4	0.7-2.3mm	1.16	0.98	701.35	0.86	20.35	9.25	31.59	9.17	5.45	30.01
PulpD	5	0.7-2.3mm	1.16	1.01	842.49	1.01	16.82	7.70	33.45	10.91	7.20	19.52
PulpD	0	all fibers	0.91	0.76	499.92	0.53	19.21	9.96	26.93	7.32	4.13	36.56
PulpD	1	all fibers	0.92	0.76	456.30	0.50	20.23	10.85	26.17	6.68	3.54	41.17
PulpD	2	all fibers	0.91	0.76	510.06	0.54	19.03	9.85	27.09	7.38	4.13	36.22
PulpD	3	all fibers	0.90	0.76	561.66	0.58	17.54	8.67	28.20	8.10	4.74	30.65
PulpD	4	all fibers	0.88	0.75	601.69	0.59	15.87	7.60	28.88	8.67	5.26	25.69
PulpD	5	all fibers	0.75	0.67	746.96	0.60	10.43	5.19	30.85	11.17	8.02	9.26
PulpE	0	P16/R30	1.93	1.82	713.54	1.36	6.37	2.20	33.15	9.91	6.01	7.04
PulpE	1	P16/R30	2.09	1.93	686.97	1.51	8.14	3.15	33.32	9.19	5.16	12.70
PulpE	2	P16/R30	1.93	1.80	687.77	1.36	7.61	2.84	33.64	9.11	5.01	12.30
PulpE	3	P16/R30	1.86	1.75	716.67	1.36	6.60	2.29	33.37	9.80	5.80	8.00
PulpE	4	P16/R30	1.86	1.75	721.81	1.35	6.16	2.13	33.41	9.96	5.99	6.90
PulpE	5	P16/R30	1.95	1.84	774.89	1.55	5.87	1.95	33.74	10.66	6.69	4.02

PulpE	0	P30/R50	1.15	1.07	677.20	0.78	7.99	3.28	32.41	9.64	5.82	10.90
PulpE	1	P30/R50	1.13	0.99	481.73	0.57	14.63	6.20	28.28	7.06	3.66	26.86
PulpE	2	P30/R50	1.11	1.00	570.57	0.65	11.82	5.42	31.05	7.94	4.19	22.76
PulpE	4	P30/R50	1.13	1.05	672.70	0.77	8.23	3.15	32.15	9.57	5.73	10.82
PulpE	5	P30/R50	1.18	1.11	742.29	0.87	6.13	2.29	33.36	10.59	6.70	4.98
PulpE	0	0.7-2.3mm	1.33	1.24	677.20	0.98	8.82	3.62	31.29	9.69	5.93	11.57
PulpE	1	0.7-2.3mm	1.14	0.98	443.54	0.55	17.56	9.32	27.00	6.72	3.48	36.80
PulpE	2	0.7-2.3mm	1.22	1.10	569.25	0.73	13.29	6.92	30.84	7.94	4.22	27.14
PulpE	3	0.7-2.3mm	1.12	1.02	467.99	0.59	11.58	4.17	25.74	7.40	4.26	18.79
PulpE	4	0.7-2.3mm	1.24	1.16	650.46	0.85	8.78	3.37	31.53	9.30	5.53	12.17
PulpE	5	0.7-2.3mm	1.27	1.20	724.56	0.93	6.25	2.31	33.00	10.35	6.45	5.90
PulpE	0	all fibers	1.28	1.19	599.60	0.99	8.40	4.41	29.77	8.66	5.11	16.64
PulpE	1	all fibers	0.97	0.84	381.70	0.46	16.11	10.36	24.91	6.04	3.02	41.47
PulpE	2	all fibers	1.10	0.99	502.80	0.67	12.42	7.37	28.74	7.29	3.79	29.92
PulpE	3	all fibers	1.00	0.90	402.12	0.53	12.07	4.25	23.72	6.65	3.72	20.83
PulpE	4	all fibers	1.17	1.09	578.36	0.79	8.94	3.49	29.38	8.53	4.94	14.47
PulpE	5	all fibers	1.21	1.14	655.74	0.86	6.00	2.23	31.18	9.73	6.01	7.13

Pulp B Stream 3 P30/R50 and Pulp E Stream 3 P30/R50 results were not available

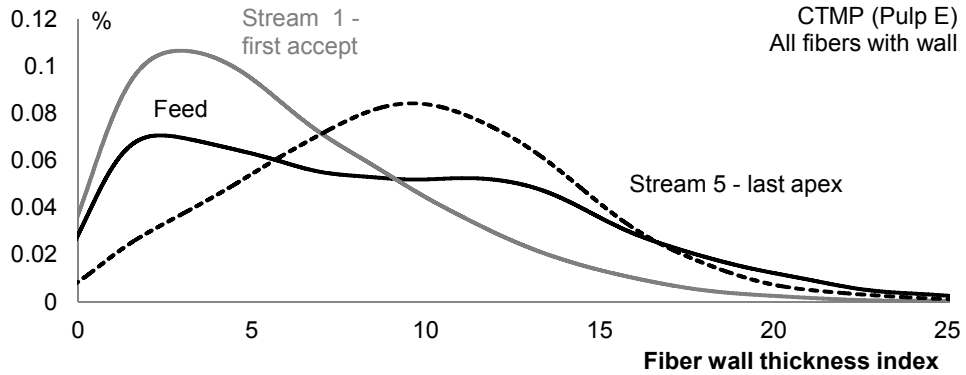

Figure A4.1.1. Example of the hydrocyclone fractionation result. Arithmetic distribution of fiber wall thickness for feed, first accept and last reject of Pulp E.

A4.2 Characteristics per hydrocyclone stream – FiberLab

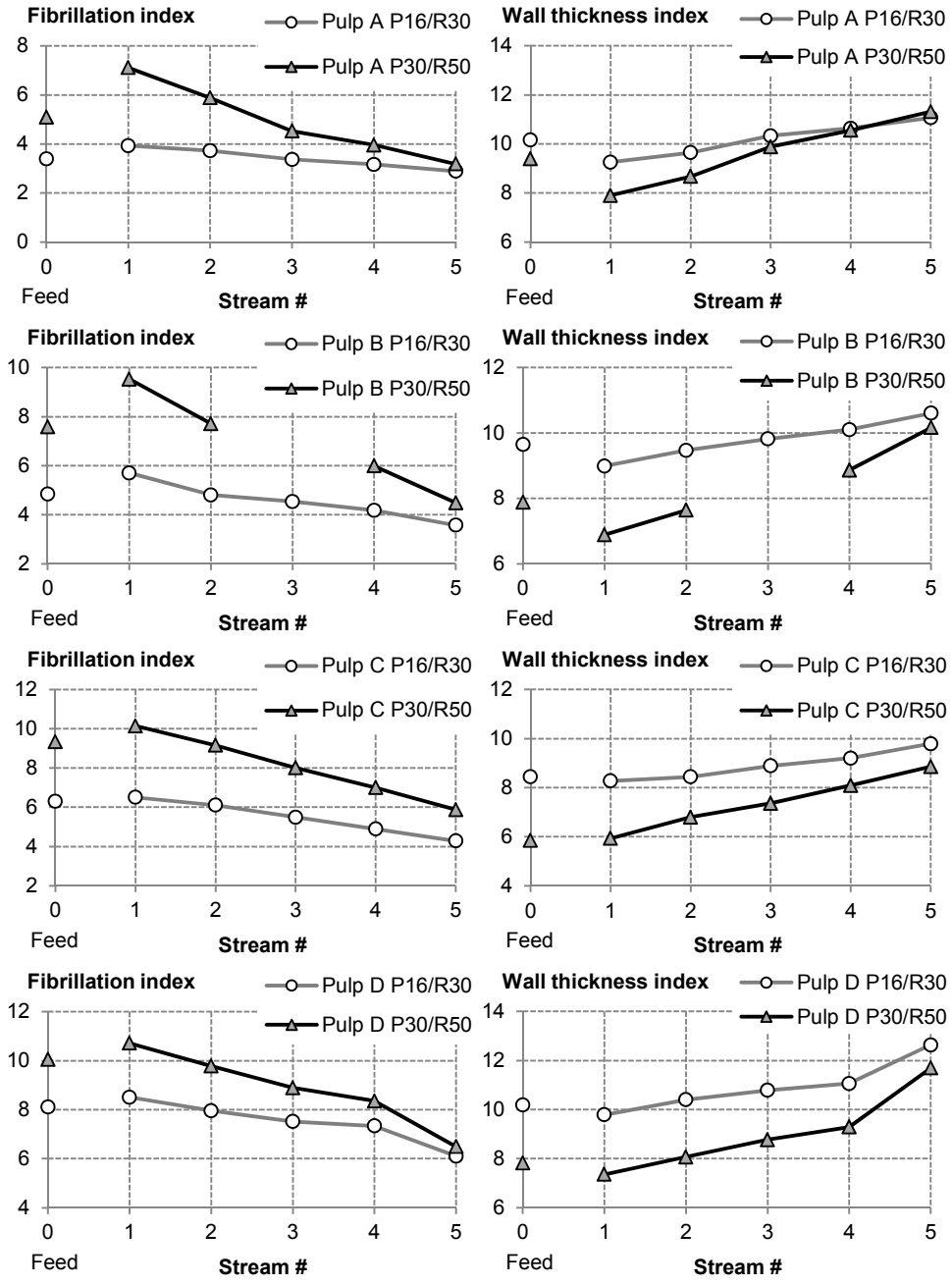

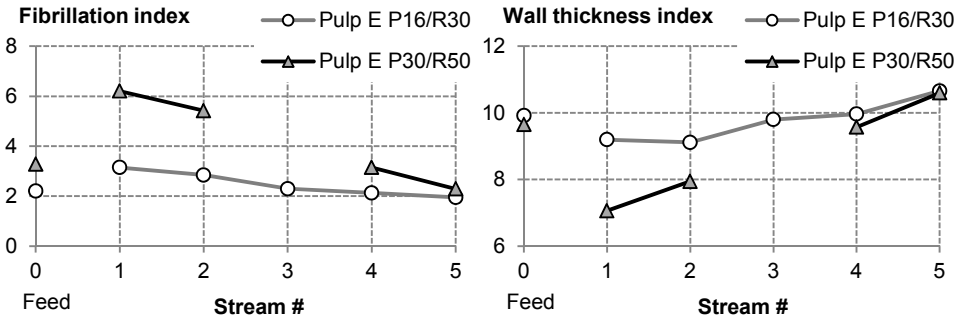

Figures A4.2.1a–j. Fibrillation index and fiber wall thickness index converged towards a common level in the last reject for the P16/R30 and P30/R50 fractions for all fractionated pulps.

Table A4.2.1. Unscreened data from FiberLab. Due to another calibration level than currently used, the levels of the fiber characteristics may differ from the filtered data (*cf.* Table A4.1.1), but rankings between the hydrocyclone streams remain.

Default averages	PulpA	PulpA	PulpA	PulpB	PulpB	PulpB	PulpC	PulpC	PulpC	PulpD	PulpD	PulpD	PulpE	PulpE	PulpE	PulpE
from FiberLab	total	16-30	30-50	total	16-30	30-50	total	16-30	30-50	total	16-30	30-50	total	16-30	30-50	50-100
Fiber width index																
0	25.3	32.63	29.57	22.3	32.13	26.7	20.27	29.57	18.23	20.3	32.47	26.23	26.2	32.8	31.67	25.27
1	21.73	32.07	26.43	20.2	31.47	24.9	19.3	29.2	20.07	19.37	31.53	25.07	20	32.53	26.5	19.53
2	23.87	32.23	28.07	22	32.17	26.4	20.73	29.63	23	20.53	32.83	26.63	22.9	32.83	29.6	21.93
3	26.8	32.93	30.77	23.9	32.2		21.87	30.57	24.2	22.2	33.37	28.33	21.93	32.63		19.37
4	28.2	33.3	31.93	27.6	32.8	28.8	23.37	31.43	26.07	23.53	33.43	29.37	26.5	32.77	31.43	24.47
5	29.87	33.7	33.57	27.4	33.1	31.13	25.4	31.9	27.93	28.7	34.93	36.67	29.6	33.2	33	28.5
Fiber wall thickness index																
0	7.97	10.47	9.67	6.9	9.97	8.07	6.17	8.73	5.23	6.27	10.4	7.9	8	10.3	10	7.5
1	6.6	9.63	8.1	5.83	9.3	7.07	5.6	8.33	5.73	5.6	10	7.47	5.23	9.53	7.3	4.77
2	7.37	9.93	8.87	6.57	9.77	7.8	6.23	8.7	6.87	6.3	10.57	8.2	6.2	9.47	8.2	5.53
3	8.67	10.7	10.13	7.37	10.13		6.67	9.17	7.47	7.03	11.03	8.9	6.43	10.17		5.33
4	9.3	10.97	10.83	8.47	10.43	9.1	7.4	9.53	8.27	7.67	11.23	9.4	7.93	10.27	9.9	7.27
5	10.27	11.37	11.63	9.23	10.97	10.43	8.3	10.1	9.1	10.4	11.9	12.8	9.43	11	10.97	9.2
Fibrillation index																
0	6.26	3.49	4.91	7.71	5.12	7.47	10.03	6.72	11.24	9.5	7.73	9.32	4.05	2.3	3.12	4.22
1	8.17	4.08	6.98	9.91	6.48	9.53	10.65	7.67	11.15	10.65	8.57	10.07	9.8	3.39	6.16	7.57
2	6.47	3.9	5.76	8.56	5.4	7.73	9.16	6.6	9.69	9.37	7.62	9.03	6.63	3.14	5.18	6.58
3	4.73	3.48	4.33	6.56	4.85		7.81	5.88	8.49	8.2	7.5	8.08	3.93	2.48		4.23
4	4.08	3.33	3.85	6.7	4.51	6	6.66	5.29	7.16	7.35	6.98	7.54	3.3	2.38	3.03	4.08
5	3.41	2.98	3.46	4.57	3.93	4.5	5.46	4.66	5.9	5.77	5.2	5.53	2.37	2.23	2.29	2.63

A4.3 Curl index

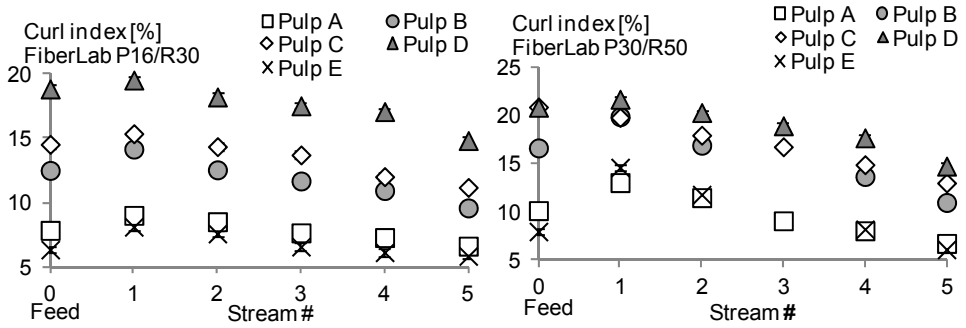

Figures A4.3.1a-b. Curl index was highest in Stream 1 and lowest in Stream 5 for the P16/R30 and P30/R50 fractions of Pulps A-E. SGW (Pulp D) had the overall highest curl index and TMP1 (Pulp A) and the CTMP (Pulp E) had the lowest.

A4.4 Z-parameter

The z-parameter indicates how big part of the fiber cross-section that is fiber wall, compared to the whole cross-sectional fiber area. The Z-parameter index (*cf.* Equation A4.4.1) calculated from FiberLab data ranked the hydrocyclone streams in accordance to the results presented in this study. For all five pulps, both for the P16/R30 and P30/R50 fractions, the lowest Z-parameter was found in Stream 1, indicating the highest amount of early wood fibers, and the highest in Stream 5, *cf.* Figures A4.4.1a-b.

$$Z-parameter(FiberLab) = \frac{4\pi * CSA}{(\pi * width)^2} * 100 \qquad \text{Eq. A4.4.1}$$

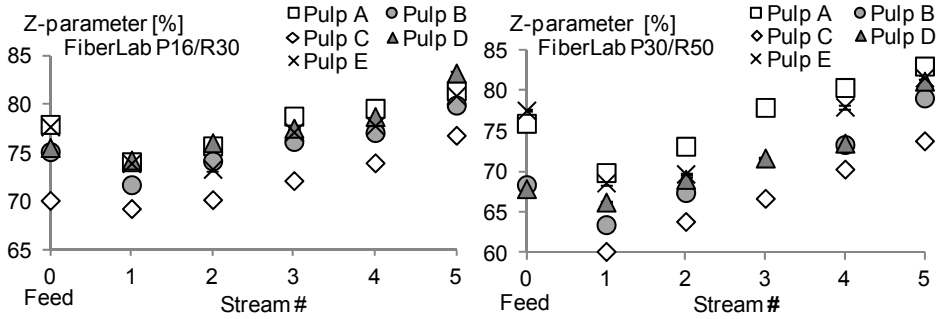

Figures A4.4.1a-b. Z-parameter calculated from the FiberLab results from Equation A4.4.1 for each hydrocyclone stream for the P16/R30 (a) and P30/R50 (b) fractions.

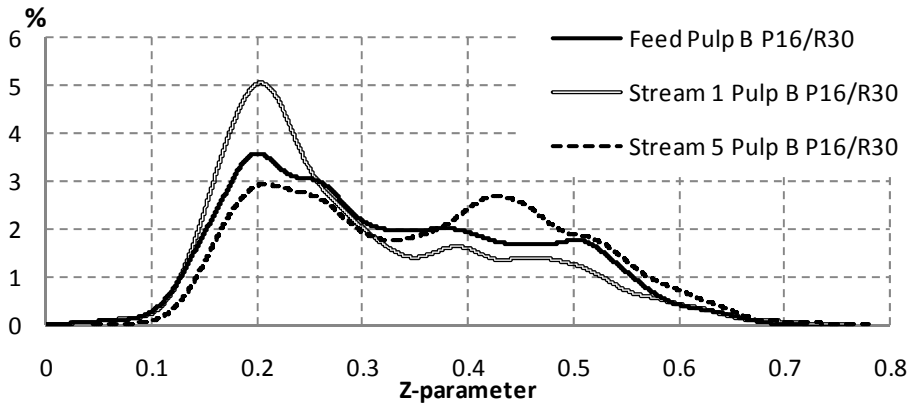

Figure A4.4.2. Arithmetic distribution of Z-parameter for Feed, Stream 1 (first accept), and Stream 5 (last reject) for Pulp B, P16/R30 fraction.

A4.5 FiberLab method deviation

Table A4.5.1. Results from FiberLab repeatability tests in evaluations of TMP from ten measurements per sample based on screened raw data (cross-sectional fiber wall thickness, curl, fibrillation >0). Fiber length 0.7-2.3 mm. "CV" is the coefficient of variation.

Fiber property	**Deviation**	
Measured and calculated	**10 "runs" per average**	**CV**
Number of evaluated fibers	29975-28362-31395	
Fiber length L_c	1.318-1.317-1.311	0.31%
Fiber length projected L_p	1.104-1.101-1.097	0.35%
Cross-sectional wall area	574.5-570.4-575.5	0.47%
Fiber wall volume index	0.856-0.848-0.850	0.44%
Curl index	21.18-21.49-21.17	0.86%
Fibrillation index	10.25-10.29-10.26	0.21%
Fiber width index	30.82-30.80-30.72	0.16%
Fiber wall thickness index	7.30-7.24-7.34	0.64%
Collapse Resistance Index CRI	3.84-3.76-3.88	1.56%
BIN=f(CRI,fibrill.)	43.8-44.2-43.7	0.59%

A4.6 Distribution width F0.90 (FiberLab)

Table A4.6.1. Distribution width (F0.90) for arithmetic distributions of fibrillation index.

Pulp	Stream 1	Stream 2	Stream 3	Stream 4	Stream 5
A P16/R30	13.5	12.9	10.8	10.1	8.6
A P30/R50	23.3	20.1	16.2	13.9	10.4
B P16/R30	18.8	16.4	15.6	14.4	12.1
B P30/R50	27.7	24.6	-	21.0	16.1
C P16/R30	21.6	20.6	19.1	17.4	15.0
C P30/R50	29.8	28.9	26.4	24.9	21.9
D P16/R30	20.4	19.3	18.6	18.4	15.6
D P30/R50	26.2	24.9	23.2	22.3	18.5
E P16/R30	12.2	11.1	8.6	7.6	7.1
E P30/R50	21.5	19.8	-	12.6	8.5

Table A4.6.2. Distribution width (F0.90) for arithmetic distributions of collapse resistance index.

Pulp	Stream 1	Stream 2	Stream 3	Stream 4	Stream 5
A P16/R30	14.2	15.0	15.8	16.2	16.6
A P30/R50	13.2	14.0	15.1	15.9	16.5
B P16/R30	14.2	14.6	14.9	15.5	15.7
B P30/R50	12.1	13.0	-	14.2	15.4
C P16/R30	13.4	13.5	14.1	14.3	14.9
C P30/R50	10.6	12.0	12.6	13.4	14.2
D P16/R30	16.3	17.1	17.3	17.9	20.4
D P30/R50	13.5	14.7	15.5	16.4	19.7
E P16/R30	14.2	13.9	14.9	14.8	15.2
E P30/R50	11.7	12.7	-	14.5	15.1

Table A4.6.3. Distribution width (F0.90) of arithmetic distributions of fiber wall thickness index and fibrillation index for the pulps that were fractionated in hydrocyclones.

Distribution width F0.90	**Fraction**	**Pulp A**	**Pulp B**	**Pulp C**	**Pulp D**	**Pulp E**
Fiber wall thick. index	P16/R30	17.6	16.8	16.8	19.2	16.0
	P30/R50	16.8	16.0	14.7	17.6	16.0
Fibrillation index	P16/R30	11.1	16.5	21.6	19.5	8.2
	P30/R50	18.2	24.4	28.3	25.3	13.3

A5. Cross-sectional SEM image analysis

A5.1 Averages from analysis

Table A5.1.1. Averages of cross-sectional SEM image analysis of Pulps A - E, P16/R30 fractions of Stream 0 (Feed), Stream 1 (first accept) and Stream 5 (last reject), and R16 fraction of Stream 0 (Feed) of Pulp E.

Pulp	Stream	Fraction	Fiber wall area (CSA)	Width	Wall thickness	CRI
PulpA	0	P16/R30	217.05	29.25	2.62	0.33
PulpA	1	P16/R30	186.74	28.93	2.26	0.25
PulpA	5	P16/R30	226.23	29.39	2.74	0.36
PulpB	0	P16/R30	215.31	30.34	2.53	0.30
PulpB	1	P16/R30	194.50	30.17	2.28	0.25
PulpB	5	P16/R30	229.56	29.36	2.77	0.36
PulpC	0	P16/R30	193.08	26.81	2.58	0.34
PulpC	1	P16/R30	180.88	26.41	2.45	0.31
PulpC	5	P16/R30	224.44	27.51	2.93	0.42
PulpD	0	P16/R30	233.12	28.24	2.95	0.41
PulpD	1	P16/R30	224.30	27.95	2.86	0.39
PulpD	5	P16/R30	267.64	28.96	3.33	0.51
PulpE	0	P16/R30	242.89	30.29	2.85	0.37
PulpE	1	P16/R30	224.71	30.41	2.59	0.29
PulpE	5	P16/R30	263.09	30.08	3.14	0.44
PulpE	0	R16	303.14	32.29	3.38	0.48

A5.2 Method variation in cross-sectional SEM image analysis

Table A5.2.1. Coefficient of variation, CV, between random thirds of data within one result file of data originating from the cross-sectional SEM micrographs method. Method variances for the whole data should be on the same or a lower level than the deviations between the thirds. "CV" is the coefficient of variation.

P16/R30	**Wall**	**Width**	**CRI**	**CSA**
CV	3.9%	6.3%	5.0%	10.7%

A6. Correlation between long fiber density and fiber dimensions

A6.1 Density

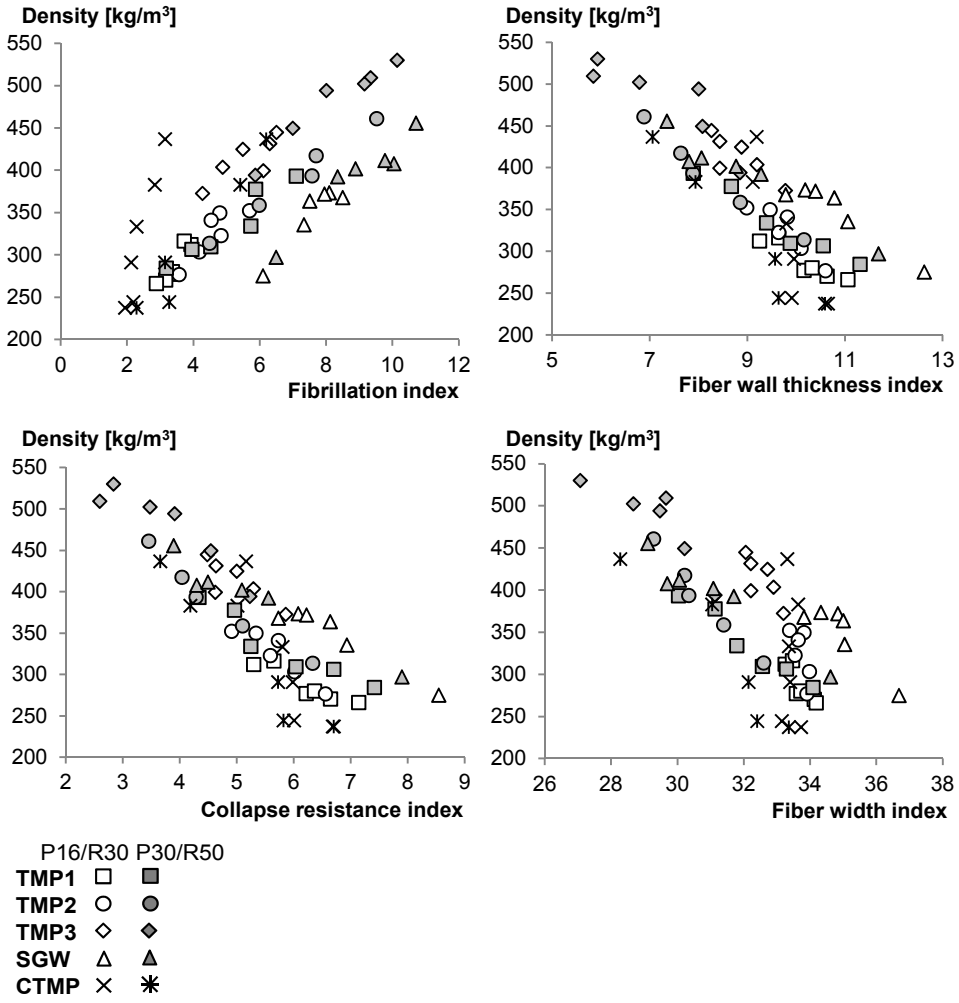

Figures A6.1.1a-d. Density (STFI density) as a function of fibrillation index (a), fiber wall thickness index (b), collapse resistance index (c) and fiber width index (d). The correlation between tensile index and arithmetic averages of fiber characteristics are found in Section 4.1.4.

A7. Weighted averages

All FiberLab data was filtered to exclude fines and broken fibers before arithmetic or weighted averages were calculated.

A7.1 Correlation between arithmetic and length weighted averages

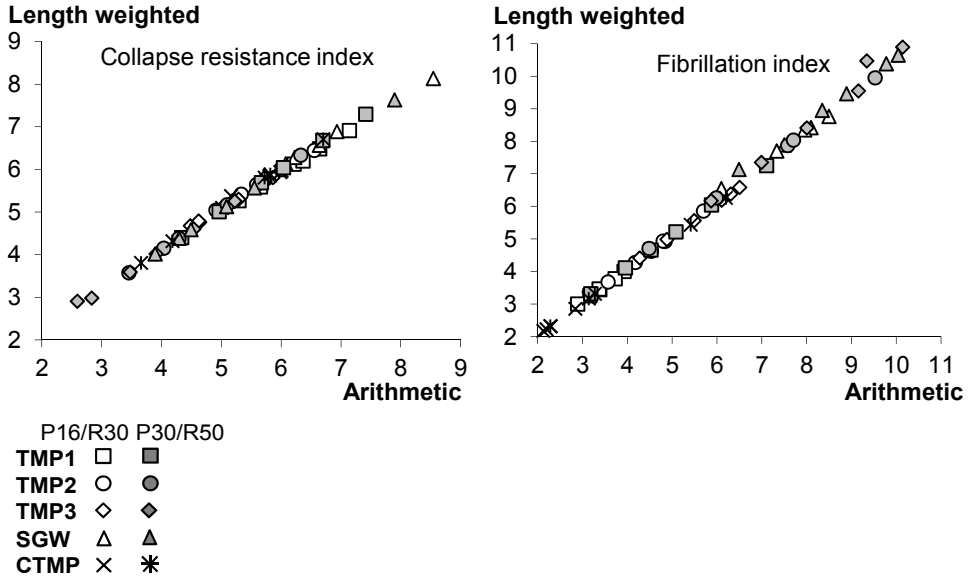

Figures A7.1a-b. Correlations between arithmetic and length weighted averages of collapse resistance index and fibrillation index of the hydrocyclone fractionated pulp fractions. The corresponding correlations for fiber wall thickness index and fiber width index are found in Paper III, Figures 3a-b.

A7.2 Correlation between arithmetic and wall volume weighted averages

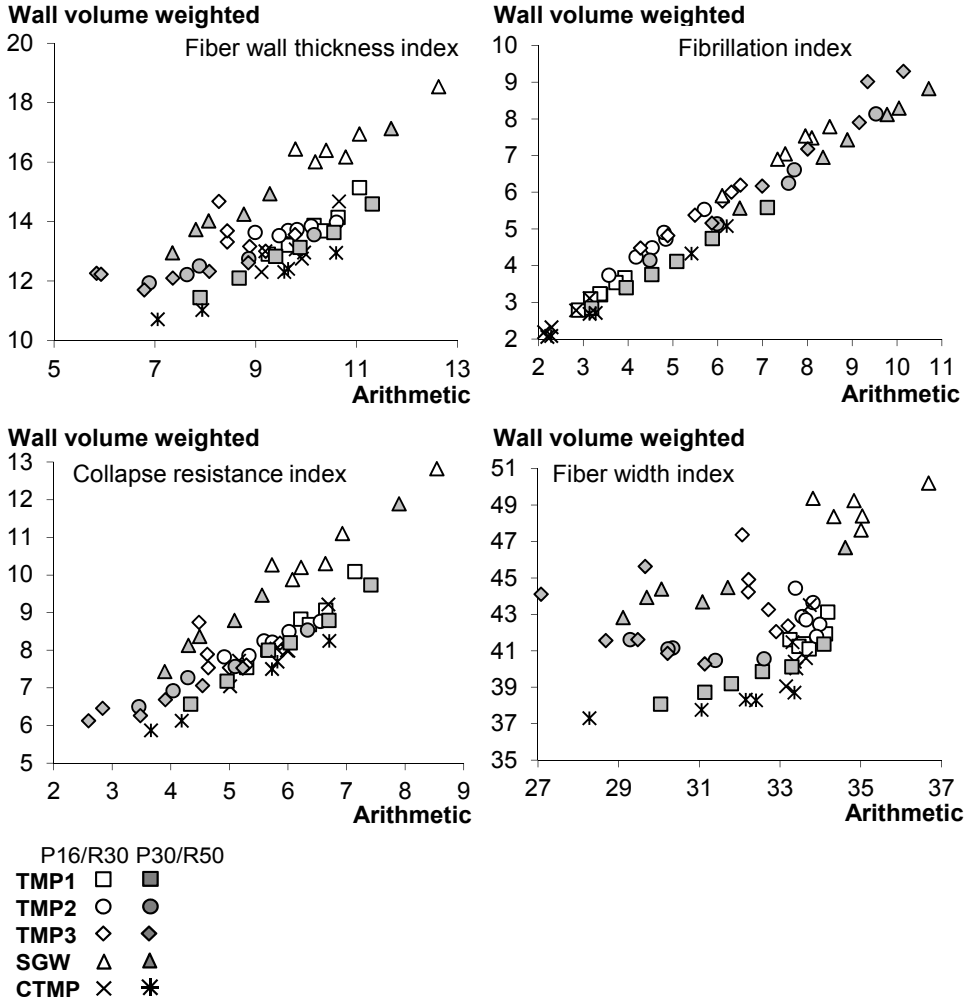

Figures A7.2a-d. Correlations between arithmetic and wall weighted averages of fiber wall thickness index, fibrillation index, collapse resistance index and fiber width index of the hydrocyclone fractionated pulp fractions.

A7.3 Correlation between arithmetic and length^2 weighted averages

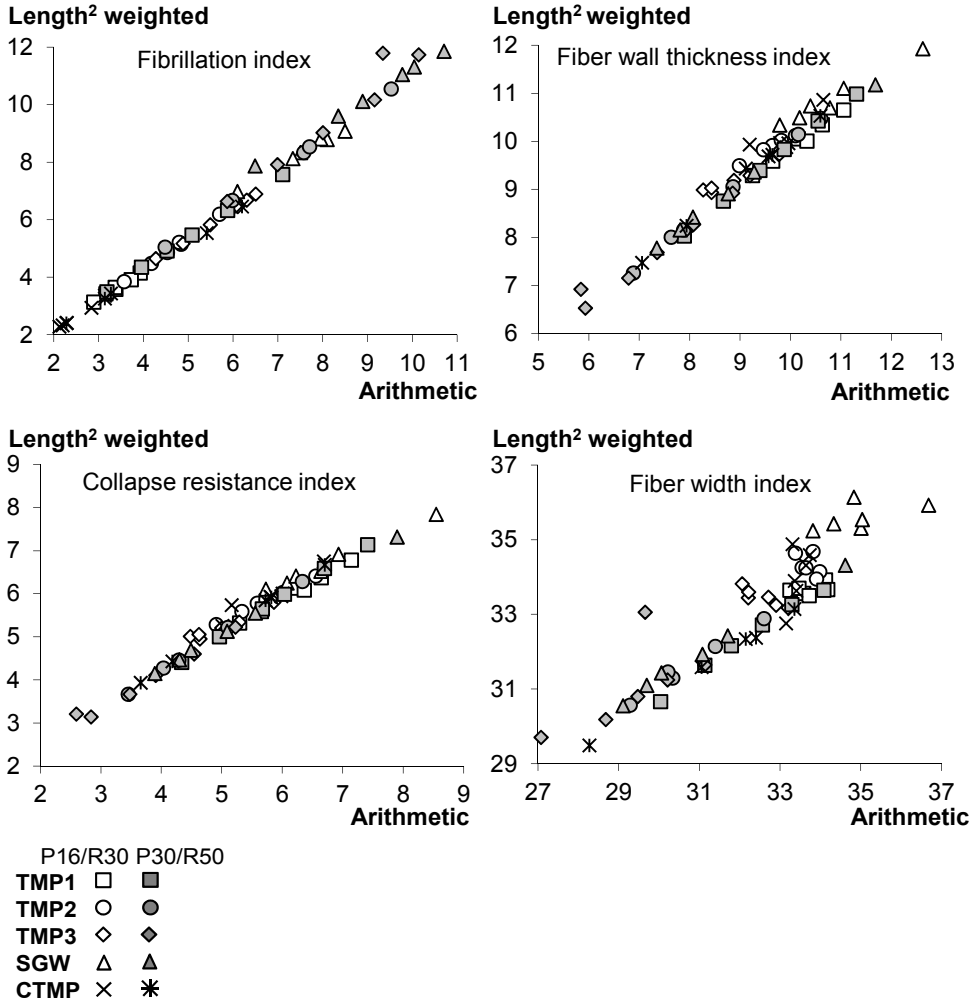

Figures A7.3.1a-d. Correlations between arithmetic and length^2 weighted averages of fibrillation index, fiber wall thickness index, collapse resistance index and fiber width index of the hydrocyclone fractionated pulp fractions.

A7.4 Correlation between wall volume weighted fiber characteristics

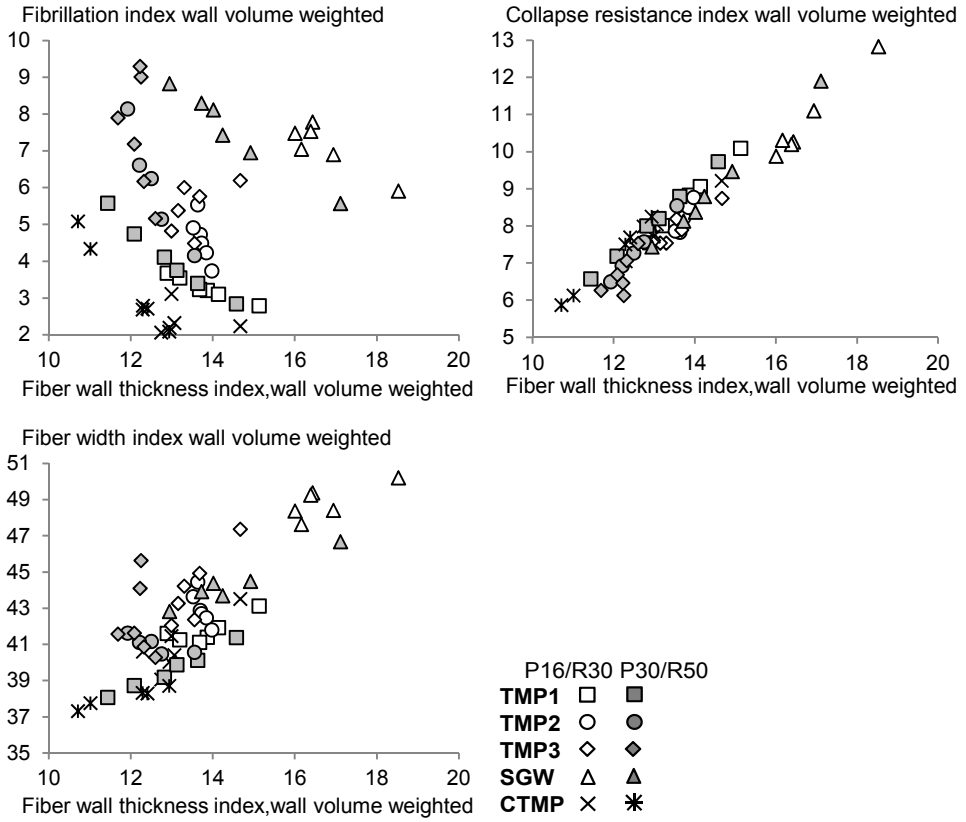

Figures A7.4.1a-c. Correlations between wall volume weighted fiber wall thickness index and wall volume weighted fibrillation index (a), wall volume weighted collapse resistance index (b) and wall volume weighted fiber width index (c).

A7.5 Correlation between tensile index and wall volume weighted fiber characteristics

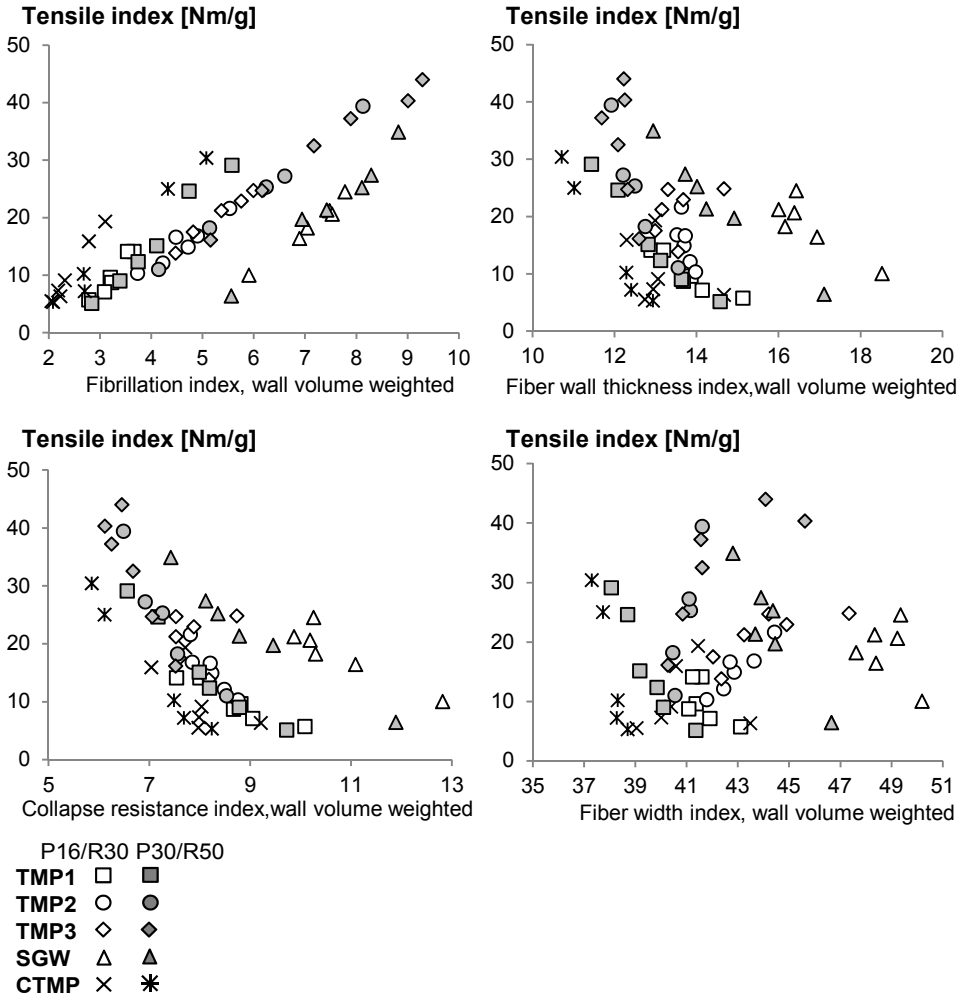

Figures A7.5.1a-d. Correlation between tensile index and wall volume weighted averages of fibrillation, fiber wall thickness, collapse resistance and fiber width indices for the P16/R30 and P30/R50 fractions of the five hydrocyclone fractionated pulps.

A8. Tensile index point distributions

Calculation example;

Pulp A P16/R30 was used as an example. Tensile index point distributions were made with tensile index on the x-axis, and the weight amount of fibers compared to the hydrocyclone feed (Table A1.6.2) in the y-axis.

Table A8.1. Data for the tensile index point distribution of Pulp A (TMP3), P16/R30 fraction.

Stream #	Tensile index Pulp A (TMP3) P16/R30 [Nm/g]	Stream #	Amount of Feed Pulp A P16/R30 [%]
5	5.7	5	17.1
4	7.1	4	16.5
3	8.7	3	23.3
2	14.1	2	20.7
1	14.1	1	22.4

From Table A8.1 above, the tensile index point distribution for Pulp A P16/R30 will be made from the points; (5.7;0), (5.7;17.1), (7.1;16.5), (8.7;23.3), (14.1;20.7); (14.1;22.4). (14.1;0). "Point distributions" are not limited to measured or predicted tensile index, but can be used in this approach for any measured or calculated property.

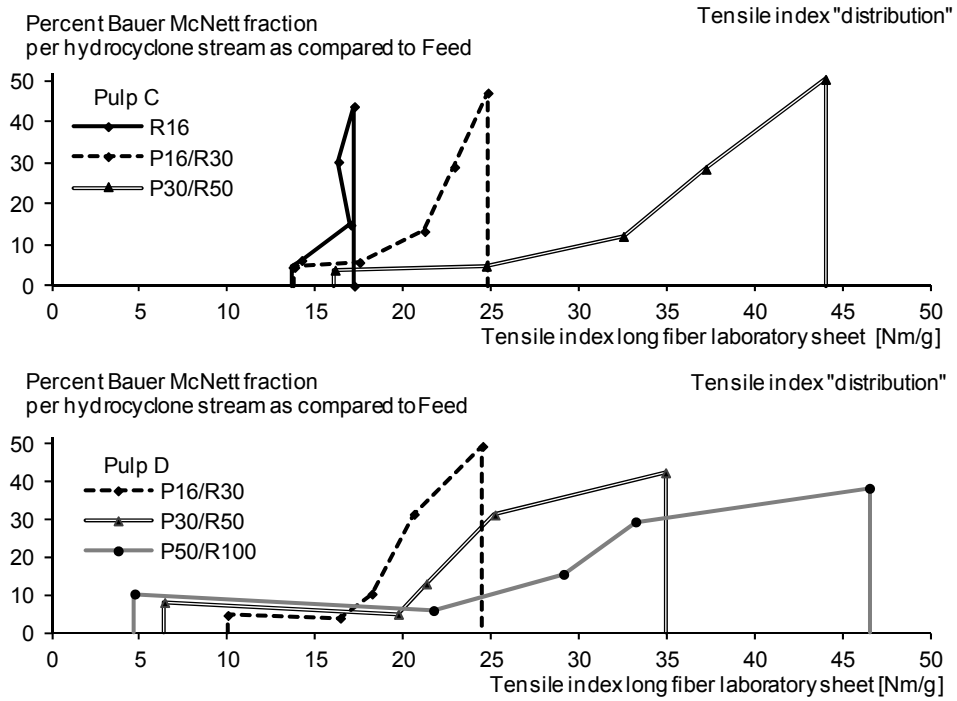

Figures A8.1a-b. Tensile index point distributions based on the tensile index and percent of fibers in each hydrocyclone stream compared to feed pulp. The resemblance between the different distributions of the Bauer McNett fractions of each pulp is high, indicating that the characteristics of the fibers are similar for the fiber length (Bauer McNett) fractions.

A9. MorFi Lab

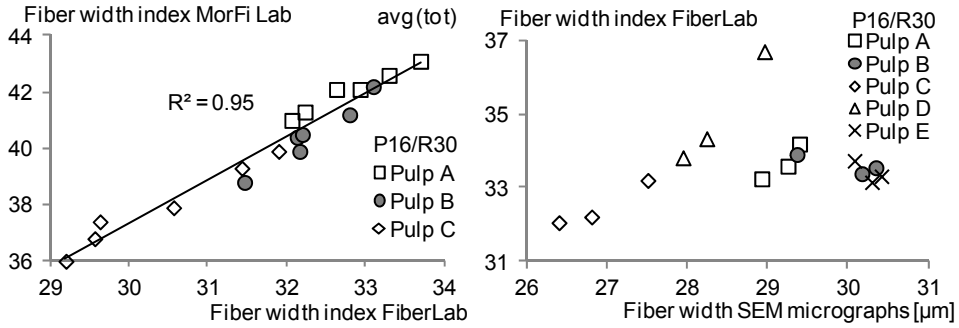

Figures A9.1a-b. Correlation between fiber width index from the FiberLab and MorFi Lab analyzers (left) and between FiberLab and cross-sectional SEM image analysis method (right). The FiberLab and MorFi Lab results are from default reports and may also include fines whereas fiber width index in the cross-sectional SEM comparison was based on data from standard methods (fines excluded).

A10. Other evaluated fiber analysis methods

A10.1 Simons' Stain

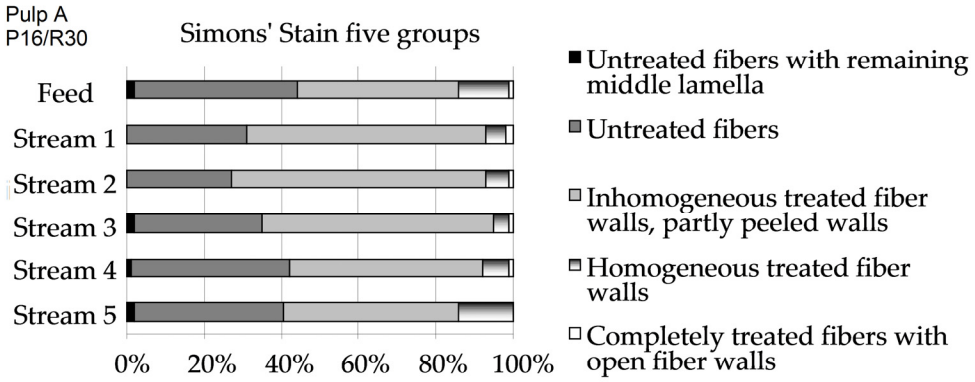

Figure A10.1.1. Results of Simons' Stain analysis of Streams 0-5, Pulp A (TMP1), P16/R30 fraction. The amount of untreated fibers was increased from Stream 1 to Stream 5 which was in accordance with the rest of the evaluated results.

A10.2 Relative bonded area with CyberBond™

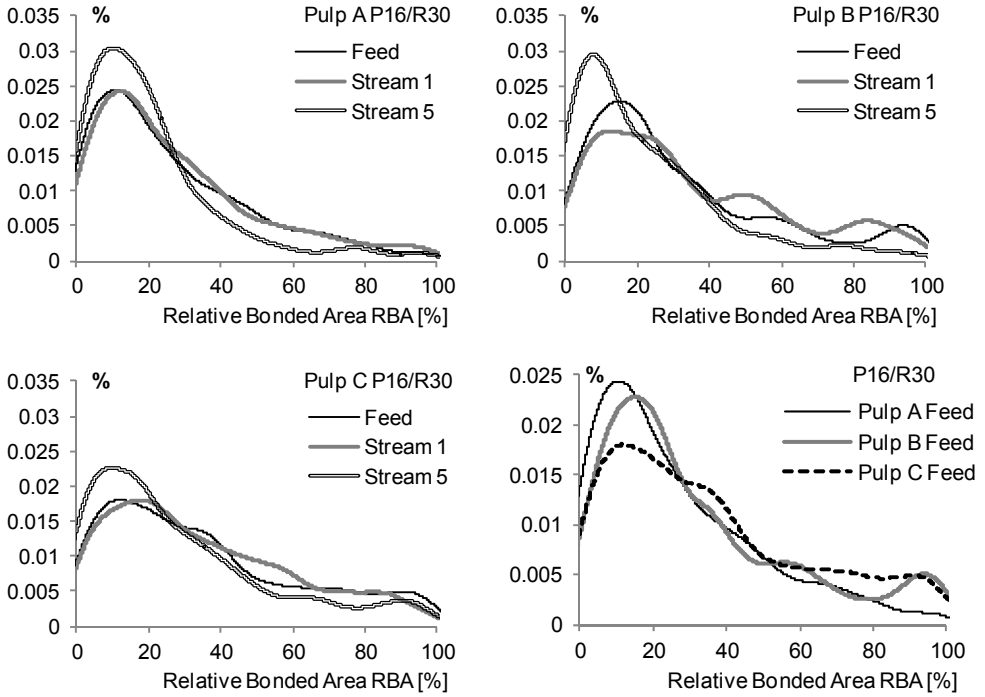

Figures A10.2a-e. Distributions of relative bonded area of Pulps A-C, Streams 0 (Feed), 1, 5 for the P16/R30 fractions (a-c) and the feed pulps (d). The distributions are based on 500 fibers and were made by KDE *via* diffusion mixing.

Table A10.2.1. Average relative bonded area from CyberBond^{TM}.

Relative bonded area RBA [%]

P16/R30	Pulp A (TMP1)	Pulp B (TMP2)	Pulp C (TMP3)
Feed	26.6	32.1	34.7
Stream 1	27.8	35.5	34.8
Stream 2	32.1	32.1	34.7
Stream 3	24.8	28.0	36.8
Stream 4	25.2	25.1	33.9
Stream 5	20.7	22.9	28.6

A10.3 Fiber flexibility and stiffness using Tam Doo and Kerekes method

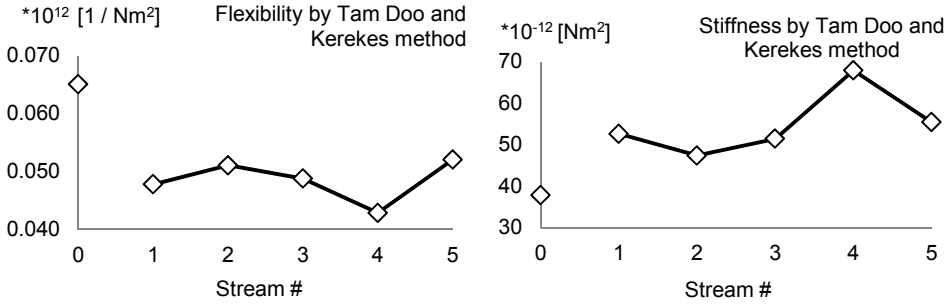

Figures A10.3.1a-b. The flexibility and stiffness of the Pulp A P16/R30 fibers were evaluated by the use of the Tam Doo and Kerekes method. No conclusions could be made from the results which were based on only 50 analyzed fibers per pulp fraction.

A11. Acoustic emission

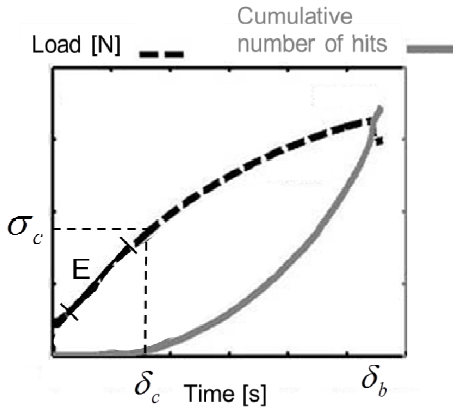

Figure A11.1. Principle of calculation of the critical strain energy Wc from cumulative graphs of acoustic events and load at constant elongation rate.

Equation A11.1 below was used to calculate the critical strain energy density Wc.

$$W_c = \frac{\sigma_c^{\,2}}{2 * E} \qquad \text{Eq. A11.1}$$

σ_c: Load at 10% of the total number of acoustic events at fracture, divided by the product specimen width and grammage of the paper.

E: Elastic modulus calculated from the initial slope of the load – elongation curve.

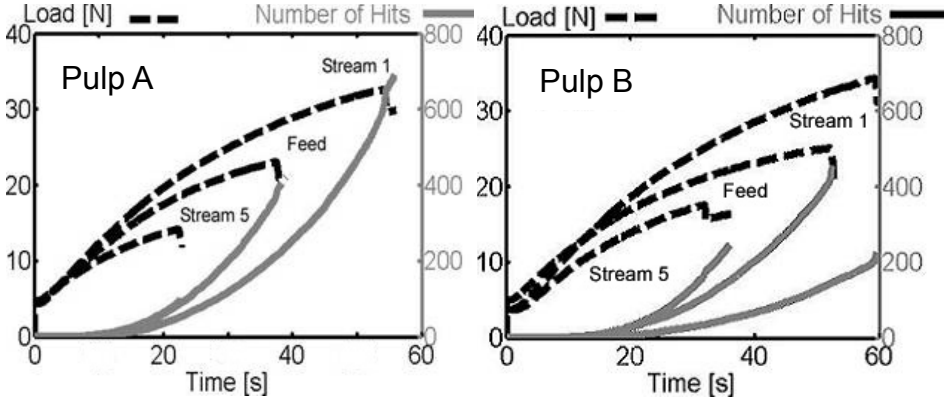

Figures A11.2a-b. The load (dotted line) and total number of acoustic events (solid grey) versus time at constant strain rate are shown for Feed, Stream 1 and Stream 5 for Pulp A (TMP1) and Pulp B (TMP2). ”Number of hits” refer to the cumulative number of hits.

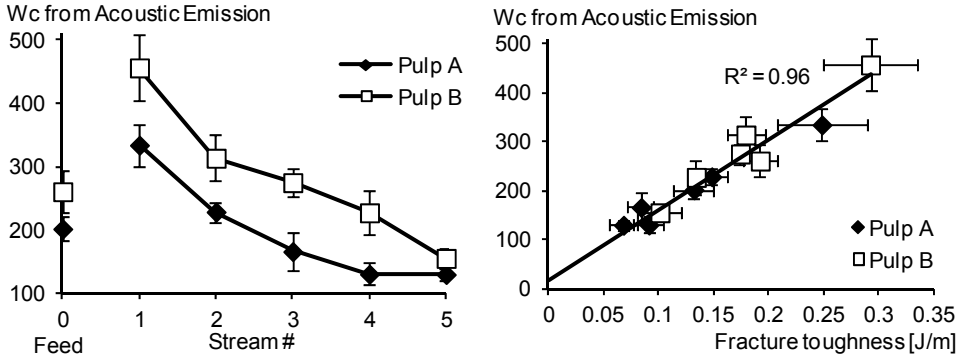

Figures A11.3a-b. W_C, the elastic energy density at onset of damage, was the highest for Stream 1 and the lowest for Stream 5 for Pulps A and B for DSF* sheets of the P16/R30 fraction (left). Gradin *et al*. (2008) showed that the elastic energy density correlated to fracture toughness for various kinds of fiber paper based products. In Paper I it was shown that W_C correlated well to fracture toughness also for sheets* made from the long fiber fraction P16/R30 (right) **Sheets made in the Formette Dynamic Sheet Former*.

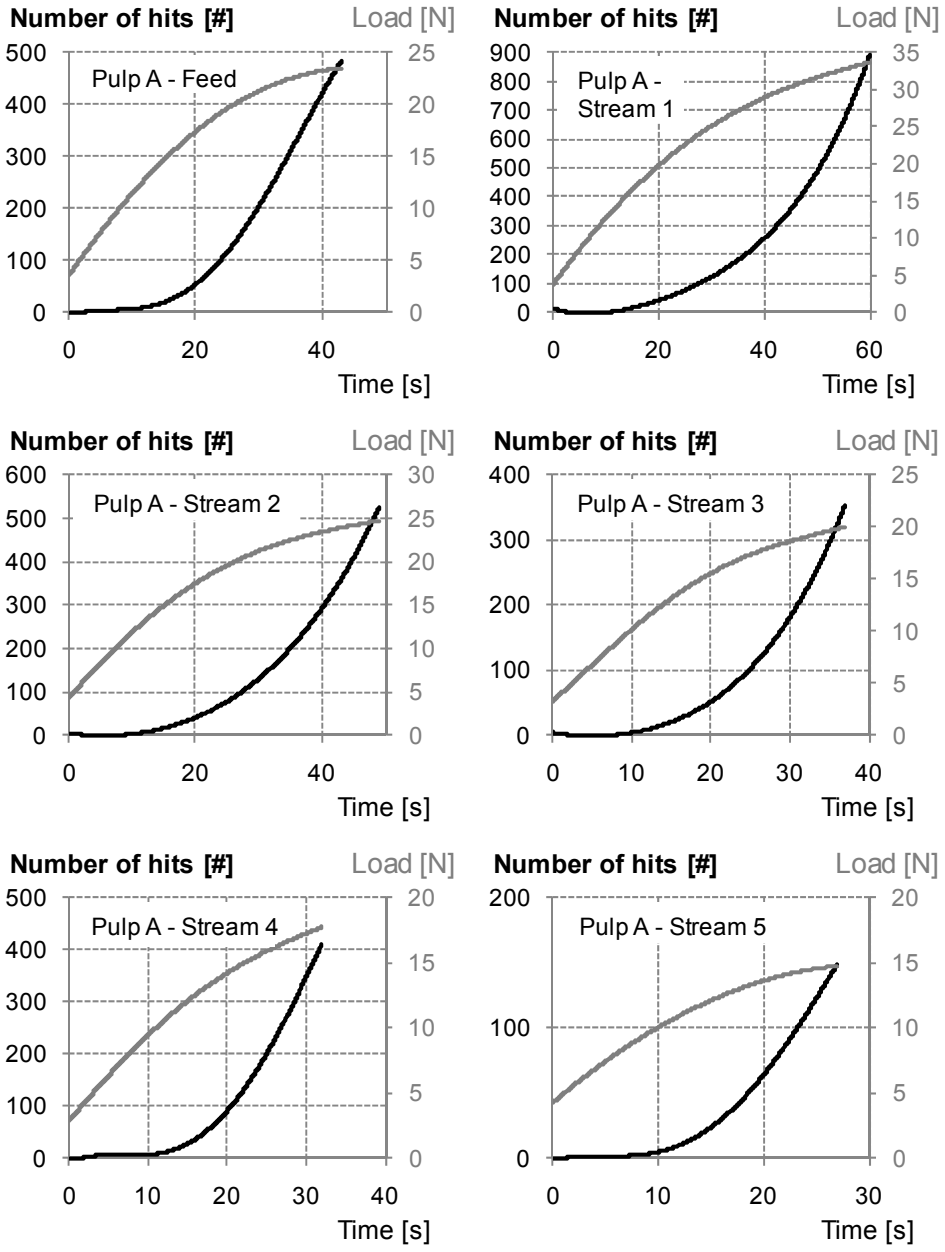

Figures A11.4a-f. Load and cumulative number of hits for the five hydrocyclone streams plus feed for the P16/R30 fractions of Pulp A.

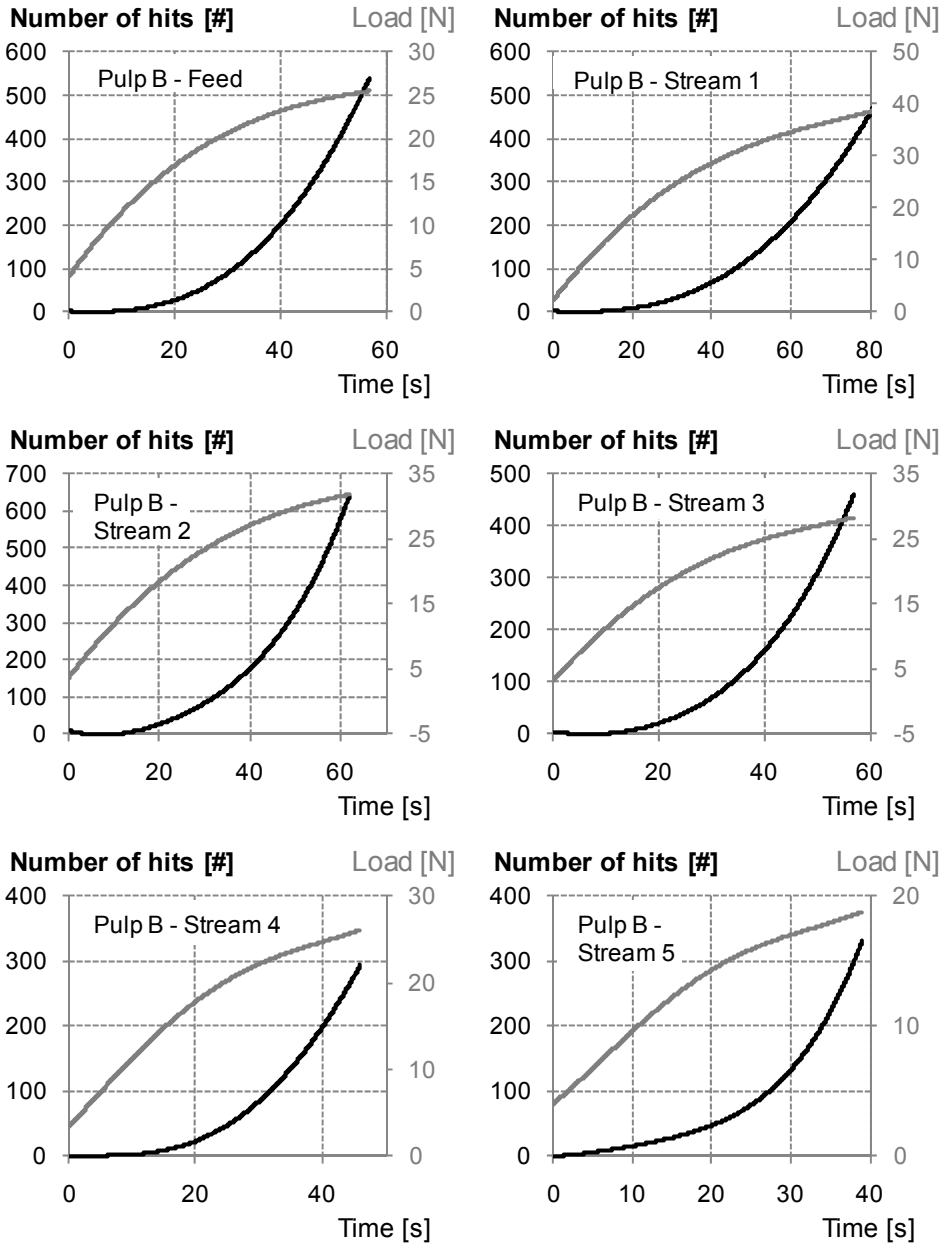

Figures A11.5a-f. Load and cumulative number of hits for the five hydrocyclone streams plus feed for the P16/R30 fractions of Pulp B.

A12. Comparison between frozen and non-frozen pulp samples

Table A12.1. Example of comparison with FS-200 fiber length analyzer between two samples of the same pulp - one that was dewatered, frozen and hot disintegrated and one that was tested directly.

	85-00_1630	**85-00_1630**
	Dewatered, frozen, hot disintegraded	No freezing or hot disintegration
FS-200		
Population distrubution FS-200 <0.2 mm (%)	37.7	37.96
Fibre length Kajaani FS-200 l/n (mm)	0.65	0.62
Fibre length Kajaani FS-200 l/l (mm)	1.61	1.56
Fibre length FS-200 Lw (mm)	2.28	2.23

Table A12.2 shows results from a comparison of fiber characteristics from the FiberLab optical analyzer. The sample 67-00 was based on a mixture of two other samples, 67-06 and 67-07. The mixture (67-00) was expected to contain approximately equal weight amounts of the samples 67-06 and 67-07 and the fiber characteristics of the mixture was expected to mirror an average of the fiber characteristics of the two part samples. 67-00 was dewatered (>30% dry content), separated into smaller parts of dense pulp, frozen, and then hot disintegrated before fiber analysis. 67-06 and 67-07 were tested directly, without dewatering.

The hot disintegrated sample (67-00) had lower curl than the two samples that were tested directly which was expected based on other trials (*cf.* Section 4.2.3). Based on this one evaluation, as seen in Table A12.2, it is possible that the fibrillation index was reduced by the dewatering – freezing – hot disintegration procedure, and that some fiber swelling occurred (slightly higher fiber wall thickness and fiber width). This would benefit from further evaluations. As the frozen pulps were only compared with other frozen pulps in this study, this may have changed the levels of some fiber characteristics but not any results and most likely no rankings.

Table A12.2. Example of comparison with FiberLab analyzer between samples that were dewatered, frozen and hot disintegrated (67-00), and samples that were tested directly (67-06 and 67-07). 67-00 was a mixture between 67-06 and 67-07 and the fiber properties of the mixed sample were expected to be arranged between the fiber properties of the other two samples.

	67-00	67-06	67-07
	Mixture of 67-06 and 67-07, then dewatered and frozen, hotdisintegrated		
FiberLab			
Fiber length FiberLab C(l) (mm)	1.33	1.31	1.39
Fiber length FiberLab ISO C(l) (mm)	1.44	1.42	1.48
Fiber length FiberLab P(l) (mm)	1.16	1.1	1.17
Fiber length FiberLab ISO P(l) (mm)	1.29	1.22	1.29
Fines FiberLab > 0.20 mm C(l) (%)	8.57	8.26	7.1
Fines FiberLab < 0.20 mm P(l) (%)	11.09	11.56	9.79
Fiber width FiberLab (l) (µm)	29	28	28.7
CWT FiberLab (l) (µm)	7.7	7.2	7.6
Fiber curl FiberLab (l) (%)	16.5	21.5	19.7
Cross Sectional Area FiberLab (l) (µm2)	581.1	555.9	584.5
Fiber volume Fiberlab (l) (10^6 µm3)	1.08	1.06	1.11
Kink FiberLab (l) (1/m)	850.7	750	660.7
Fibrillation FiberLab (%)	11.99	14.03	13.28

APPENDIX B. BIN MODEL

B1.1 BIN model based on arithmetic averages

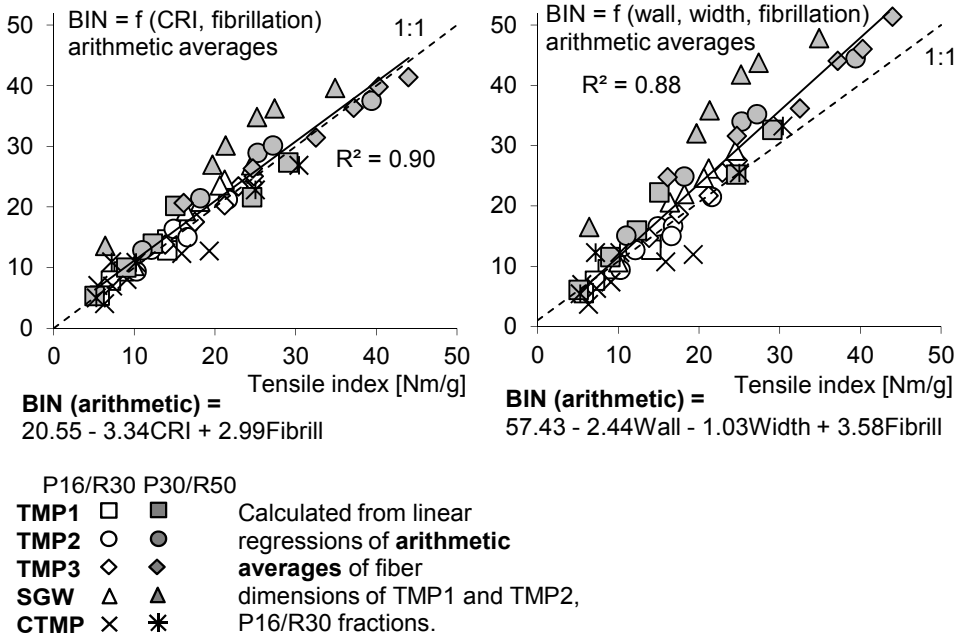

Figures B1.1.1a-b. The two figures show the correlation between tensile index and the factor *BIN* which was derived from linear regressions of fiber dimensions. In the left figure, *BIN* is based on arithmetic averages of collapse resistance index (CRI) and fibrillation index. Collapse resistance index is based on fiber wall thickness index and fiber width index. In the right figure, the same data was used but fiber wall thickness and fiber width were used separately in the *BIN* model. The model based on collapse resistance index and fibrillation showed higher coefficient of determination and closer alignment to the 1:1 line than the model where fiber wall thickness and width were used separately. It was found that fiber width used as a separate factor reduced the correlation between *BIN* and tensile index for long fiber laboratory sheets, and the current *BIN* model is based on only fiber wall thickness index and fibrillation index.

B1.2 *BIN* model based on wall volume weighted averages

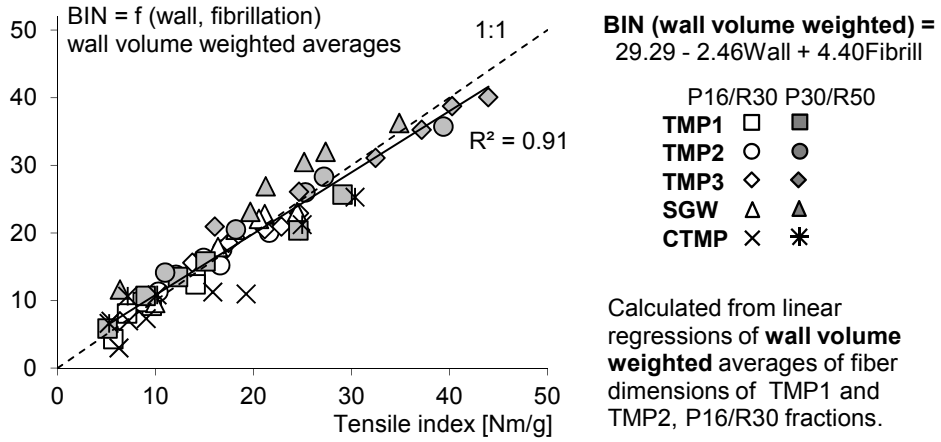

Figure B1.2.1. *BIN* based on wall volume weighted averages of fiber wall thickness and fibrillation resulted in high correlation to tensile index of long fiber laboratory sheets, and close alignment to the 1:1 line. This model is recommended if the BIN model is used to predict averages of laboratory sheets. If the *BIN* model is used in producing weighted *BIN* distributions, a model based on arithmetic averages (*cf.* Figure 4.8) is currently recommended.

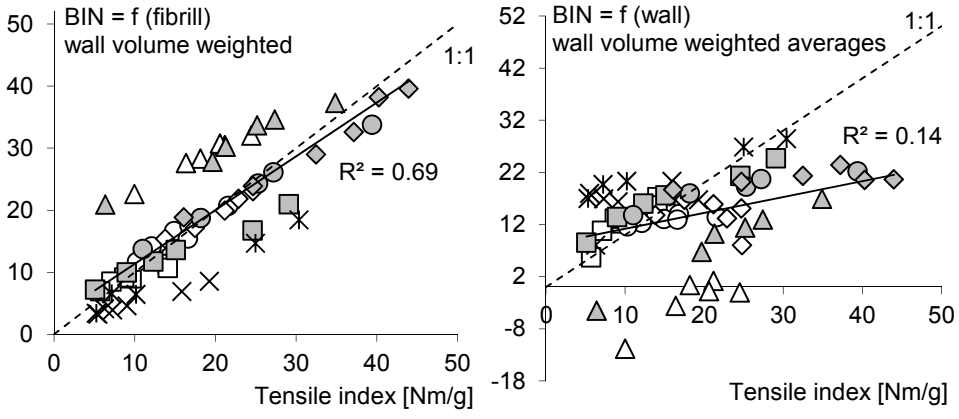

BIN (wall volume weighted) =
-7.08 + 5.02Fibrillation

BIN (wall volume weighted) =
83.55 - 5.15Wall

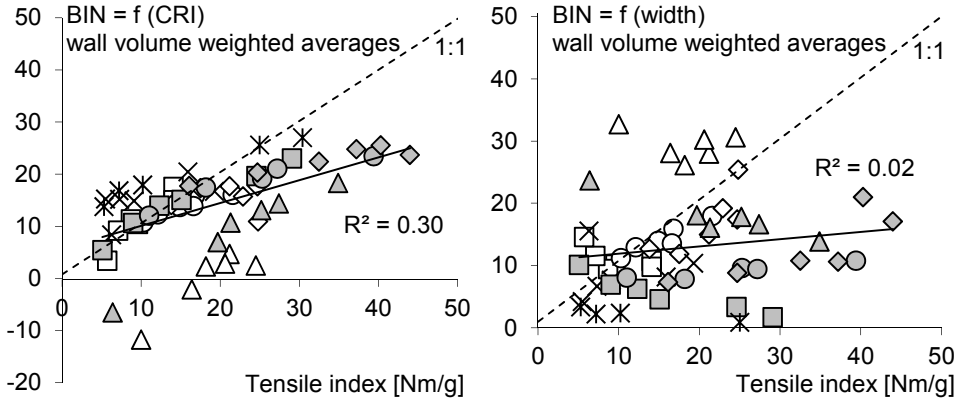

BIN (wall volume weighted) =
59.72 - 5.56CRI

BIN (wall volume weighted) =
-95.66 + 2.56Width

	P16/R30	P30/R50	
TMP1	□	■	Calculated from linear
TMP2	○	●	regressions of **wall volume**
TMP3	◇	◆	**weighted** averages of fiber
SGW	△	▲	dimensions of TMP1 and TMP2,
CTMP	×	✳	P16/R30 fractions.

Figures B1.2.2a-d. *BIN* based on only fibrillation index (a), fiber wall thickness index (b), collapse resistance index, CRI (c) and fiber width index (d) resulted in poor correlations to the measured tensile index of the long fiber laboratory sheets.

B1.3 BIN averages and width of distribution for mixtures of news / SC TMP

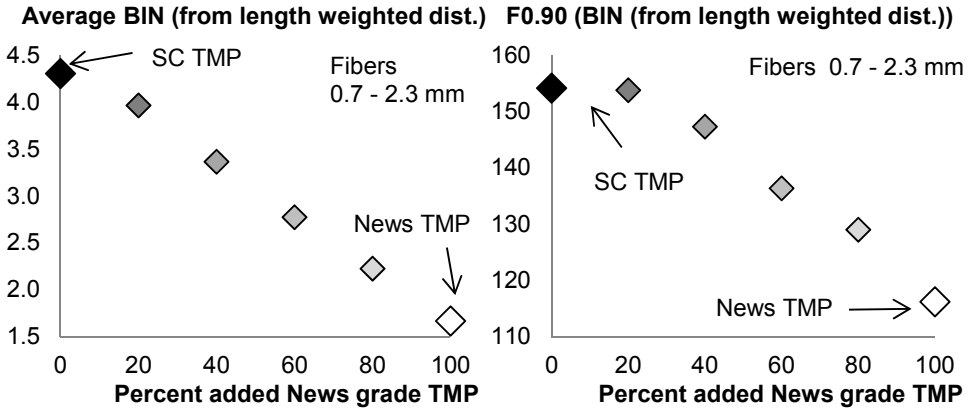

Figures B1.3a-b. Averages and characteristic width of distribution (F0.90) of *BIN* for the mixtures made in laboratory between news- and SC grade TMPs. Increasing amounts of news grade TMP in the mixtures resulted in both decreased average *BIN* and decreased characteristic width (F0.90) of the *BIN* distributions.

B2. Examples of *BIN* method in process

B2.1 *BIN* before and after screens

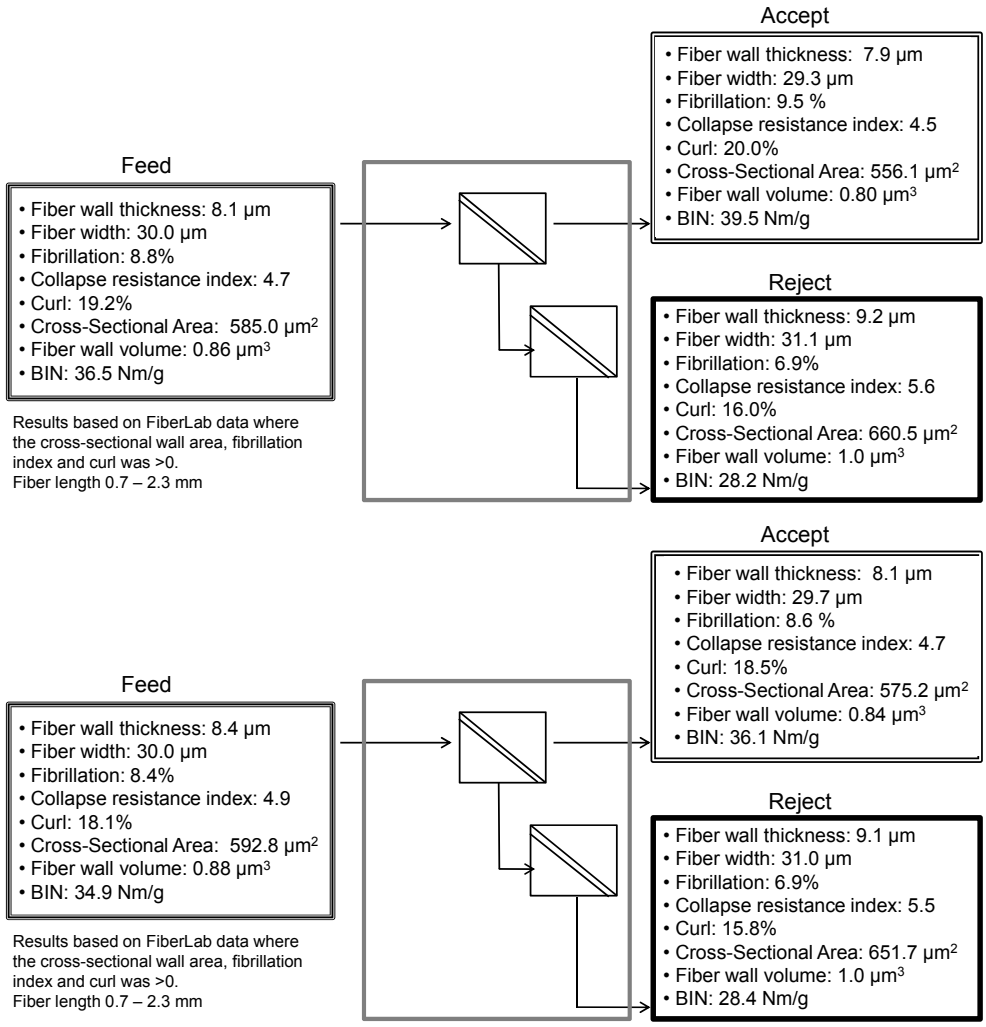

Figures B2.1.1a-b. Examples of how the averages of *BIN* and other fiber characteristics changed over screening in a TMP process. *BIN* was calculated from fibrillation index and collapse resistance index. As expected, average *BIN* increased with decreased fiber wall thickness index and increased fibrillation index in the accept. The reject had lower *BIN* than the accept and feed. over screens in a TMP process. Samples were collected at two different occasions.

B2.2 *BIN* over a process line

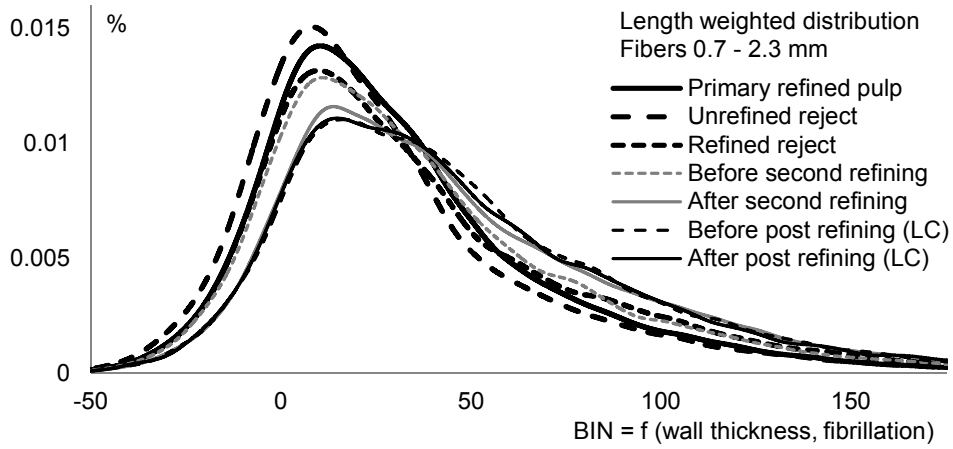

Figure B2.2.1. *BIN* distributions for samples following a TMP process line using double disc refiners. The raw material was *Picea abies*. The *BIN* distributions moved to a higher *BIN* level throughout the process. It can also be seen that the low consistency refining (LC) did not have any effect on *BIN* as discussed in Section 4.2.3.

Table B2.2.1. Averages and characteristic width of distribution, F0.90, of the samples collected throughout the process above (*cf.* Figure B2.2.1).

Sample point	Average *BIN*	F0.90(*BIN*)
Primary refined pulp (double disc refiner)	33.7	130.5
Unrefined reject	29.7	132.0
Refined reject	38.7	146.9
Before second stage refining	39.2	142.6
After second stage refining (double disc refiner)	48.2	154.1
Before post refining (LC refiner)	48.2	150.8
After post refining	48.3	154.0

APPENDIX C. UTILIZED STATISTICS

C1. Averages from combined parameters

Collapse Resistance Index was calculated based on fiber wall thickness index and fiber width index according to Equations 3.5 and 3.6 in Section 3.

In Paper I, the default averages of FiberLab data was used in the calculations of collapse resistance index (*cf.* Equation 3.5a). In Papers II-V, data was instead based on FiberLab raw data and collapse resistance index was calculated for each fiber before an average value was calculated (*cf.* Equation 3.6a). It was discovered that the average value of collapse resistance index differed very much depending on how the average was calculated – from single fibers or from averages of width and wall thickness. The rankings between the pulp samples remained unchanged, but numerical levels were up to 30% higher when average collapse resistance was calculated from averages of fiber wall thickness and fiber width compared to when averages were calculated based on the collapse resistance of single fibers.

The two approaches of calculating averages for a combined factor "a" a=a*b, for N number of fibers are seen below;

Alternative 1. Using averages to calculate a new average a (*cf.* Paper I)

$$a_{avg(1)} = \bar{b} \times \bar{w}$$

Alternative 2. Calculating average a from the sum of a for every fiber from i=1 to N; (*cf.* Papers II-V)

$$a_{avg(2)} = \frac{1}{N} \sum_{i=1}^{i=N} (b_i \times w_i)$$

It was concluded that the differences between the two methods were found in the nonlinear scatter, which in the normal distribution is commonly zero for an average value from a large amount of data, but which is only positive in the case of a square product as for the Collapse Resistance Index. The scatter is derived below.

$$a = b \times w$$

for a series of data $x_i,\ldots, x_N$ and ε_b and ε_w is the scatter of b and w in thus series.

Calculating average a for each fiber (Alternative 2, Papers II-V), and summarizing the average from single fiber averages, results in the equation;

$$a_i = \frac{1}{N} \sum_{i=1}^{N} (b_i \times w_i) \qquad \text{Eq. C1.1}$$

Any scatter of property w or b is included in the average a_i.

Calculating the average *a* from the already calculated averages of *b* and *w* (Alternative 1, Paper I) results in the equation below (Equation Eq. C1.2). ε is the scatter in fiber property for each fiber.

$$b = \bar{b}_i \times \varepsilon_b$$
$$w = \bar{w}_i \times \varepsilon_w$$
$$a_{avg} = \frac{1}{N}\sum_{i=1}^{N} b \times w = \frac{1}{N}\sum_{i=1}^{N} (\bar{b} \times \varepsilon_b) \times (\bar{w} \times \varepsilon_w) = \quad \text{Eq.C1.2}$$
$$= \frac{1}{N}\sum_{i=1}^{N} \bar{b}_i \times \bar{w}_i + \frac{1}{N}\sum_{i=1}^{N} \bar{b}_i \times \varepsilon_{wi} + \frac{1}{N}\sum_{i=1}^{N} \bar{w}_i \times \varepsilon_{bi} + \frac{1}{N}\sum_{i=1}^{N} \varepsilon_{bi} + \varepsilon_{wi}$$

For nonlinear equations which include using the square wall thickness index in the calculation of collapse resistance index, the scatter will not become zero, as for linear equations. Equation C1.3 below shows that the scatter in the nonlinear equation will always be positive, and therefore affect the average "a" (a_{avg}).

For linear equations, the average scatter will become zero, and the two middle factors in Equation C1.2 can be removed. Remaining is the same expression as in Equation C1.3 below, with the addition of the enhanced nonlinear scatter.

$$a_{avg} = \frac{1}{N}\sum_{i=1}^{N} \bar{b}_i \times \bar{w}_i + \frac{1}{N}\sum_{i=1}^{N} \varepsilon_{bi} + \varepsilon_{wi} \quad \text{Eq. C1.3}$$

When the square of any fiber parameter is used and the equation becomes nonlinear, the a_{avg} calculated according to Alternative 1 above will therefore always be higher than for Alternative 2 (a_i).

To avoid the effect of nonlinear scatter in calculating averages based on other fiber characteristics, it is therefore recommended to calculate the fiber characteristic for single fibers before calculating its average value.

C2. Deviation of products of independently measured data

Standard deviation

The variance and standard deviation over a number of measured data points was calculated as follows (Eq. C2.1 and C2.2);

$$\sigma^2 = \text{variance} = \frac{1}{N}\sum_{i=1}^{N}(Z_i - \overline{Z})^2 \quad (Eq.C2.1)$$

$$\sigma = s\tan dard\ deviation = \sqrt{\text{var}\, iance} \quad (Eq.C2.2)$$

$$\overline{Z} = \text{average of measured points}$$

Some parameters were calculated as the product of two independently analyzed parameters. One example was tensile index; the average tensile index was calculated from the product of two independently measured average values; tensile strength and grammage of sheet. The standard deviation σ for an uncorrelated property K, defined as below, was calculated according to Equation C2.3.

$$\overline{K} = \frac{\overline{X}}{\overline{Y}}$$

$$\frac{\sigma_K{}^2}{\overline{K}^2} = \frac{\sigma_X{}^2}{\overline{X}^2} + \frac{\sigma_Y{}^2}{\overline{Y}^2} \rightarrow$$

$$\sigma_K = \overline{K}\sqrt{\frac{\sigma_X{}^2}{\overline{X}^2} + \frac{\sigma_Y{}^2}{\overline{Y}^2}} \quad (Eq.\ C2.3)$$

Coefficient of variation CV

Repeatability in sampling and measurement was estimated as the coefficient of variation, CV. The general equation for coefficient of variation was calculated as:

$$CV_Z\,[\%] = \frac{\sigma_Z}{\overline{Z}} * 100 \qquad \text{Eq. C2.4}$$

For two uncorrelated averages $\overline{X}$ and $\overline{Y}$ forming the product $\overline{K}$, the following is valid;

$$\overline{K} = \frac{\overline{X}}{\overline{Y}}$$

The coefficient of variation was calculated according to Equation C2.5 which was derived below.

$$CV_K{}^2 = CV_X{}^2 + CV_Y{}^2$$

$$CV_K = \sqrt{CV_X{}^2 + CV_Y{}^2} \qquad \text{Eq. C2.5}$$

95% confidence intervals

The 95% confidence interval Δ around an average $\overline{Z}$ was calculated according to:

$$\overline{Z} \pm \Delta$$

$$\Delta = \frac{t * \sigma}{\sqrt{n}} \qquad \text{Eq. C2.6}$$

where:

σ = standard deviation = ROT (variance)
t = t-factor, based upon number of measurement points, *cf.* Table C2.1 below
n = number of measured points

Table C2.1. t-distribution used for calculating 95% confidence intervals of fiber dimensions and laboratory sheets properties.

n	t for 5% uncertainty	n	t for 5% uncertainty
4	2.78	16	2.12
5	2.57	17	2.11
6	2.45	18	2.10
7	2.36	19	2.09
8	2.31	20	2.09
9	2.26	25	2.06
10	2.23	30	2.04
11	2.20	40	2.02
12	2.18	60	2.00
13	2.16	120	1.98
14	2.14	∞	1.96
15	2.13		

For a factor combined from two independently measured, uncorrelated parameters, the 95% confidence intervals were estimated by using the average standard deviation for K, S_K, calculated in Equation C2.7 below, together with *t* and *n* from Table C2.1 above, for the property of the lowest amount of measured points. The 95% confidence interval for products of independently measured data was then calculated according to Equation C2.8.

$$\overline{K} = \frac{\overline{X}}{\overline{Y}}$$

$$s_X = \sqrt{AVERAGE\ VARIANCE(X)}$$

$$s_Y = \sqrt{AVERAGE\ VARIANCE(Y)}$$

$$s_K = \overline{K}\sqrt{\frac{{s_X}^2}{\overline{X}^2} + \frac{{s_Y}^2}{\overline{Y}^2}} \quad (Eq.C2.7)$$

$$95\%\,CONF.INT(K):$$

$$\frac{t\ (LOWEST\ NUMBER\,OF\ MEASURED\ POINTS) * s_K}{\sqrt{n}\ (LOWEST\ NUMBER\,OF\ MEASURED\ POINTS)} (Eq.C2.8)$$